International
Progress Report

IPR-01-45

Äspö Hard Rock Laboratory

TRUE Block Scale project

Selective pressure build-up tests in borehole KI0025F

Bengt Gentzschein

GEOSIGMA AB

Mansueto Morosini

SKB

October 1998

Svensk Kärnbränslehantering AB
Swedish Nuclear Fuel
and Waste Management Co
Box 5864
SE-102 40 Stockholm Sweden
Tel +46 8 459 84 00
Fax +46 8 661 57 19

Äspö Hard Rock
Laboratory

Report no.
IPR-01-45
No.
F56K
Author
Gentzschein, Morosini
Date
Checked by
Date
Approved
Christer Svemar
Date
02-08-23

Äspö Hard Rock Laboratory

TRUE Block Scale project

Selective pressure build-up tests in borehole KI0025F

Bengt Gentzschein

GEOSIGMA AB

Mansueto Morosini

SKB

October 1998

Keywords: Build-up test, flow, KI0025F, mocxel indentification, pressure, transient, transmissivity, UHT 1

Abstract

Selective flow and pressure build-up tests were conducted in borehole KI0025F as part of the characterisation of the TRUE Block Scale volume at the Äspö HRL. In all, six test intervals were characterised using the SKB UHT equipment. After completion of the tests, test data were subject to preliminary evaluation using Jacobs approximation of Theis well function. At a later stage the test data were analysed with the help of the interpretation software Saphire (Kappa Engineering).

Sammanfattning

Som en del av karakteriseringen av True Block Scale-området utfördes selektiva flödes- och tryckuppbyggnadstester i borrhål KI0025F. Med utrustningen SKB UHT karakteriserades sex testintervaller. Efter avslutning av försöken, användes testdata till preliminära uträkningar med Jacobs approximation av Theis brunnsfunktion. Vid ett senare stadium analyserades testdata med hjälp av utvärderingsprogrammet Saphire (Kapa Engineering).

CONTENTS

1 Background 9

2 Objectives 11

3 Scope 13

4 Equipment Used 15

5 Performance and Evaluation 23
5.1 Test Principles 23
5.2 Test Cycle and Procedures 23
5.3 Calibration 24
5.4 Data Processing 25
5.5 Preliminary Evaluation 26
5.6 Evaluation Using Saphir 27
5.7 Sources of Error 31
5.8 Specifics and Evaluation 31
5.8.1 Section 43.0 - 44.0 m 31
5.8.2 Section 86.0 - 87.0 m 34
5.8.3 Section 165.3 - 166.3m 35
5.8.4 Section 166.3 - 167.3 m 39
5.8.5 Section 167.3 - 168.3 m 41
5.8.6 Section 186.0 - 193.8 m 42

6 Results 49

7 Discussions 51
7.1 Moye vs. Saphir 51
7.2 Jacob vs. Saphir 52
7.3 Storage coefficient 53
7.4 Skinfactor 56

8 Conclusions 59

9 References 61

10 Appendices 63

Appendix 1: Borehole logg of KI0025F
Appendix 2: Description of the UHT 1 diagrams
Appendix 3: Symbols and calculations of the UHT 1 diagrams
Appendix 4: Parameter equations used for the Saphir evaluation.
Appendix 5: Diagrams of the test in section 43.0 - 44.0 m
Appendix 6: Diagrams of the test in section 86.0 - 87.0 m
Appendix 7: Diagrams of the test in section 165.3 - 166.3 m
Appendix 8: Diagrams of the test in section 166.3 - 167.3 m
Appendix 9: Diagrams of the test in section 167.3 - 168.3 m
Appendix 10: Diagrams of the test in section 186.0 - 193.8 m

List of Figures

Figure 1-1 Updated structural model of the TRUE Block Scale Volume. Planar section at Z=-450 masl (Hermansson and Follin). Horizontal projection of tentative geometry of borehole KI0025F.

Figure 4-1 Overview of the UHT 1-system

Figure 4-2 Upper packer (above) and lower packer (below

Figure 4-3 Hoisting rig

Figure 5-1 Hydraulic Test Fact Sheet. Evaluation of section 43.0 - 44.0 m using Saphir

Figure 5-2 Hydraulic Test Fact Sheet. Evaluation of section 87.0 - 88.0 m using Saphir

Figure 5-3 Hydraulic Test Fact Sheet. Evaluation of section 165.3 - 166.3 m using Saphir

Figure 5-4 Hydraulic Test Fact Sheet. Evaluation of section 166.3 - 167.3 m using Saphir

Figure 5-5 Hydraulic Test Fact Sheet. Evaluation of section 167.3 - 168.3 m using Saphir

Figure 5-6 History plot of pressure for section 186.0 - 193.8 m in KI0025F

Figure 5-7 Hydraulic Test Fact Sheet. Evaluation of section 186.0 - 193.8 m using Saphir

Figure 5-8 Pressure and pressure derivative for the build-up phase in section 186.0-193.8 m of borehole KI0025F

Figure 7-1 Difference in calculated transmissivities with methods of Moye, Jacob and Saphir as a function of the skinfactor calculated with Saphir

Figure 7-2 Pressure response in section 187-196 m in borehole KA2563A due to hydraulic testing activities in borehole KI0025F. Reference to the test numbers is in Table 3-2.

Figure 7-3 Interference test response in KA2563A 187-196 m for different response time when flowing KI0025F(complete length) ; 0, 0.5 and 1 h

List of Tables

Table 3-1 Pressure build-up tested intervals of borehole KI0025F

Table 3-2 A complete list of tests conducted in borehole KI0025F, June 1997

Table 5-1 Conceptual interpretation sequence of Saphir

Table 5-2 Modelling results for section 43.0 – 44.0 m.

Table 5-3 Modelling results for section 87.0 – 88.0 m.

Table 5-4 Modelling results for section 165.3 – 166.3 m.

Table 5-5 Modelling results for section 166.3 – 167.3 m.

Table 5-6 Modelling results for section 167.3 – 168.3 m.

Table 5-7 Modelling results for section 186.0 – 193.8 m.

Table 6-1 Test data from pressure build-up tests in borehole KI0025F

Table 6-2 Preliminary evaluated hydraulic parameters from pressure build-up tests in borehole KI0025F

Table 6-3 Parameter results from evaluation using Saphir, all hydraulic tests conducted in KI0025F

Table 7-1 Preliminary evaluated parameters and Saphir-evaluated parameters from pressure build-up tests in borehole KI0025F

Table 7-2 Aquifer parameters in section 187 -196 m of KA2563A calculated for different response times.

Table 7-3 Sensitivity of transmissivity and storage coefficient calculated for section 187-196 m of KA2563A to different shut-in flow rates in KI0025F

Table 7-4 Storage coefficients from TRUE-1 and LPT-2 experiments at Äspö

1 BACKGROUND

During 1996 characterization work for the TRUE Block Scale Project commenced at Äspö with drilling of borehole KA2563A from the spiral tunnel. Characterization data from this borehole and data from boreholes KA2511A and KA3510A have been used to update the structural model of the south-western part of the Äspö HRL (Hermanson and Follin, 1997). On the basis of this updated model and the identified centre of gravity for further investigations, several alternative borehole positions were considered. Eventually, a borehole location in the ”I-drift/niche” was selected, cf. Figure 1.1, from which an approximately 200 m long 76 mm diameter triple tube borehole directed near south was drilled.

A suite of borehole characterization techniques have been conducted in KI0025F, including borehole deviation surveying, borehole image processing (Stråhle 1997) borehole radar measurements (Carlsten 1997), core logging, double packer flow logging (Gentzschein 1997) and UCM acoustic flow logging (Gustafsson 1997). An overview of the results from the charcterization is shown in Appendix 1, which also shows the cumulative inflow of water to the borehole during drilling. The borehole image survey, in conjunction with the core logging resulted in a detailed description of the fractures in the test sections according to Appendix 1.

This report details the flow and pressure build-up tests performed in intervals of the borehole selected on the basis of the performed characterization in the hole.

The tests were carried out with the new test equipment (UHT 1) specially designed by SKB for use underground. The intention was to have on-site follow up of the tests such that their performance and duration was optimized.

After completion of the tests, test data were subject to preliminary evaluation using Jacobs approximation of Theis’ well function. At a later stage the test data were analyzed with the help of the interpretation software Saphir (Kappa Engineering)

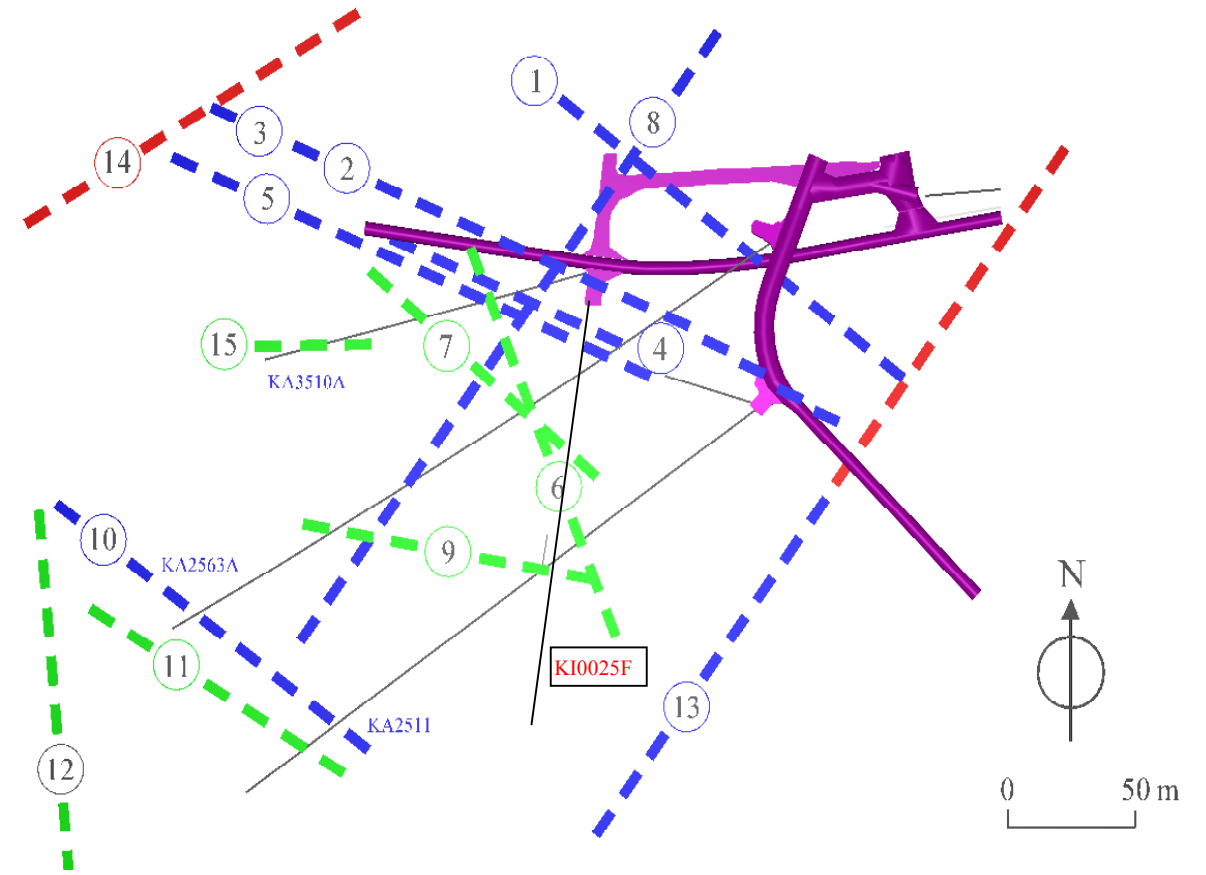

Figure 1-1 *Updated structural model of the TRUE Block Scale Volume. Planar section at Z=-450 masl (Hermanson and Follin 1997). Horizontal projection of tentative geometry of borehole KI0025F .*

2 OBJECTIVES

The objectives of the investigations were to;

- perform flow and pressure build-up tests in selected parts of borehole KI0025F which either may be regarded as boundaries to future hydraulic and transport experiments, or which may be actual target features for future experiments

- produce the necessary output files of flow and pressure as a function of time such that state of the art evaluation of formation parameters and flow dimension could be evaluated.

The objectives of the evaluation of the hydraulic tests undertaken in KI0025F were to

- establish the flow model
- assess the aquifer parameters
- detect and identify hydraulic boundaries
- compare preliminary evaluation (Jacob) with evaluation using Saphir.

3 SCOPE

Borehole KI0025F is drilled due south with a downward inclination of 20^{o} to a total length of 193.8 m. The nominal diameter of the hole is 75.85 mm. The upper 60 metres of the borehole have been reamed to a final diameter of 76.55 mm. The core mapping and the available BIPS images show that the borehole sample an essentially homogeneous body of Äspö diorite. Occasional minor bodies of greenstone and fine-grained granite are intersected at some locations. Major transmissive zones have been noted at:

L=4.9 m (Q=40 l/min, cement grouted)
L=165.3-166.3 m (Q=35 l/min) and at
L=187.7-193.8 m (Q=35 l/min).

Minor inflows in the range 2-3 l/min where found at approximately
L=45 m and
L=86 m

The tests were performed in selected test sections of borehole KI0025F, using either double or single packer arrangement. The exact position and length of the test sections were based on the results of the detailed flow logging with a double packer and the BIPS data. The tested intervals (sections) in KI0025F are summarized in Table 3-1

Table 3-1 Pressure build-up tested intervals of borehole KI0025F

Test section (m)	Length of measurement section (m)	Date of test	Comment
43.0 - 44.0	1	970618	
87.0 - 88.0	1	970618	
165.3 - 166.3	1	970619	
166.3 - 167.3	1	970619	
167.3 - 168.3	1	970623	
186.0 - 193.8	7.8	970624	Single packer test

Five of the successful tests were preceded by tests, which had to be interrupted due to equipment failure or due to difficulties in keeping a constant pressure head during the test. A complete list of tests is shown in Table 3-2

Table 3-2 A complete list of tests conducted in borehole KI0025F, June 1997

Test section (m)	Date/ Time of test	Data file	Comment
43.0 - 44.0	970617/ 09:54:38	KI0025F1.HT2	Non-convergence of P & Q
43.0 - 44.0	970617/ 12:51:01	KI0025F2.HT2	Non-convergence of P & Q
43.0 - 44.0	970618/ 13:44:03	KI0025F3.HT2	Non-convergence of P & Q
43.0 - 44.0	970618/ 14:54:11	KI0025F4.HT2	Successful test
87.0 - 88.0	970618/ 18:06:16	KI0025F5.HT2	Borehole valve leakage
87.0 - 88.0	970618/ 18:06:16	KI0025F6.HT2	Successful test
87.5 - 88.5	970618/	No data file	Only flow measurement
87.75 - 88.75	970618/	No data file	Only flow measurement
165.3 - 166.3	970618/ 22:26:54	KI0025F7.HT2	Pressure recovery over the night
165.3 - 166.3	970619/	KI0025F8.HT2	Jammed borehole valve. Data file is missing
165.3 - 166.3	970619/ 09:50:09	KI0025F9.HT2	Successful test
166.3 - 167.3	970619/ 11:36:59	KI025F10.HT2	Valves were erronously set
166.3 - 167.3	970619/ 13:48:58	KI025F11.HT2	Unstable P & Q
166.3 - 167.3	970619/ 14:27:41	KI025F12.HT2	Successful test
167.3 - 168.3	970623/ 11:18:05	KI025F13.HT2	Successful test
0 - 193.8	970623/ 18:27:18	KI025F14.HT2	Pressure recovery over the night
186.0 - 193.8	970624/ 11:13:30	KI025F15.HT2	Air in the hoses
186.0 - 193.8	970624/ 12:54:45	KI025F16.HT2	Data fetch
186.0 - 193.8	970624/ 12:54:45	KI025F17.HT2	Successful test

4 EQUIPMENT USED

The underground hydraulic test system (UHT 1) developed by SKB (Almén and Hansson, 1996) was used for the tests.

UHT 1 is constructed for underground hydraulic testing in boreholes with 56 mm and 76 mm diameter. Maximum borehole length is 300 m and the maximum working depth is 500 metres below sea level.

The main parts of the system (Figure 4-1) are

- Down-hole equipment with packers and pipe string
- Hoisting rig
- Mini container including a system control unit, a measurement control unit and a data export and plotting unit

The down-hole equipment consists of two inflatable Polyurethane packers, see Figure 4.2, separated by pipe(s), a mechanically operated valve, a pipe string and two pressure lines. The sealing length of each packer is 1.0 m and they are inflated using water pressurized by nitrogen. The pipe between the packers and a by-pass opening at the upper gable of the outer packer equalize the ground water pressure on both sides of the measurement section. The down-hole valve is after packer inflation opened by pushing the pipe string 87- 105 mm towards the bottom of the borehole and is shut by pulling the pipe string the same distance. One of the two pressure hoses (polyamide) is connecting the packers and the pressurizing system. The second pressure hose establishes hydraulic contact between the measurement chamber and a transducer (P) positioned in the Mini container.

The pressure in the section between the outer packer and the collar is shut in using a sealing device at the casing collar. The device consists of a rubber cone with openings for the pipe string and for the two pressure hoses. The device enables movement of the test tool in the borehole without de-pressurizing the entire borehole completely. A quick-coupling at the sealing-device and a pressure line to a pressure transducer in the container makes it possible to measure the borehole pressure (P_a).

The pipe string is made of aluminium with threaded pipe joints of stainless steel . The outer/inner diameter is 33/21 mm and the length of individual pipe segments is 3 metres. There are also 1 m pipes and 0.5 m pipes.

The test tool and the pipe string are lowered into the borehole using a hoisting rig, which is operated by a control panel and a power unit with a hydraulic motor (Figure 4-3). The pipe holders on the feeder beam are opened hydraulically, but are closed by means of disc springs. On the control panel there are 3 manometers showing the system pressure and the pressure on each side of the piston. With the help of the piston pressure

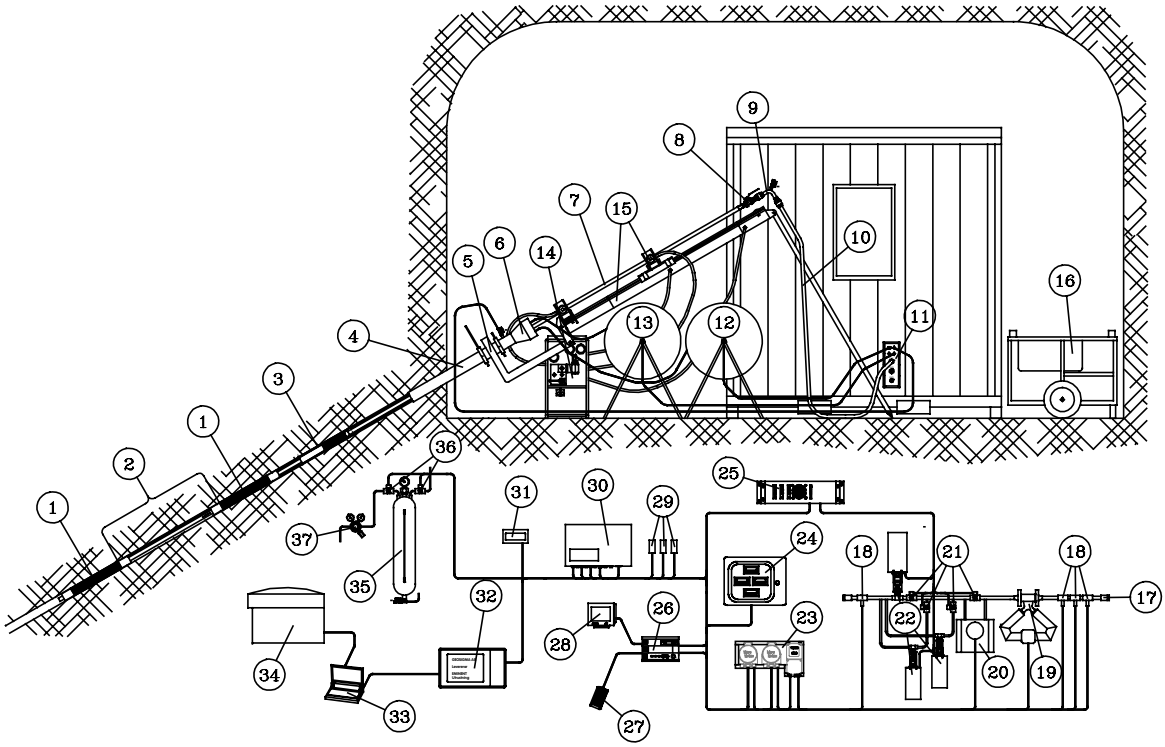

Figure 4-1 *Overview of the UHT 1-system*

1. Packer
2. Measurement section
3. Test valve
4. Casing
5. Extension beam
6. Sealing device
7. Pipe string
8. Adapter
9. Tube bend with air evacuation valve
10. Measurement hose from borehole
11. Wall lead-in
12. Hose reel, packer
13. Hose reel, section pressure
14. Control board, hoisting rig
15. Feed beam, hoisting rig
16. Power unit, hoisting rig
17. Inlet to container
18. Sensors, pressure, temperature, electrical conductivity
19. Flow meter BIG
20. Flow meter small
21. Valves
22. Regulation valves
23. Amplifier to Flow meter unit
24. Display for Flow meter unit
25. Stepping motor
26. Regulation computer
27. Regulation computer, key board
28. Regulation computer, monitor
29. Pressure transducers
30. Data scan box
31. External display
32. Measurement computer (SPC Rabbit)
33. Evaluation computer (Compaq)
34. Laser Jet printer
35. Pressure tank, packer inflation
36. Solenoid valves
37. N_2-gas governor

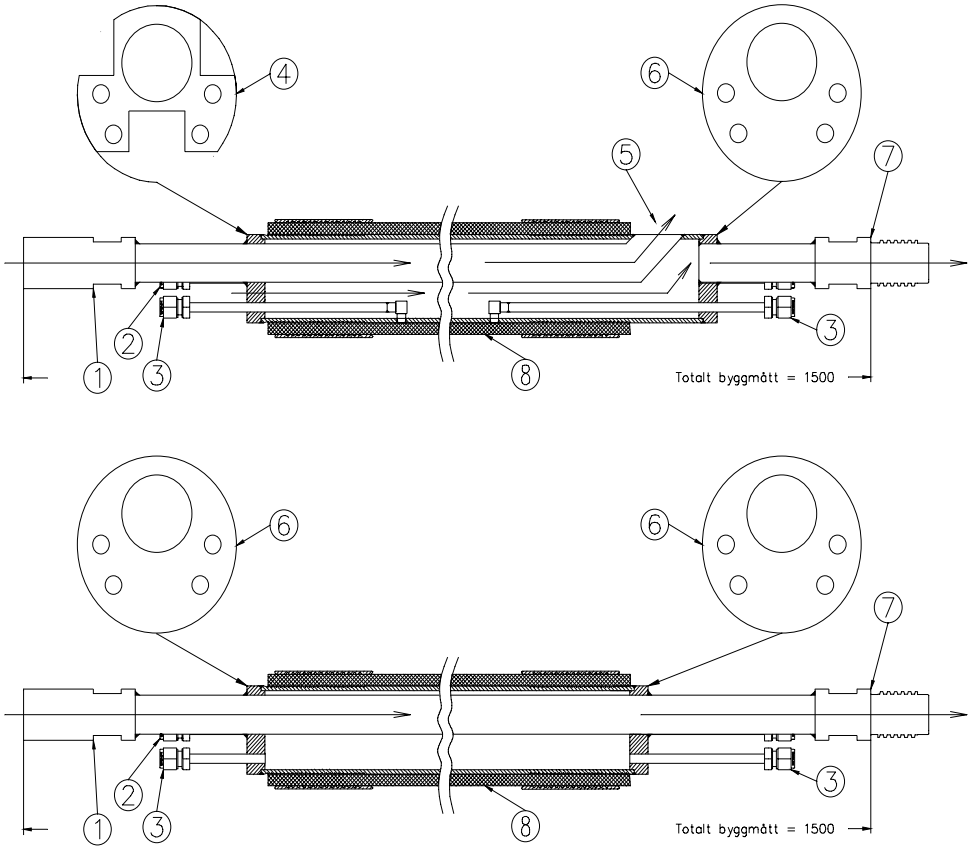

Figure 4-2 *Upper packer (above) and lower packer (below)*

1. Female pipe joint, ϕ = 33 mm, Double O-ring gasket
2. Hydraulic lead-through
3. Packer inflation cannular tube
4. Packer gable, the openings connect borehole intervals on both side of the packer.
5. The hydraulic connection to the test section
6. Packer gable
7. Male pipe joint, ϕ = 33 mm, Double O-ring gasket
8. Polyurethane

and a specially devised diagram, the lifting force can be calculated for each situation. The pipe holders are automatically opened and closed when the pipes are hoisted or lowered.

A casing extension and a beam extension are mounted on the borehole casing to fit the hoisting rig (Figure 4-3).

The mini container is made of steel and has the outer dimension 2.5x1.7x2.6 m. Its walls are insulated using covered white plates and the floor is covered with an aluminium sheet. It is furnished with a table, cupboards and shelves for keeping tools, spare parts etc. The container accommodates the monitoring equipment and the computers and the printer, necessary to retrieve and plot data, respectively.

The electrical system of the container is connected to 16 A three-phase AC. Inside the container there are two 230 V electrical systems. One of them is directly connected to the power net, the second, which feeds the measurement instruments is also connected to an UPS-unit (auxiliary power supply) to avoid data losses during a power failure.

The pipe system in the container is connected to a lead-through in the wall. On the outside of the lead-through, different hoses from the borehole are connected with the help of quick-couplings.

The pressure transducers, of type Druck PTX 630, measure absolute pressure, and are mounted on a board on one of the container walls. There are two sets of transducers with different pressure ranges. The standard set of pressure transducers are, cf. Section 5:

Interval/packer	**Number**	**Transducer id**	**Range (alternative range)**		
Test section	2	P and P_b	6	MPa	(1 MPa)
Borehole	1	P_a	6	MPa	(1 MPa)
Packers	1	P_{pack}	8	MPa	(2 MPa)

The pressure transducers are connected to the borehole through cannular tubes, hydraulic hoses and polyamide hoses.

The technical specifications of the pressure transducers are:

Supply voltage:	9 - 30 VDC
Output current:	4 - 20 mA
Linearity and hysteresis:	± 0.1 % of full scale
Temperature error :	± 0.3 % of full scale in the range -2 ^{o}C - +30 ^{o}C

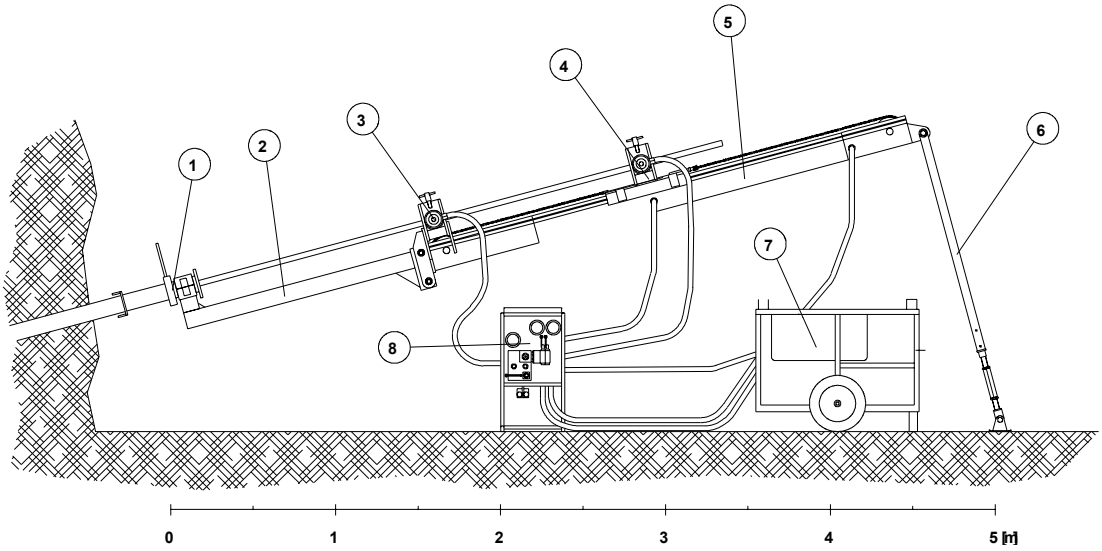

Figure 4-3 *Hoisting rig*

1. Casing extension
2. Beam extension
3. Pipe holder
4. Pipe holder
5. Feed beam
6 . Legs
7 . Power supply unit
8 . Control panel

The technical specifications of the pressure transducers are:

Supply voltage:	9 - 30 VDC
Output current:	4 - 20 mA
Linearity and hysteresis:	± 0.1 % of full scale
Temperature error :	± 0.3 % of full scale in the range -2 ^{o}C - +30 ^{o}C

The flow meter unit enables monitoring and regulation of the flow during constant pressure tests and constant flow tests, respectively. The flow regulation is operated and controlled using a digital computer. The main parts of the flow meter unit are:

- Two mass flow meters of type Coriolis-meters, flow range: 0.001-100 L/min
- Valves to regulate the flow rate
- A water filter
- Two pressure transducers, measuring the pressure at the inlet and the outlet of water, respectively.
- A temperature sensor

Further more there are:
- a display unit with four displays
- a cylinder with an electric conductivity sensor
- an amplifier to the flow meter unit and the conductivity sensor.

All flow is lead through the large flow meter (Q_{big}) irrespective if the little one (Q_{small}) is in use or not. The technical data of the main components of the flow meter unit are as follows:

Flow meter Q_{small}

Type :	Micro Motion mass flow meter
Range:	0 - 1.00 Kg/minute
Accuracy:	±0.4 % of current value ± zero stability (0.0001 Kg/minute)
Pressure drop at max.flow:	c. 500 KPa
Maximum working pressure:	7 MPa

Flow meter Q_{big}

Type :	Micro Motion mass flow meter
Range:	0 - 100 Kg/ minute
Accuracy:	± 0.15 % of current value ± zero stability (0.003 Kg/minute)
Hysteresis:	< 0.1 %
Pressure drop at max. flow:	c. 500 KPa
Maximum working pressure:	5 MPa

Pressure transducers, inlet and outlet

Type :	Druck Transmitter PTX 1400
Range:	0 - 6 Mpa
Linearity and hysteresis:	± 0.1 %

Temperature sensors

Type :	GEOSIGMA BG01
Range:	0 - +32 ^{o}C
Accuracy:	±0.25 ^{o}C

Electrical Conductivity meter

Type :	Kemotron 2911
Sensor:	Kemotron 9221, 4-electrode
Range:	Adjustable, 14 intervals within the range 0 - 20 000 mS/m
Accuracy, amplifier:	±0.25 % of current value
Accuracy, cell constant:	±0.5 %
Maximum working pressure:	5 MPa
Temperature sensor:	Pt 100

When performing constant pressure tests, as was the case with the tests in KI0025F, the constant pressure is maintained by a standard PC (Intel 486, 100 MHz, 4MB RAM and 200 MB HDD, CRT monitor). The pressure is kept constant by regulating the water flow rate. A specially designed software opens and shuts regulation valves such that a constant pressure according to a preset value is achieved. The program is written in TURBO-C and run on a DOS platform

The UHT 1 measurement system is controlled by, and operated from a 120 MHz Pentium laptop computer. The software used is DM2 (Datascan Technology) , which also constitutes the platform for the Hydro Monitoring System (HMS) at the Äspö HRL. DM2 is a standard program, but has been supplemented with additional programs.

All sensors are connected to the AD-converter unit (Datascan 7320)
In addition there is a Datascan-unit for digital I/O (Datascan 7035).

The data produced by UHT 1 are evaluated in a second computer, a portable Compaq 100 MHz Pentium. The operating system is Windows 95, but the evaluation programs are run in on a DOS platform. Data files from the test are transferred to the evaluation computer during or after each test.

The UHT 1-system also includes a HP Laser Jet 5p, which is printing
either evaluation plots from the evaluation computer, or display images from the measurement computer.

5 PERFORMANCE AND EVALUATION

5.1 TEST PRINCIPLES

The tests were performed as flow and pressure build up tests. During the flow phase the ambient pressure in the test section was generally lowered with c.2 MPa (200 m water column), with the exception of test section 166.3 - 167.3 m. This is a low permeable section and the pressure was lowered c. 0.7 MPa. The resulting flow was registered as a function of time. Subsequently the test section was shut in and the pressure was allowed to recover to ambient pressure. Either the flow or the recovery phase can be evaluated using theories for transient flow.

5.2 TEST CYCLE AND PROCEDURES

The test cycle adopted for the flow and pressure build up tests in borehole KI0025F, following mobilization on the borehole, was the following;

1) The packer assembly was inserted to the desired test location using the hoisting rig. Estimated duration : 5 - 30 minutes depending on the distance to the (next) test position.
2) Packer expansion waiting for creeping effects in the packer material (polyurethane) to diminish enough to permit start of test. Time : Minimum 20 minutes
3) Evacuation of air from the pipe string and the measurement hose.
4) Opening of test valve and regulation of water flow under constant pressure (dP=20 bars) conditions (Flow Phase) during which the flow was registered as a function of time. The exact length of the flow phase was decided on the basis of plots of flow as a function of time generated by the system. Time : 32 - 63 minutes.
5) Closing of test valve followed by pressure recovery (Build-up Phase) during which pressure was registered as a function of time. The exact length of the build-up phase was decided on-site using diagnostic plots generated by the test system. Time : 22 - 125 minutes.
6) Packer deflation. Time : 3 - 5 minutes.
7) Transfer of packer assembly to the next test section. Estimated time: 5 - 30 minutes depending on the distance to the next test position.

After the test in the measurement section 87.0 - 88.0 m a more detailed localization of the flowing section (fracture) was performed. The procedure used was defined by Peter Andersson for the SELECT flow and pressure build up tests;

1. After completion of the pressure build up test according to the list above the packer assembly was moved 0.5 m further into the borehole.
2. The packers were expanded during 5 minutes
3. The resulting flow was measured and recorded. N.B. dP = 20 bars
4. If the flow was more than 50% of the flow recorded under the flow phase of the preceeding "actual" test, the packer assembly was moved another 0.25 m into the borehole. If not cf. #5.
5. If the flow was less than 50% of the flow recorded during the flow phase of the preceding "actual" test, the packer assembly was moved out 0.75m
6. The packers were expanded for 5 minutes.
7. The resulting flow was measured and recorded. N.B. dP = 20 bars
8. The packers were deflated and moved to the next test section in accordance with the list above.

5.3 CALIBRATION

The flow meters Q_{small} and Q_{big}, see chapter 4, were calibrated using graduated cylinders and a stop watch. Two flows were measured for each flow meter for the purpose of calibration, and each level was measured twice.

The pressure transducers P_a, P_b and P_{pack}, see chapter 4, were calibrated with the help of the reference pressure system established in the Äspö HRL tunnel. The transducers were connected to two hoses, filled with water of known density. The hoses respectively lead up to two different but known reference water levels (at KK0120 and KK2850) along the tunnel. The levels are well determined which enables calculation of the calibration constants. The position of the pressure sensors and the barometric pressure are also used in the calibration process. The elevation of the sensors were surveyed prior to the tests and the barometric pressure was measured with a Druck DPI 700 digital pressure indicator, which have a factory-listed accuracy of 0.05% of full scale (2 bar).

The temperature sensor and the electric conductivity sensor were only zero-point calibrated. The temperature sensor was compared with a high-accuracy portable thermometer of good quality. The conductivity sensor was calibrated using a liquid solution with a well determined electric conductivity.

The results of the calibrations were inputted into the measurement computer and the calibration constants were automatically calculated.

5.4 DATA PROCESSING

The parameters, measured by the UHT-1 measurement system are:

P	Pressure of the test section
P_a	Pressure of the borehole intervals around the test section
P_{pack}	Packer pressure
T_{surf}	Water temperature (surface)
Q_1	Water flow rate Q_{small}
Q_2	Water flow rate Q_{big}
P_b	Pressure of the test section (same as P)
Elcond	Electrical conductivity

The operative system of the measurement computer is OS9000. The measurement program is based on a program called

- DM2-386

Additionally there are three modules (standard programs)
- CALC-386 (for special transformation of data)
- SEQ-386 (creates automatic sequenses of measurements, data storing.)
- MIMICMAN (creates graphical interfaces with process images)
- CONTR-386 (controller for regulation of flow/pressure)

These programs are supplemented with a number of application programs.

- Menu programs for entering data(calibration constants, background data)
- Report generator which creates an out put file (MIO-format)
- Drive routine for extra display
- Calibration programs

The program ”KERMIT” is used to transfer data from the measurement computer to the evaluation computer.

The program SHELL.EXE starts all the programs in the evaluation computer. SHELL.EXE is a commercial program from WordPerfect. The data file transferred from the measurement computer has a MIO-format (Appendix 3). This file is converted to a number of files, which enables plotting of the different diagrams. The same plot program creates plots both on the screen and on the printer. The programs in the evaluation computer are:

- IPPLOT.EXE Conversion program from ERGO-data (B. Johansson)
- SKBPLOT.EXE Plot program from ERGO-data (B. Johansson)
- PLTCNV.EXE File selection program. From GEOSIGMA (G. Nyberg)
- RUNBAT.EXE File selection program and start of BATCH file. From GEOSIGMA (G. Nyberg)

The plot program generates three types of diagrams :

- A diagrams (**A1 - A5**) show pressure, flow and temperature variations during the whole test cycle.**A0** is a flyleaf showing background data as well as measured and calculated data from the test.

- B diagrams (**B1 - B6**) show pressure and flow variations during the flow phase in logarithmic and semilogarithmic scale. Also other parameter transformations are plotted.

- C diagrams (**C1 - C9**) show pressure and flow variations during the pressure buildup phase in logarithmic and semilogarithmic scale. Also other transformations of parameters and time are plotted.

A more detailed description of the diagrams is found in Appendix 2. In Appendix 3 the symbols and the parameters of the diagrams are described.

5.5 PRELIMINARY EVALUATION

In one of the C-diagrams (C4) the pressure build-up is plotted versus the equivalent time, dt_e , in minutes. The equivalent time is defined as

$$dt_e = \frac{t_p \cdot dt}{t_p + dt}$$ where

t_p = time in minutes when the test section was open
dt = elapsed time after shutting the valve to the test section.

The diagram was used for a preliminary evaluation of the tests in KI0025F according to standard routines for evaluation of pressure build-up tests at the Äspö HRL (Rhén and Nilsson, 1991). The following geohydrological parameters was determined:

- specific capacity, Q/s (m^2 /s)
- transmissivity, T (m^2 /s) where

Q = water flow rate (m^3 /s).
s = pressure change (m) during the test

The transmissivity was calculated using Jacob's semilogarithmic approximation of Theis well function (Rhén and Nilsson, 1991):

$$T = 0.183 \cdot \frac{Q}{\Delta s}$$

where

Δs = the pressure change in metres during a decade along the straight line in the semi-logarithmic diagram (m)

The average hydraulic conductivity of the tested section, $\bar{K}$, can be calculated as

$$\bar{K} = T / L \qquad (L = \text{The length of the test section(m)})$$

The UHT 1 system automatically calculates a steady-state value of the hydraulic conductivity of the test sections using Moye´s formula (Moye 1967):

$$K = \frac{Qp \times 1000 \times 9.81}{L \times dP_{om}} \cdot \cdots \cdot C$$

where

Qp = flow rate of the test section at the end of the flow phase(m^3/s)

dP_{om} = Average of Po - P during the flow phase (KPa)

P = hydraulic head of the test section

Po = hydraulic head of the test section before flow start.

$C = [1 + \ln(L/2r_w)]/ 2\pi$

L = Length of the test section (m)

r_w = borehole radius (m)

The steady-state hydraulic conductivity is printed on the flyleaf of each test section (as K_{oss}).

5.6 EVALUATION USING SAPHIR

Hydraulic tests were conducted as sequences of constant pressure drawdown phase followed by a pressure buildup phase, see section 5.1. The analysis has also been performed with the well test interpretation software Saphir v 2.20H by Kappa Engineering. The focus of the analysis has mainly been on the build-up phase. A brief derivation of the governing equations is given in Appendix 4.

The interpretation is based on the theories of transient radial flow behaviour in a porous medium that is governed by the diffusion equation. In particular, Saphir utilises the

Jacob approximation to the well function throughout the calculation of the aquifer and wellbore parameters. Theories of well test interpretation are given in many references e g Earlougher (1977), de Marsily (1986). The adoption of these theories for the present analysis in fractured rock may be partly justified through the geometrical analogy between a borehole intersecting a confined granular aquifer and a borehole intersecting a fracture or fracture zone whose water is mainly derived from the expansion of water upon release of pressure. Previous experience of tests in fractured rock has shown that in many cases (not all) the pressure response agrees with the confined, homogeneous, radial flow model.

The general approach is to identify the flow regimes during a test by means of log-log and semi-log plots of pressure vs time for the buildup phase but also of flow vs time for the constant pressure flow phase. This will yield a first estimate of the transmissivity (T) [Equation 1] and skin (ξ) parameters (Appendix 4), where β is the matched parameter $C_D e^{2\xi}$

$$T = \frac{Q}{2\pi(\Delta p)_{match}}$$

$$\xi = \frac{1}{2} \ln \left(\beta \cdot \frac{Sr_w^2}{T (\Delta t)_{match}} \right)$$

It is necessary to identify the wellbore storage unit slope line on the log-log plot and the horizontal line on the pressure derivative log-log plot where the pressure derivative p'_D is 0.5 in order to obtain a first estimate of the parameters. When such a match is obtained the following relation applies, [Equation 2],

$$T = \frac{1}{4\pi} \cdot \frac{Q}{\Delta p'_{IARF}}$$

This identification will also provide the time interval during which the pressure match yields the IARF (= Infinite Acting Radial Flow) response. It should be recognised that the pressure derivative is the same as the calculated slope of the pressure function vs time function on a semi-log plot shown on a log-log plot. This definition is advantageous since it is still valid when analysing tests with multiple rates. During IARF the pressure derivative response due to multiple rates is the same for the case of drawdown and build-up [Equation 3] (Appendix 4),

$$\Delta p'_{MRDd} = \Delta p'_{MRBu} = \frac{Q}{4\pi T} = \frac{1}{2} \cdot \frac{(\Delta p)_{match}}{(p_D)_{match}}$$

These aquifer parameters are then used as first estimates in the nonlinear regression calculation of parameters. When only one flow rate is involved during drawdown the pressure history is calculated with the Jacob equation according to

$$\Delta p_{Dd}(\Delta t) \approx \frac{(\Delta p)_{match}}{(p_D)_{match}} \cdot \frac{1}{2}\left[\ln\left(\frac{(t_D)_{match}}{(\Delta t)_{match}} \cdot \Delta t \right) + 0.80909 \right]$$

When multiple flow rates are involved the complete test sequence is generated through superposition of multiple rates (these equations are given in Appendix 4 for the pressure drawdown and build-up cases) and compared with the measured data.

Aquifer parameters that are derived through type-curve matching are utilised as input values for a non-linear regression fitting between data and model. The non linear regression is performed with the objective to minimise the sum of the squared differences between modelled and measured head. This regression also allows the fitting parameters, K, skin and C to be fixed or be variable. With the use of the new estimates of the aquifer and wellbore parameters a new model is generated and compared to the data by means of confidence intervals for the fitted parameters.

When merging data and model the closest type curve is selected or interpolation is done between the closest type curves. The pressure match is done on the stabilised part of the pressure derivative and the time match is done on the early part affected by Well Bore Storage.

In the superposition routine of Saphir the well function is approximated with its series expansion. Through this approximation a small error is introduced when superposing multiple rates and it is desirable not to have an excessive number of flow rates. Typically we have about 150-200 different flow rates during the pressure drawdown. Thus, a simplification of the rate history is adopted in that very small rate fluctuation during the pressure drawdown are averaged to one rate in order to decrease the number of time intervals to superpose. The reduction in number of flow rates during the pressure drawdowns were in the order of 50-70% of which the majority occur at the beginning of the drawdown phase when a constant pressure drawdown is targeted.The modelling of the complete test history proved particularly valuable in cases of short tests and non-unique character in the log-log diagnostic plots.

The stepwise interpretation during a Saphir session, in the case of the KI0025F tests, is summarised in Table 5.1.

Table 5.1 Conceptual interpretation sequence of Saphir

1. Import the test data into Saphir
2. Identify the flow phase to analyse, drawdown or build-up
3. Produce a semilog multirate plot
4. Calculate the slope of of the semilog plot, will produce the pressure derivative dp'
5. Plot the dp and dp' on a traditional log-log plot
6. Identify the WBS unit slope and dp'=0.5 line on the log-log plot
7. Perform a log-log match on dp and p
8. Calculate the transmissivty according to equation 1 and 2 for the constant rate case while according to equation 3 for the multiple rate case.
9. Calculate the WBS constant (C) from the time match: $(\Delta t)_{match} \Rightarrow C \Rightarrow C_D$
10. Calculate the skin (ξ) from the correlation parameter $C_D e^{2\xi}$ for constant rate case, while for the multiple rate case the skin is derived from the intercept of the semi-log multirate plot.
11. Use the calculated parameters T, C_D and skin (ξ) to generate a pressure drawdown log-log plot and a pressure history plot.
12. Perform a reiterative non-linear regression between the calculated and measured pressure drawdown. This will also produce a confidence interval on the fitting parameters (K, T and skin).
13. Plot the drawdown and absolute pressure history to make ocular inspection of agreement between model and data.
14. If necessary redo all of the above with a different model until an acceptable agreement is obtained on both the dp and p plot.

5.7 SOURCES OF ERROR

The accuracy of the pressure transducers, the flow meters, the temperature sensor and the electrical conductivity sensor is described in chapter 4. The packer inflation influences the accuracy of hydraulic tests. The generated flow in a double packer section caused by the packers to be used in the tests in KI0025F, have been tested in the laboratory, cf. Lindström (1997). The results show that after 20 minutes of inflation, the flow is c. 0.6 ml/min. and after 40 minutes the generated flow is approximately 0.4ml/min. Consequently, the effect of packer creep induced flow is most pronounced for low-transmissive test sections.

5.8 SPECIFICS AND EVALUATION

In a granitic rock mass typically consisting of Äspö diorite, the flow of groundwater is entirely controlled by fractures and fissures. Borehole KI0025F is core drilled with a diameter of 76mm from an elevation of –448 masl in a southerly direction. The inclination is approximately 20^{o} down reaching a depth of about 194 m at an elevation of -510m masl.

Prior to the hydraulic testing a suite of borehole characterization techniques were applied, including borehole deviation surveying, borehole image processing (Stråhle 1997), borehole radar measurements (Carlsten 1997), core logging, double packer flow logging (Gentzschein 1997) and UCM acoustic flow logging (Gustafsson 1997). An overview of the results from the characterization is shown in Appendix 1, which also shows the cumulative inflow of water to the borehole during drilling. The borehole image survey (BIPS), in conjunction with the core logging resulted in a detailed description of the fractures in the test sections according to Appendix 1.

5.8.1 Section 43.0 - 44.0 m

Three attempts were made before an acceptable test was carried out, see Table 3.2. This was due to difficulties in keeping a constant pressure during the flow phase. The dP (the pressure drop during the flow phase) was increased from c. 1 MPa (specified in the QA-plan) to c. 2 MPa. Furthermore the constants in the algorithm of the regulation software were altered. After these changes the UHT 1-system worked better. However, between the second and the third test the mechanical borehole valve could not be closed. It was found to be broken. The valve was replaced before the testing continued.

The borehole pressure (Pa) outside the test section increased throughout the test (from 4120 kPa to 4185 kPa). The borehole was shut in at 13.25 while the packer inflation started at 13.45. The diagnostic plot A2 shows that there is a small flow (0.024 l/min.) during the recovery.

Test controlling parameters and test data are compiled in the table below.

Parameter	Unit	Value	Explanation
Po	kPa	4161.58	Initial formation pressure
P	kPa	variable	Section pressure
dPom	kPa	2025.19	Average of Po - P during flow phase
tp	s	3793	Flowing time
Qp	m^3/s	$1.47 \cdot 10^{-5}$	Flow rate at the end of flow phase
dtf	s	941	Recovery time
Koss	m/s	$4.05 \cdot 10^{-8}$	Steady state hydraulic conductivity

Preliminary evaluation

Using the evaluation method described in section 5.5, three geohydrological parameters, Transmissivity (T), average hydraulic conductivity (K_{ave}) and specific capacity (Q/s) have been calculated:

$$T = 1.3 \cdot 10^{-5} \ m^2/s$$
$$K_{ave} = 1.3 \cdot 10^{-5} \ m/s$$
$$Q/s = 7.1 \cdot 10^{-8} \ m^2/s$$

The evaluation technique is shown in the semi-logarithmic plot C4 of Appendix 5

Evaluation using Saphir

In the following a storage coefficient of $5.5 \cdot 10^{-6}$ is adopted on the ground laid out in the discussion chapter (Chapter 7).

The log-log plot of dP and dP' of the pressure build-up in Figure 5-1a show an early wellbore storage phase (WBS) of appreciable duration followed by a derivative interpreted as steady. Although the early part of the derivative plot is incomplete the section behaves as a damaged well which consequently is causing the high positive skin of 72 in the modelling. Throughout the test the guard zone displays a linearly increasing pressure of about 60 kPa, from 4123 to 4183 kPa over a time period of about 6000 seconds. This is not correlated to any of the pressure disturbances induced in the test section and is therefore interpreted as being a general pressure trend in the borehole. Since the pressure trend is relatively small it was not corrected for in the test, and it is believed not to impact on the results of the analysis in any conclusive way.

Modelling was performed with WBS and skin as inner boundaries and an infinite acting radial flow (IARF) reservoir model. The resulting match between data and model is excellent for the pressure recovery dP while not so good for the derivative, Figure 5-1a. However, good confidence may be attributed to the model since the modelling of the pressure vs time history (Figure 5-1b) reveals quite a good fit with the measured data. The results of the modelling and the calculated aquifer parameters are presented in Table 5-2.

ÄSPÖLABORATORIET

Figure 5-1

Hydraulic Test Fact Sheet: KI0025F, 43.0 - 44.0m

Test Information

Company: SKB	Test Name: #4, Bu2
Site: Äspö tunnel	Test Date: 1997-06-18
Borehole: KI0025F	Project: TRUE Block Scale
Section: 43.0-44.0m	Testing Company: Geosigma AB
Test Type: Pressure buildup following constant head test	Analysis by: M. Morosini (SKB)

a) Diagnostic Plot

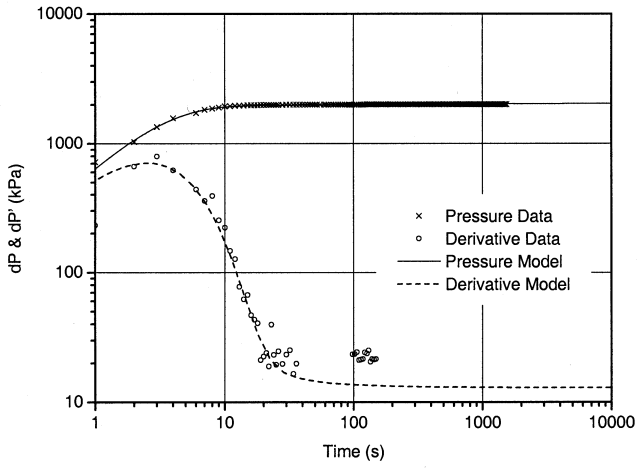

b) Pressure History and Model Plot

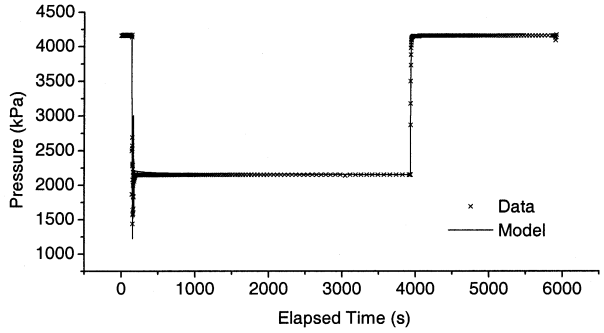

c) Flowrate History Plot

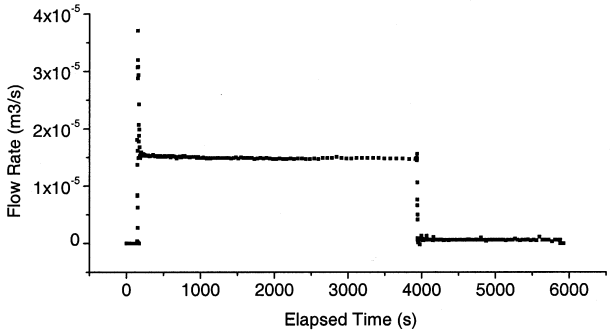

Modelling Info

Input parameters:

$Q_{shut\text{-}in}$ = 0.9 L/min
$P_{shut\text{-}in}$ = 2150 kPa
P_i = 4157kPa
$r = r_w$ = 0.038m
Storage Coefficient = $5.5*10^{-6}$
Smoothing = 0.2

Output parameters:

Well: Wellbore storage & skin
Aquifer: IARF
Boundary: None
$C = 1.9*10^{-11} m^3/Pa$
P_i = 4195kPa
Skin = 72
Transmissivity = $9.0*10^{-7}$ m^2/s

Comment

Three steeply diping fractures in Äspö diorite with a total aperture of 6mm are identified.

File: KI0025F#4Bu2.OPJ

Table 5-2 Modelling result for section 43.0 – 44.0m.

S (fixed) Storativity [-]	**Skin** [-]	**T** Transmissivity [m^2/s]	**Pi** Measured/Modelled [kPa]	**Flow regime**	**Outer boundary**
$5.5 \cdot 10^{-6}$	72	$9.0 \cdot 10^{-7}$	4157/4195	IARF	None detected

5.8.2 Section 87.0 m - 88.0 m

During the first test in this interval the mechanical test valve was leaking. It was then decided to keep the test valve completely open and regulate the flow using the ball valve at the end of the pipe string outside the borehole. This increased the WBS volume from 4.5 L to 40 L.

As was the case with the previous test, the borehole pressure (Pa) increased throughout the test (from 4190 kPa to 4215 kPa). The diagnostic plot A2 also shows that there is a small flow (0.036 l/min) during the recovery.

Test controlling parameters and test data are compiled in the table below.

Parameter	Unit	Value	Explanation
Po	kPa	4224.59	Initial formation pressure
P	kPa	variable	Section pressure
dPom	kPa	2013.42	Average of Po - P during flow phase
tp	s	3338	Flowing time
Qp	m^3/s	$5.7 \cdot 10^{-6}$	Flow rate at the end of flow phase
dtf	s	1799	Recovery time
Koss	m/s	$1.6 \cdot 10^{-8}$	Steady state hydraulic conductivity

After the pressure build-up test a detailed qualitative localisation of the flowing section (fracture) was performed according to the procedure described in section 5.2. The resulting flow is tabulated below.

Section (m)	dP (kPa)	Flow (l/min)
87.0 – 88.0	-2000	0.39
87.5 – 88.5	-2000	0.47
87.75 – 88.75	-2000	0.04

Preliminary evaluation

Using the evaluation method described in section 5.5, three geohydrological parameters, Transmissivity (T), average hydraulic conductivity (K_{ave}) and specific capacity (Q/s) have been calculated:

$$T = 5.1 \cdot 10^{-7} \ m^2/s$$
$$K_{ave} = 5.1 \cdot 10^{-7} \ m/s$$
$$Q/s = 2.8 \cdot 10^{-8} \ m^2/s$$

The evaluation technique is shown in the semi-logarithmic plot C4 of Appendix 6.

Evaluation using Saphir

The guard zone pressure displays a continuously increasing pressure of about 30 kPa during the test sequence. It is presumed that this trend is also present in the test section but was not corrected for since it is relatively small and is not apparent in the transients of the test. Clear response to packer inflation and deflation are evident but not to the flow and shut-in events.

The constant pressure phase reached a flow of 0.34 L/min before shut in. The ensuing pressure build-up plot show the initial WBS slope and a damaged well character in the derivative followed by what appears to be an almost horizontal derivative , Figure 5-2a. Hence, the model that best fits the data is a WBS and skin inner boundary followed to IARF behaviour. The fit is quite good for the dP while not as good in the dP'. Again, the confidence in the adopted model is reinforced by the modelling with the complete test history, Figure 5-2b. The results from the modelling, including the calculated aquifer parameters are summarised in Table 5-3.

Table 5-3 Modelling results for section 87.0 – 88.0m.

S (fixed) Storativity [-]	**Skin** [-]	**T** Transmissivity [m^2/s]	**Pi** Measured/Modelled [kPa]	**Flow regime**	**Outer boundary**
$5.5 \cdot 10^{-6}$	33	$1.8 \cdot 10^{-7}$	4194/4284	IARF	None detected

5.8.3 Section 165.3 m - 166.3 m

The first test in this section failed since the mechanical test valve did not open properly. The second attempt was more successful. The diagnostic plot A3 shows a correlation between a pressure decrease in the borehole outside the test section and the opening/closing of the test valve.

ÄSPÖLABORATORIET

Figure 5-2

Hydraulic Test Fact Sheet: KI0025F, 87.0-88.0m

Test Information

Company: SKB	Test Name: #6, Bu2
Site: Äspö tunnel	Test Date: 1997-06-18
Borehole: KI0025F	Project: TRUE Block Scale
Section: 87.0-88.0m	Testing Company: Geosigma AB
Test Type: Pressure buildup following constant head test	Analysis by: M. Morosini (SKB)

a) Diagnostic Plot

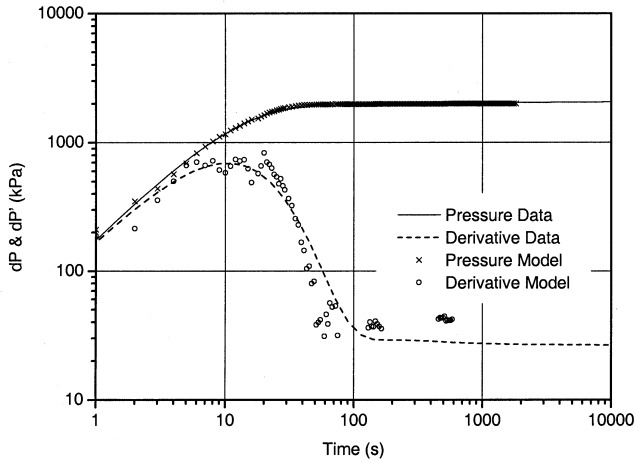

b) Pressure History and Model Plot

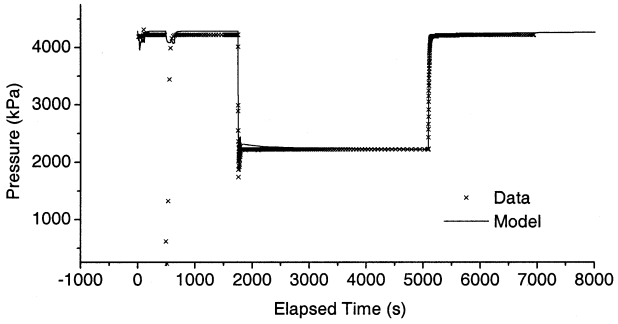

c) Flowrate History Plot

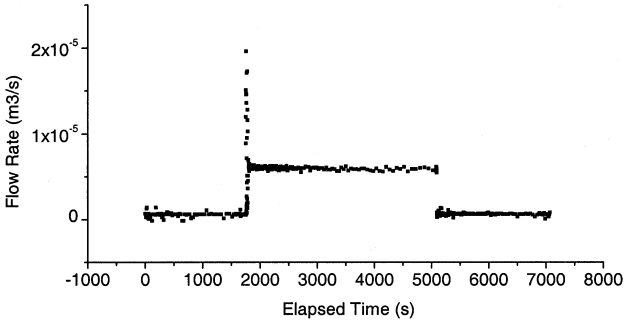

Modelling Info

Input parameters:

$Q_{shut\text{-}in}$ = 0.39 L/min
$P_{shut\text{-}in}$ = 2213 kPa
P_i = 4194Pa
$r = r_w$ = 0.0038m
Storage Coefficient = $5.5*10^{-6}$
Smoothing = 0.1

Output parameters:

Well: Wellbore storage & skin
Aquifer: IARF
Boundary: None
$C = 3.2*10^{-11} m^3/Pa$
P_i = 4284 kPa
Skin = 33
Transmissivity = $1.8*10^{-7}$ m^2/s

Comment

Three fractures with cavities were identified in Äspö diorite. They have a total aperture of 5mm.

File: KI0025F#6Bu2.OPJ

The controlling test parameters and test data from section 165.3-166.3 m are compiled in the table below.

Parameter	Unit	Value	Explanation
Po	kPa	4239.00	Initial formation pressure
P	kPa	variable	Section pressure
dPom	kPa	1997.40	Average of Po - P during flow phase
tp	s	2684	Flowing time
Qp	m^3/s	$2.27 \cdot 10^{-4}$	Flow rate at the end of flow phase
dtf	s	1338	Recovery time
Koss	m/s	$6.35 \cdot 10^{-7}$	Steady state hydraulic conductivity

Using the evaluation method described in section 5.5, three geohydrological parameters, Transmissivity (T), average hydraulic conductivity (K_{ave}) and specific capacity (Q/s) have been calculated:

$$T = 1.2 \cdot 10^{-5}\ m^2/s$$
$$K_{ave} = 1.2 \cdot 10^{-5}\ m/s$$
$$Q/s = 1.1 \cdot 10^{-6}\ m^2/s$$

The evaluation technique is shown in the semi-logarithmic plot C4 of Appendix 7

Evaluation using Saphir

Diagnostic log-log plots of dP and dP' vs time show a non-existent WBS period followed by a stable almost horizontal derivative interpreted as representing IARF, Figure 5-3a . The shape of the derivative does not suggest the well to be damaged although the skin losses are quite high. Similarly as in the case of the previous section the model best fitting the data is one with WBS and skin as inner boundaries and IARF for the reservoir model.

Both the match with dP in the log-log plot and the complete test history, Figure 5-3b show very good agreement with the measured data, while it is not as good for the log-log derivative. The guard zone responds to the flow events in the test section. This is interpreted as a manifestation of a hydraulic connection through the fractures between the test and the guard zone. There is however no indication that this would produce a boundary in the diagnostic log-log plot. The results from the modelling and the calculated aquifer parameters are shown in Table 5-4.

Table 5-4 Modelling results for section 165.3 – 166.3m.

S (fixed) Storativity [-][-]	**Skin** [m^2/s]	**T** Transmissivity [kPa]	**Pi** Measured/Modelled	**Flow regime**	**Outer boundary**
$5.5 \cdot 10^{-6}$	25	$5.7 \cdot 10^{-6}$	4238/4266	IARF	None detected

Figure 5-3

Hydraulic Test Fact Sheet: KI0025F, 165.3-166.3m

Test Information

Company: SKB	Test Name: #9, Bu2
Site: Äspö tunnel	Test Date: 1997-06-19
Borehole: KI0025F	Project: TRUE Block Scale
Section: 165.3-166.3m	Testing Company: Geosigma AB
Test Type: Pressure buildup following constant head test	Analysis by: M. Morosini (SKB)

a) Diagnostic Plot

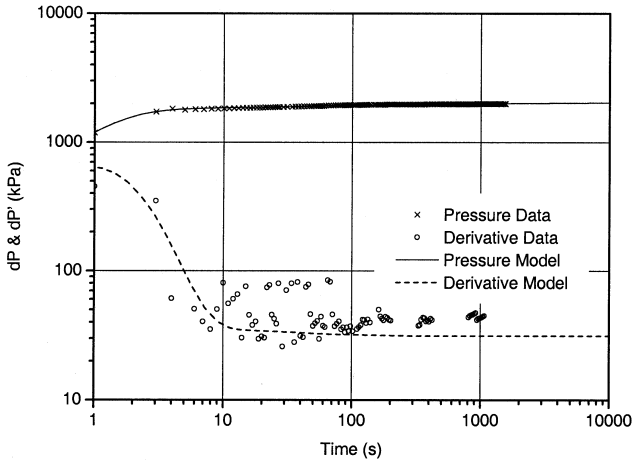

b) Pressure History and Model Plot

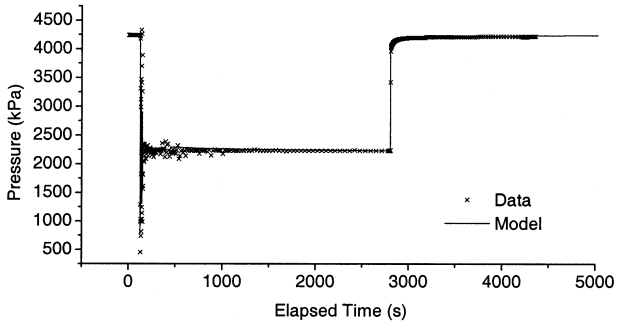

c) Flowrate History Plot

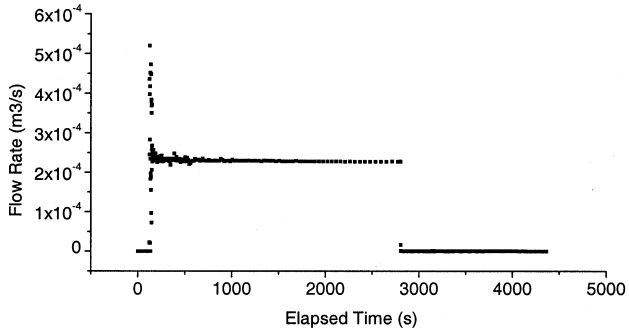

Modelling Info

Input parameters:

$Q_{shut\text{-}in}$ = 13.5 L/min
$P_{shut\text{-}in}$ = 2231 kPa
P_i = 4238kPa
$r = r_w$ = 0.038m
Storage Coefficient = $5.5*10^{-6}$
Smoothing = 0.12

Output parameters:

Well: Wellbore storage & skin
Aquifer: IARF
Boundary: None
$C = 1.1*10^{-10} m^3/Pa$
P_i = 4266kPa
Skin = 25
Transmissivity = $5.7*10^{-6}$ m^2/s

Comment

One open fracture with an aperture of 5mm was identified. Additionly, there are eight fractures with cavities with a total aperture of 23mm.

File: KI0025F#9Bu2.OPJ

5.8.4 Section 166.3 m - 167.3 m

In this interval it was difficult to establish a constant pressure and a stable flow. The differential pressure (dP) was changed between -2 MPa and -1 MPa and eventually fixed at -0.7 MPa before an acceptable small variation in flow and pressure was achieved. NB. the period for stabilising the pressure was long (c. 130 s). Test controlling parameters and test data are compiled in the table below.

Parameter	Unit	Value	Explanation
Po	kPa	4232.99	Initial formation pressure
P	kPa	variable	Section pressure
dPom	kPa	709.46	Average of Po - P during flow phase
tp	s	1823	Flowing time
Qp	m^3/s	$8.61 \cdot 10^{-5}$	Flow rate at the end of flow phase
dtf	s	1354	Recovery time
Koss	m/s	$6.79 \cdot 10^{-7}$	Steady state hydraulic conductivity

Using the evaluation method described in section 5.5, three geohydrological parameters, Transmissivity (T), average hydraulic conductivity (K_{ave}) and specific capacity (Q/s) have been calculated:

$T = 8.8 \cdot 10^{-6}$ m^2/s
$K_{ave} = 8.8 \cdot 10^{-6}$ m/s
$Q/s = 1.2 \cdot 10^{-6}$ m^2/s

The evaluation technique is shown in the semi-logarithmic plot C4 of Appendix 8.

Evaluation using Saphir

The diagnostic plot (Figure 5-4a) does not show any characteristics or a well-defined shape in the dP or dP'. Different models were tested and in conjunction with the matching of the complete test sequence (i.e. drawdown and build-up) a good fit was obtained with the WBS/skin inner boundary and IARF reservoir model (Figure 5-4b). Note that no WBS is evident in the measured data. The guard zone responds to the flow events in the test section, which is interpreted as being a result of hydraulic connection between the test section and the guard zone, through the fracture system. Again, this appears not to have any consequences for the test interpretation. The results of the modelling, including the calculated aquifer parameters are presented in Table 5-5.

Table 5-5 Modelling results for section 166.3 – 167.3m.

S (fixed) Storativity [-]	**Skin** [-]	**T** Transmissivity [m^2/s]	**Pi** Measured/Modelled [kPa]	**Flow regime**	**Outer boundary**
$5.5 \cdot 10^{-6}$	20	$5.0 \cdot 10^{-6}$	4232/4258	IARF	None detected

ÄSPÖLABORATORIET

Figure 5-4

Hydraulic Test Fact Sheet: KI0025F, 166.3-167.3m

Test Information

Company: SKB	Test Name: #12, Bu2
Site: Äspö tunnel	Test Date: 1997-06-19
Borehole: KI0025F	Project: TRUE Block Scale
Section: 166.3-167.3m	Testing Company: Geosigma AB
Test Type: Pressure buildup following constant head test	Analysis by: M. Morosini (SKB)

a) Diagnostic Plot

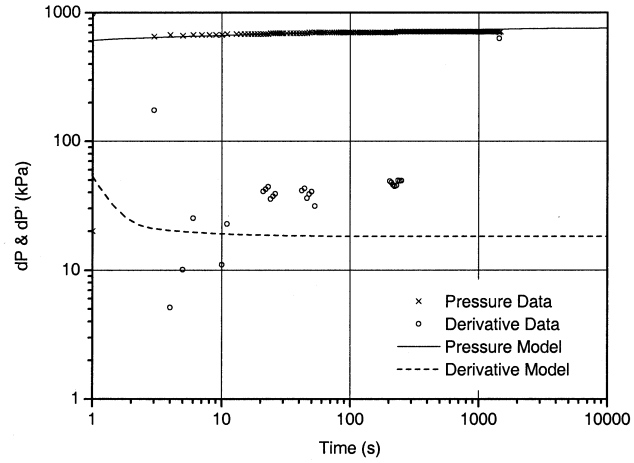

b) Pressure History and Model Plot

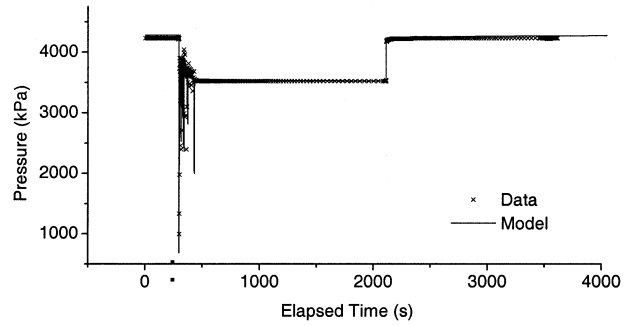

c) Flowrate History Plot

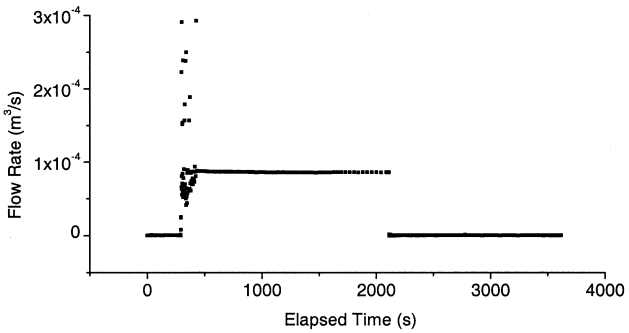

Modelling Info

Input parameters:

$Q_{shut\text{-}in}$ = 5.1 L/min
$P_{shut\text{-}in}$ = 3522 kPa
P_i = 4233kPa
$r = r_w$ = 0.038m
Storage Coefficient = $5.5*10^{-6}$
Smoothing = 0.35

Output parameters:

Well: Wellbore storage & skin
Aquifer: IARF
Boundary: None
$C = 3*10^{-12} m^3/Pa$
P_i = 4258kPa
Skin = 20
Transmissivity = $5.0*10^{-6}$ m^2/s

Comment

One open fracture with an aperture of 6mm and two fracture with cavities with apertures of 1 and 2mm respectively. The lithology is Äspö diorite

File: KI0025F#12Bu2.OPJ

5.8.5 Section 167.3 m - 168.3 m

After the test the pump of the hydraulic unit broke down, but the test was performed satisfactorily. Initially the flow decreased steadily. After c. 100 seconds it stabilized at approximately c. 2.3 10^{-5} m^3/s. This flow pattern deviates from the flow of previous tests. In the earlier tests the flow varied around a level that eventually became the stable flow.

Also in this test there is a correlation between the pressure drop of the test section and the pressure decrease in the borehole interval outside the tested interval.
Test controlling parameters and test data are compiled in the table below.

Parameter	Unit	Value	Explanation
Po	kPa	4250.35	Initial formation pressure
P	kPa	variable	Section pressure
dPom	kPa	1791.89	Average of Po - P during flow phase
tp	s	1945	Flowing time
Qp	m^3/s	$2.30 \cdot 10^{-5}$	Flow rate at the end of flow phase
dtf	s	2522	Recovery time
Koss	m/s	$7.17 \cdot 10^{-8}$	Steady state hydraulic conductivity

Preliminary evaluation

Using the evaluation method described in section 5.5, three geohydrological parameters, Transmissivity (T), average hydraulic conductivity (K_{ave}) and specific capacity (Q/s) have been calculated:

$$T = 8.3 \cdot 10^{-6}\ m^2/s$$
$$K_{ave} = 8.3 \cdot 10^{-6}\ m/s$$
$$Q/s = 1.3 \cdot 10^{-7}\ m^2/s$$

The evaluation technique is shown in the semi-logarithmic plot C4 of Appendix 9.

Evaluation using Saphir

The most striking characteristic in the diagnostic log-log plot for this test (Figure 5-5a) is the short duration of the horizontal part of the derivative. Virtually all data are from the WBS influenced period and very few from the phase characterising the reservoir. Nevertheless an attempt to model the data was performed where the only option for a model which could be supported by the data is the WBS/skin inner boundary and an IARF reservoir model. The resulting model to the dP is not fitting too well to the data, except for the later part. However, the suitability of the model is supported by the match with the complete test sequence (drawdown and build-up) in Cartesian coordinates, Figure 5-5b. The calculated aquifer parameters are summarized in Table 5-6. The difficulties in matching the model to the data may also suggest that the adopted model of

radial homogenous flow in a granular porosity medium may not be adequate here. Trials with time shifting in order to straighten the initial derivative resulted in a worse match between model and experimental data for the whole test sequence.

Table 5-6 Modelling results for section 167.3 – 168.3m.

S (fixed) Storativity [-]	**Skin** [-]	**T** Transmissivity [m^2/s]	**Pi** Measured/Modelled [kPa]	**Flow regime**	**Outer boundary**
$5.5 \cdot 10^{-6}$	39	$8.10 \cdot 10^{-7}$	4249/4279	IARF	None detected

5.8.6 Section 186.0 m - 193.8 m

Since the hydraulic power unit was out of order (see section 5.8.5) the single packer configuration was manually lowered to the test position which entailed a borehole pressure equal to or close to the atmospheric pressure.

The test was carried out according to plan without problems. The stabilization of the flow is similar to the flow pattern of the previous test section, see section 5.8.5.

Test controlling parameters and test data are compiled in the table below.

Parameter	Unit	Value	Explanation
Po	kPa	4183.49	Initial formation pressure
P	kPa	variable	Section pressure
dPom	kPa	1972.08	Average of Po - P during flow phase
tp	s	2000	Flowing time
Qp	m^3/s	$4.54 \cdot 10^{-4}$	Flow rate at the end of flow phase
Pp	kPa	2175.7	Pressure at the end of flow phase
dtf	s	7505	Recovery time
Koss	m/s	$2.60 \cdot 10^{-7}$	Steady state hydraulic conductivity

Preliminary evaluation

Using the evaluation method described in section 5.5, three geohydrological parameters, Transmissivity (T), average hydraulic conductivity (K_{ave}) and specific capacity (Q/s) have been calculated:

$T = 5.7 \cdot 10^{-6}$ m^2/s
$K_{ave} = 7.3 \cdot 10^{-7}$ m/s
$Q/s = 2.3 \cdot 10^{-6}$ m^2/s

The evaluation technique is shown in the semi-logarithmic plot C4 of Appendix 10.

Figure 5-5

Hydraulic Test Fact Sheet: KI0025F, 167.3-168.3m

Test Information

Company: SKB	Test Name: #13, Bu2
Site: Äspö tunnel	Test Date: 1997-06-23
Borehole: KI0025F	Project: TRUE Block Scale
Section: 167.3-168.3m	Testing Company: Geosigma AB
Test Type: Pressure buildup following constant head test	Analysis by: M. Morosini (SKB)

a) Diagnostic Plot

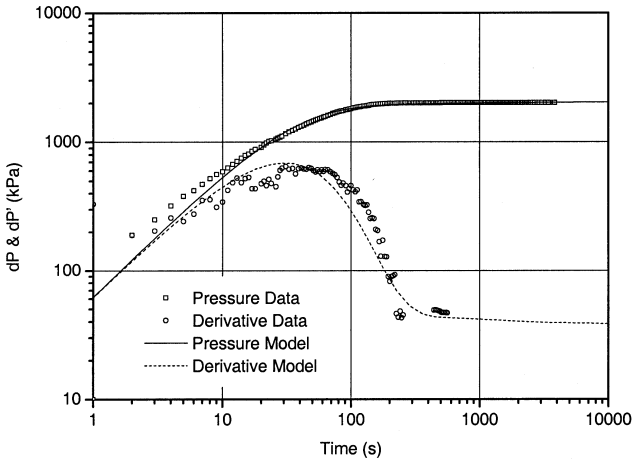

b) Pressure History and Model Plot

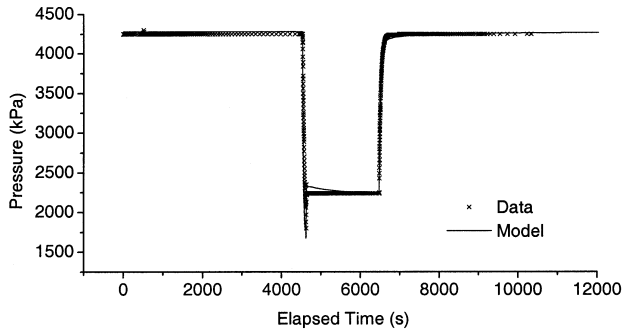

c) Flowrate History Plot

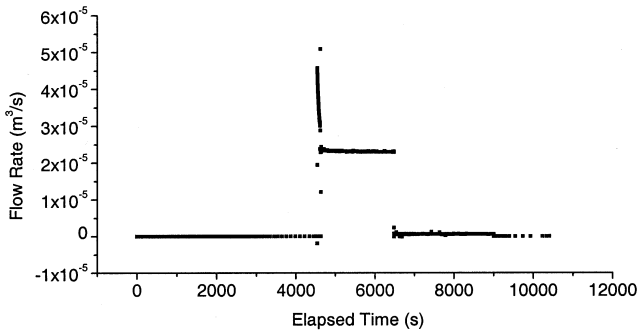

Modelling Info

Input parameters:

$Q_{shut\text{-}in}$ = 1.38 L/min
$P_{shut\text{-}in}$ = 2242 kPa
P_i = 4249kPa
$r = r_w$ = 0.038m
Storage Coefficient = $5.5*10^{-6}$
Smoothing = 0.2

Output parameters:

Well: Wellbore storage & skin
Aquifer: IARF
Boundary: None
$C = 3.5*10^{-10} m^3/Pa$
P_i = 4279 kPa
Skin = 39
Transmissivity = $8.1*10^{-7}$ m^2/s

Comment

Four fractures in Äspö diorite were identified. One open with 1mm aperture and three with cavities with a total aperture of 5mm.

File: KI0025F#13Bu2.OPJ

Evaluation using Saphir

The UCM flow logging (Gustafsson 1997) shows a main inflow of about 64 L/min which is interpreted as a fracture towards the bottom of the hole at about 193.5m and an inflow of 10 L/min (evenly distributed?) in the remainder of the section. The flow from the whole section is 72 L/min.

A history plot with pressure and flow data is shown in Figure 5-6. This is the data set from which the constant pressure phase and pressure build-up phase are extracted for interpretation.

It was noted that the guard zone responded to the pressure disturbances slightly. During the flowing phase the section above (guard zone) experienced a dP of 60 kPa for an induced average dP in the test section of 1972 kPa. The hydraulic connection between the two sections is not perceived to impact on the calculation of aquifer parameters due to the large differences between these two dP's.

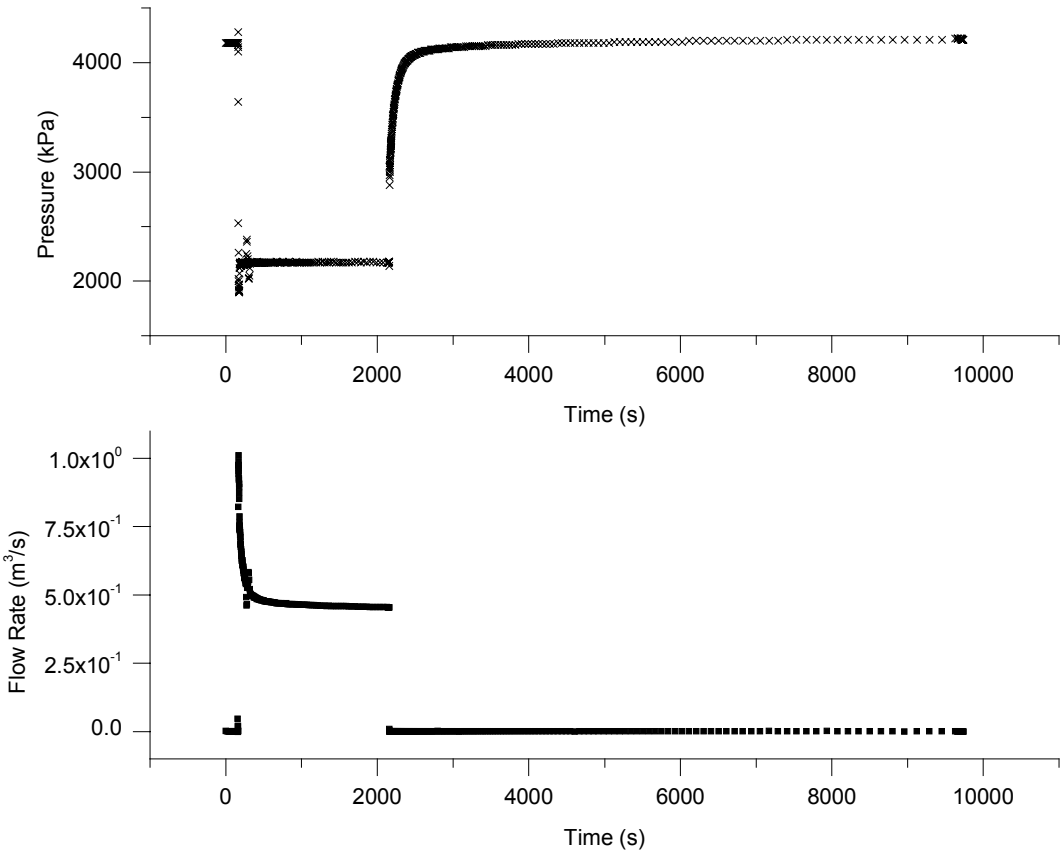

Figure 5-6 *History plot of pressure and flow for section 186.0 - 193.8m in KI0025F*

ÄSPÖLABORATORIET

Figure 5-7

Hydraulic Test Fact Sheet: KI0025F, 186.0-193.8m

Test Information

Company: SKB	Test Name: #17, Bu2
Site: Äspö tunnel	Test Date: 1997-06-24
Borehole: KI0025F	Project: TRUE Block Scale
Section: 186.0-193.8m	Testing Company: Geosigma AB
Test Type: Pressure buildup following constant head test	Analysis by: M. Morosini (SKB)

a) Diagnostic Plot

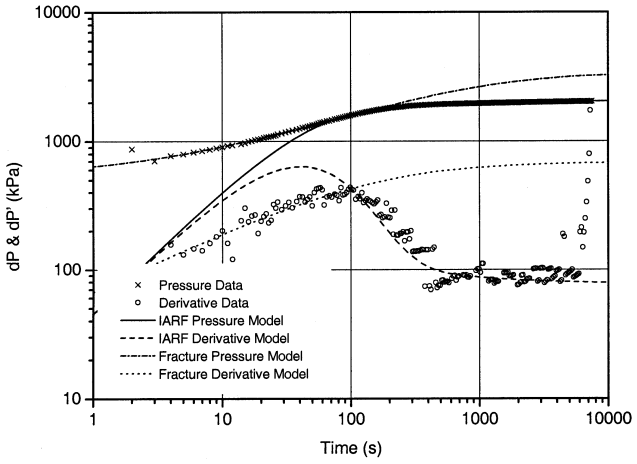

b) Pressure History and Model Plot

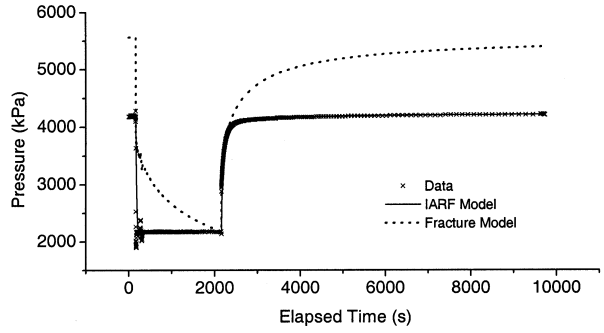

c) Flowrate History Plot

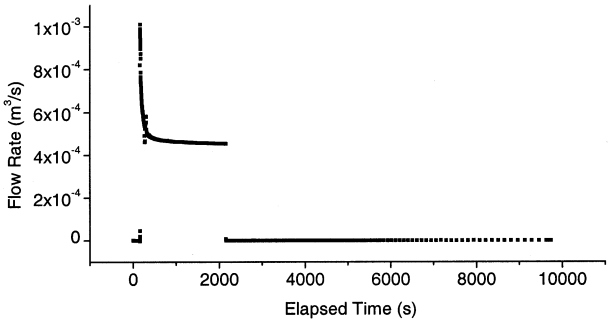

Modelling Info

Input parameters:

$Q_{shut\text{-}in}$ = 27 L/min
$P_{shut\text{-}in}$ = 2176 kPa
P_i = 4183kPa
$r = r_w$ = 0.038m
Storage Coefficient = $5.5*10^{-6}$
Smoothing = 0.05

Output parameters:

Well: Wellbore storage & skin
Aquifer: IARF
Boundary: None
$C = 3.9*10^{-9} m^3/Pa$
P_i = 4234kPa
Skin = 5.9
Transmissivity = $4.56*10^{-6}$ m^2/s

Well: Finite K Fracture
Aquifer: IARF
Boundary: None
$C = 7.1*10^{-13} m^3/Pa$
P_i = 5563kPa
Skin = 0.4
Transmissivity = $5.13*10^{-7}$ m^2/s

Comment

This is a heavily fractured section in fine grained granite. Particularly toward the bottom where clay material caused very slow drilling progress. It also produced major inflow of about 62 L/min. Many fractures were found, almost all with cavities.

File: KI0025F#12Bu2New.OPJ

The main tool for interpreting the pressure build-up phase is the plot of the logarithmic pressure drawdown (dP) and pressure drawdown derivative (dP') versus the logarithm of time, Figure 5-7a and 5-8. This test displays the most interesting pressure transient behaviour. From the log-log plot some features are detected which are characteristic for certain flow regimes (boundary conditions).

a) the wellbore storage (WBS) line on the dP plot is missing
b) an initial hump on the derivative plot
c) large separation between dP and dP' in log-log representation, a factor of 4
d) straight line with 0.25 slope of dP during 10 and 100s
e) horizontal stabilisation of the pressure derivative

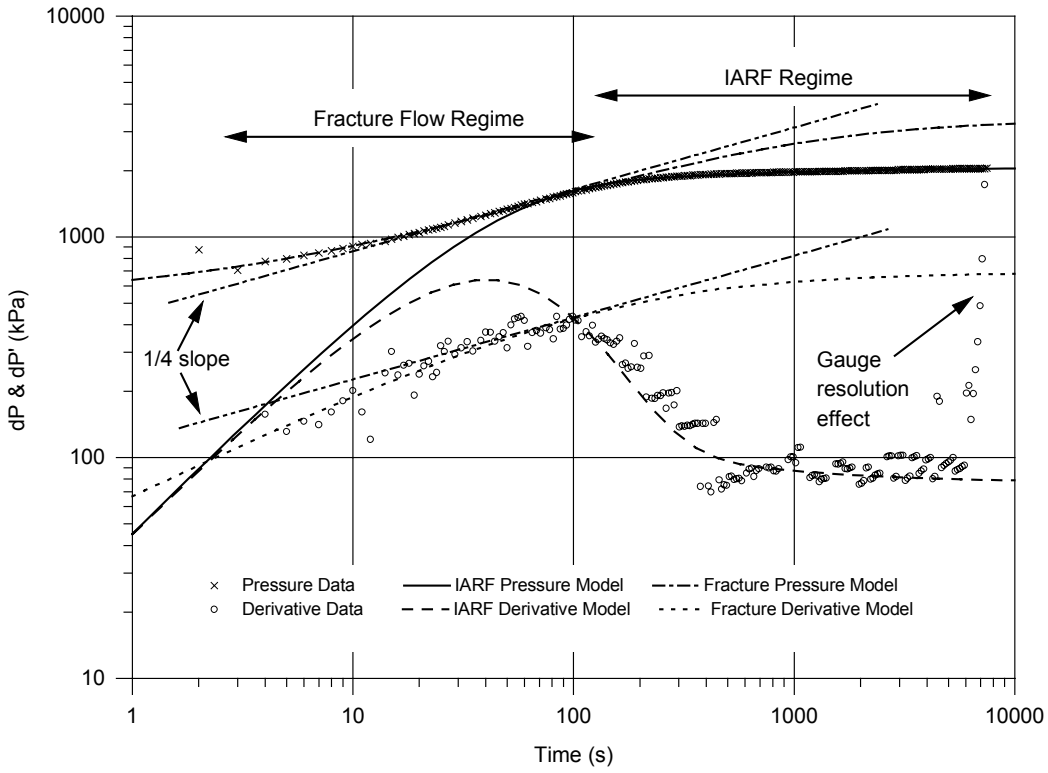

Figure 5.8 *Pressure and pressure derivative for the buildup phase in section 186.0 – 193.8m of borehole KI0025F.*

The above mentioned characteristic features may have a number of different causes which are discriminated based on a collective judgement using other information about the test section; geology, drilling etc. Different boundary conditions were modelled to the data. During early time when the flow is controlled by the wellbore and its neighbourhood the WBS/skin and the fracture boundary were modelled. At intermediate time when the aquifer is dominating the flow and pressure response, a homogeneous IARF regime was modelled. While at late time an infinite aquifer and a no flow linear boundary were modelled.

The best match between model and data was obtained when the early part was modelled with a finite conductivity fracture and the intermediate and late time region with an IARF model.

Various degrees of smoothing to produce the pressure derivative were tested (L= 0.1-2) with the result that only the phase after the hump in the derivative showed significantly different shapes with bearing on the flow concept and on the calculated parameters.

The very late time steep derivative is a smoothing artefact and does not represent a physical entity. The composite (fracture and IARF) match with the data is shown in Figure 5-8. The finite conductivity fracture is the only model which could reproduce the large dP and dP' separation in the log-log plot. In support of this hypotheis the following arguments should also be mentioned:

- the UCM flow logging result showing one major fracture contributing 86% of the inflow to the test section
- the 0.25 slope of the dP which is characteristic for a finite conductivity vertical fracture flow model
- the approximate factor 4 separation between dP and dP' during this period being characteristic for a finite conductivity vertical fracture

The pressure behaviour during the intermediate time region when the pressure derivative is declining and eventually stabilises appears to be an unambiguous indication of the transition from fracture storage flow to matrix supported flow.

Hence, conceptually, the preferred model as shown in Figure 5-4 is a flow regime where water is released according the following;

WBS (undetected) $\Rightarrow$ "single" fracture flow $\Rightarrow$ IARF

Results of the modelling including calculated aquifer parameters are presented in Table 5-7.

Table 5-7 Modelling results for section 186.0 – 193.8m.

S (fixed) Storativity [-]	**Skin** [-]	**T** Transmissivity [m^2/s]	**Pi** Measured/Modelled [kPa]	**Flow regime**	**Outer boundary**
$5.5 \cdot 10^{-6}$	0.3/11	$0.5/4.6 \cdot 10^{-6}$	4183/4234	Fracture/IARF	None detected

6 RESULTS

Important test data from the pressure build-up tests in KI0025F are summarised in Table 6-1

Table 6-1 Test data from pressure build-up tests in borehole KI0025F

Test section (m)	Po (kPa)	dPom (kPa)	Flow time (s)	Qp (m^3/s)	Recovery time (s)
43.0 - 44.0	4161.58	2025.19	3793	$1.47 \cdot 10^{-5}$	1941
87.0 - 88.0	4224.59	2013.31	3342	$5.71 \cdot 10^{-6}$	1795
165.3 - 166.3	4239.00	1997.40	2684	$2.27 \cdot 10^{-4}$	1338
166.3 - 167.3	4232.99	709.46	1823	$8.61 \cdot 10^{-5}$	1354
167.3 - 168.3	4250.35	1791.89	1945	$2.30 \cdot 10^{-5}$	2522
186.0 - 193.8	4183.49	1972.08	2000	$4.54 \cdot 10^{-4}$	7505

Po = Initial formation pressure. dPom = Average of Po - P during flow phase (P = Section pressure). Qp = Flow rate at the end of flow phase

The preliminary evaluation of the hydraulic parameters is described in section 5.5. Table 6-2 summarises the results from the six pressure build-up tests in KI0025F.

Table 6-2 Preliminary evaluated hydraulic parameters from pressure build-up tests in borehole KI0025F

Test section (m)	T (m^2/s)	$\bar{K}$ (m/s)	Q/s (m^2/s)	K_{ss} (m/s)
43.0 - 44.0	$1.3 \cdot 10^{-5}$	$1.3 \cdot 10^{-5}$	$7.1 \cdot 10^{-8}$	$4.1 \cdot 10^{-8}$
87.0 - 88.0	$5.1 \cdot 10^{-7}$	$5.1 \cdot 10^{-7}$	$2.8 \cdot 10^{-8}$	$1.6 \cdot 10^{-8}$
165.3 - 166.3	$1.2 \cdot 10^{-5}$	$1.2 \cdot 10^{-5}$	$1.1 \cdot 10^{-6}$	$6.4 \cdot 10^{-7}$
166.3 - 167.3	$8.8 \cdot 10^{-6}$	$8.8 \cdot 10^{-6}$	$1.2 \cdot 10^{-6}$	$6.8 \cdot 10^{-7}$
167.3 - 168.3	$8.3 \cdot 10^{-6}$	$8.3 \cdot 10^{-6}$	$1.3 \cdot 10^{-7}$	$7.2 \cdot 10^{-8}$
186.0 - 193.8	$5.7 \cdot 10^{-6}$	$7.3 \cdot 10^{-7}$	$2.3 \cdot 10^{-6}$	$2.6 \cdot 10^{-7}$

T = The transmissivity calculated with Jacobs semi-logarithmic approximation of Theis ´ well function.
$\bar{K}$ = T/L , (L= test interval length). Average hydraulic conductivity.
Q/s = The specific capacity, see section 5.5.
K_{ss} = Steady state hydraulic conductivity calculated by the UHT 1- system

The parameters calculated from *Saphir-analysis* of the different tests are compiled in Table 6-3 below. In all cases the established flow model, after the effects of wellbore, is that of an infinite acting radial flow (IARF) aquifer without encountering outer boundaries. From the log-log plots it is seen that some tests display a somewhat short duration of the derivative curve after the effects of wellbore. Confidence in the proposed models is greatly enhanced when simulating the complete test sequence including pressure drawdown and pressure recovery. These results are presented in the Cartesian plots.

For analysis of the build-up phase the initial pressure (P_i) is adjusted in order to produce the actual shut-in pressure. After the initial simulation it is optional whether to fix P_i at a certain value or not. It was chosen not to fix the P_i during the simulation of the complete test sequence since this produced a better match of the shut-in period that was analyzed, as well as for the complete duration of the test. The initial pressure also depends on the flow rate history, other disturbances such as interference from other wells and the model chosen. The resulting discrepancy between calculated and measured P_i is between 0.6% and 2%. The actual initial pressure is shown in Table 6-3.

Table 6-3 Results from evaluation using Saphir, all hydraulic tests conducted in KI0025F.

PARAMETERS	**TESTED SECTION IN KI0025F (m)**					
	43–44	**87–88**	**165.3–166.3**	**166.3-167.3**	**167.3-168.3**	**186.0-193.8**
Fixed input parameters						
S (-) Storage Coefficient	$5.5\cdot10^{-6}$	$5.5\cdot10^{-6}$	$5.5\cdot10^{-6}$	$5.5\cdot10^{-6}$	$5.5\cdot10^{-6}$	$5.5\cdot10^{-6}$
H (m)Section Length	1	1	1	1	1	7.8
r_w (m) Section Radius	0.0038	0.0038	0.0038	0.0038	0.0038	0.0038
Derivative smoothing	0.2	0.1	0.12	0.35	0.2	0.05
Duration of drawdown / build-up (s)	3793 / 1941	3342 / 1795	2684 / 1338	1823 / 1354	1945 / 2522	2000 / 7505
Calculated output parameters						
Flow regime(s)	IARF	IARF	IARF	IARF	IARF	Fract /IARF
C (m^3/Pa) Wellbore Storage	$1.9\cdot10^{-11}$	$3.2\cdot10^{-11}$	$1.1\cdot10^{-10}$	$3\cdot10^{-12}$	$3.5*10^{-10}$	$7.1\cdot10^{-13}$ / $3.9\cdot10^{-9}$
Skin (-)	72	33	25	20	39	0.4 / 6
T (m/s^2) Transmissivity	$9.0\cdot10^{-7}$	$1.8\cdot10^{-7}$	$5.7\cdot10^{-6}$	$5.0\cdot10^{-6}$	$8.1\cdot10^{-7}$	$5\cdot10^{-7}$ / $4.6\cdot10^{-6}$
X_f (m) fract.½ length	n/a	n/a	n/a	n/a	n/a	6
P_i (kPa) measure/model	4157 / 4195	4194 / 4284	4238 / 4266	4232 / 4258	4249 / 4279	4183 / 42347 IARF simul.

7 Discussion

During the tests it is convenient to calculate a preliminary transmissivity by simple and quick methods. Here, we employed the Moye's steady state method and Jacobs transient semilog method with Agarwall time. In the following the discussion concerns the difference in calculated aquifer parameters between different methods, on how the storage coefficient was derived at, and the skinfactor. Table 7.1 compares test parameters obtained from the preliminary evaluation and parameters from the Saphir-evaluation.

Table 7.1 Preliminary evaluated parameters and Saphir-evaluated parameters from pressure build-up tests in borehole KI0025F

Test section (m)	T_{Jacob} (m^2/s)	T_{Moye} (m^2/s)	T_{Saphir} (m^2/s)
43.0 - 44.0	$1.3 \cdot 10^{-5}$	$4.1 \cdot 10^{-8}$	$9.0 \cdot 10^{-7}$
87.0 - 88.0	$5.1 \cdot 10^{-7}$	$1.6 \cdot 10^{-8}$	$1.8 \cdot 10^{-7}$
165.3 - 166.3	$1.2 \cdot 10^{-5}$	$6.4 \cdot 10^{-7}$	$5.7 \cdot 10^{-6}$
166.3 - 167.3	$8.8 \cdot 10^{-6}$	$6.8 \cdot 10^{-7}$	$5.0 \cdot 10^{-6}$
167.3 - 168.3	$8.3 \cdot 10^{-6}$	$7.2 \cdot 10^{-8}$	$8.1 \cdot 10^{-7}$
186.0 - 193.8	$5.7 \cdot 10^{-6}$	$2.0 \cdot 10^{-6}$	$5 \cdot 10^{-7}$ / $4.6 \cdot 10^{-6}$

7.1 Moye vs Saphir

A comparison of obtained transmissivities from Moye's steady state method and Saphir is shown in Figure 7-1 as a function of the skin factor that was obtained from the Saphir analysis. This figure reveals that

- transmissivities obtained from Saphir are always higher than those based on the Moye method, two to twenty times higher.
- there is a positive ratio of correlation between the difference in T-values and the skin factor. The higher the skin the greater is the difference in T-values between the two methods.

Such a correlation is expected, it is attributed to the skin, since Moye's method does not account for skin, while Saphir does. Furthermore, pseudo-stedy state is reached during the tests, as required by Moye's method, and no outer boundaries are encountered, the IARF regime has been reached during the test time interval where the parameters are calculated. Non-compliance with steady-state and outer boundary conditions might otherwise have scattered the points much more.

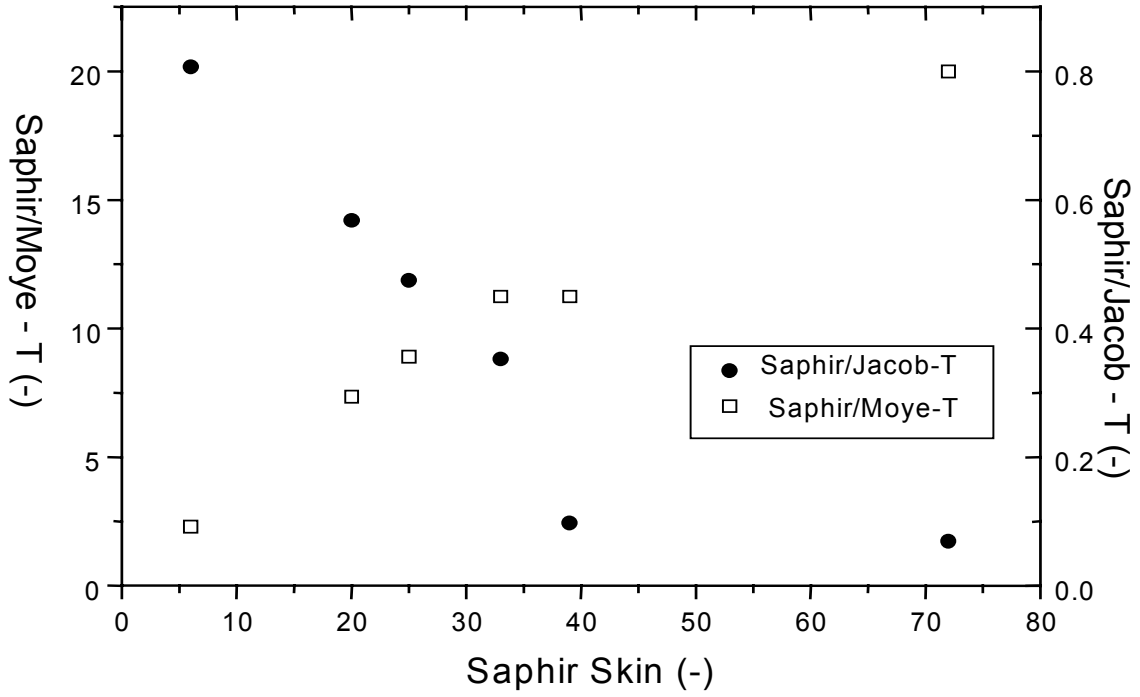

Figure 7-1 *Ratio between calculated transmissivities with methods of Moye, Jacob and Saphir as a function of the skinfactor calculated with Saphir.*

An explanation of the difference between Moye and Saphir transmissivities can possibly be that Saphir- evaluation is mainly based on the theories of transient radial flow behaviour in a porous medium (section 5.6), but that predominantly (pseudo) spherical flow occurred during the tests. Most of the data curves of the log-log plots from the recovery period were rather flat, indicating higher-dimension flow**.** It is possible that if an evaluation model taking higher dimension flow into consideration (e.g. a transient spherical flow model) was used the calculated T-values and skin factors would be lower.

7.2 Jacob vs. Saphir

A different relationship is obtained when Jacob and Saphir tranmissivities are analysed as shown in Figure 7-1. From this plot it is evident that transmissivities calculated by the Jacob's method are always higher that those obtained with Saphir. The correlation ratio of T-values with the skin is negative. This relationship is believed to be due to the different approaches adopted for Jacob and Saphir in arriving at a T-value.

The transmissivity due to Jacob does not depend on the skin value and is calculated from the part of the semi-log plot where the IARF has been established. While with Saphir it should be recognized that modelling of a build-up test as shown in the log-log plot is done iteratively by adjusting K, C and skin so as to minimize the sum of the

squared differences of the pressure between measured and modelled value. Additionally, the interpretation is also aiming at obtaining modelled parameters that at the same time will generate a match for the whole pressure history, i e drawdown and build-up**.** Thus, effectively performing two different matches with actual data, where both have to provide an acceptable agreement with the data utilising the same parameters and model. The effect of the skin is that the pressure is displaced in absolute terms but it does in no way change the shape of the drawdown curve. This can not be noticed in a Jacob analysis but will be quite evident in a history match. One might have a very good match in the log-log plot but a terrible history match.

Hence the Saphir analysis takes into account both the pressure build-up shown in the log-log plot and the complete pressure history of the test. The Jacob analysis only extracts a T-value from the pressure build-up without consideration of any pressure matching.

7.3 Storage coefficient

In the analysis of single hole tests it is necessary to have an independent *a priori* estimate of either the skin or the storage coefficient (S) and solve for the other parameters e g hydraulic conductivity, fracture length etc. The choice of storage coefficient is provided by analysing the pressure response in the nearby borehole KA2563A which is constantly monitored through the Hydro Monitoring System (HMS). The outlined procedure to arrive at an S value is approximative since the test was not designed as an interference test. Consequently it lacks synchronisation of clocks between HMS and UHT 1 as well as a dense pressure measurement at the observation section. The data sets from the two boreholes show a time difference of about one hour. This is due to the summertime that is not implemented in the HMS system. With the above circumstances considered it was decided to analyse a large and well-defined pressure build-up response in section 3 (187-196m) of KA2563A. The sequence of pressure responses in this section to the testing activities in KI0025F is shown Figure 7-2. This response was generated when the complete length of KI0025F was allowed to flow at atmospheric pressure for about 5 hour while retrieving the hoisting rig during the demobilisation phase upon completion of the hydraulic testing activities. Then the hole was shut-in and the subsequent pressure recovery is the period that is analysed, indicated as “Analysed pressure build-up“ in Figure 7-2.

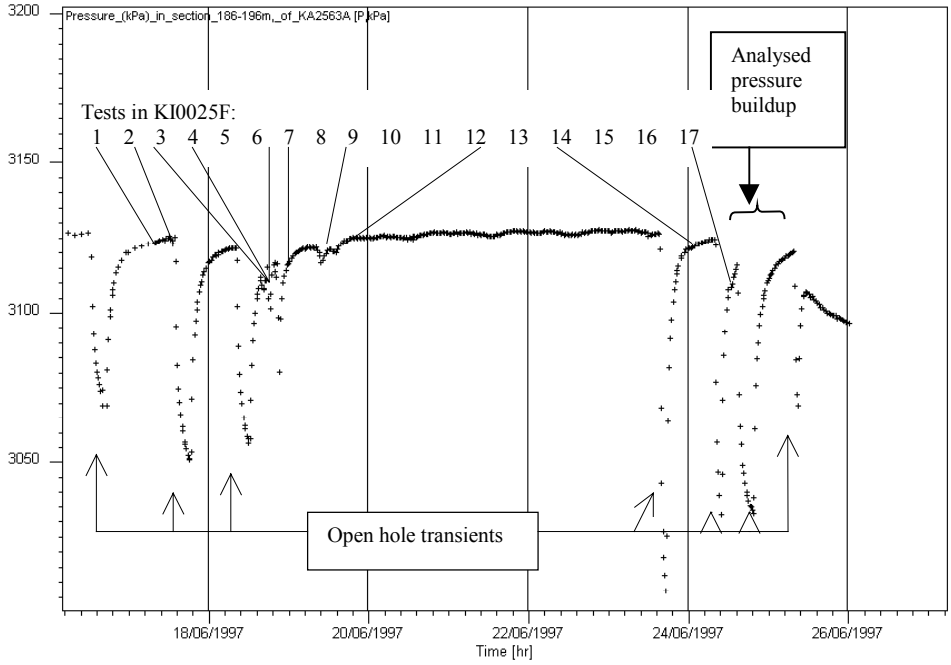

Figure 7-2 *Pressure response in section 187.0-196m in borehole KA2563A due to hydraulic testing activities in borehole KI0025F. Reference to the test numbers is in Table 3.2.*

Uncertainties also rest in the unknown response time of the pressure pulse and the unknown flow rate prior to shut-in. The response time is the difference in time from the onset of the disturbance at the active well (KI0025F) to the onset of the pressure response at the observation well (KA2563A). To address the issue a sensitivity analysis was performed on T and S for response time of 0min, 30min and 60min. These choices were governed by the judgement that the response time can not be more than one hour since this is the extreme case where duration of the flow event in KI0025F and the corresponding pressure event in KA2563A differ by 9 minutes, i e $dt_{P(KA2563A)} - dt_{Q(KI0025F)} = 9$ min. This is the time error due to inaccurate time record.

Figure 7-3 shows the plot of log (dP) vs log (dt_e) for the pressure build-up with the different time delays.

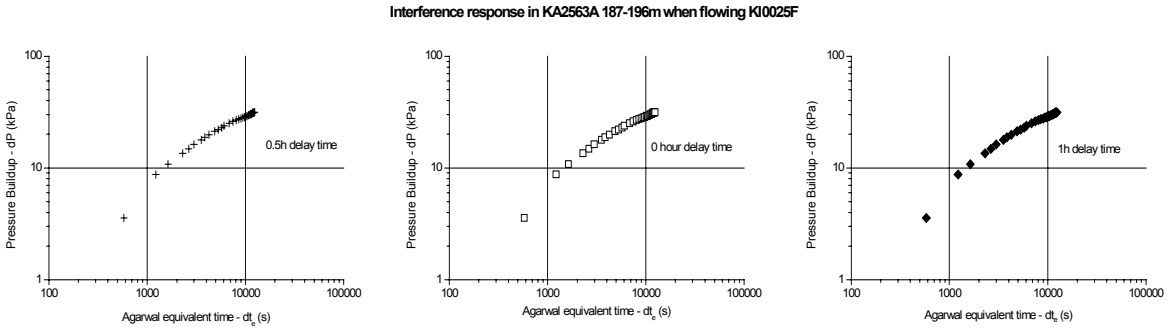

Figure 7-3 *Interference test response in KA2563A 187-196 m for different response time when flowing KI0025F (complete length) ; 0, 0.5 and 1 h.*

Although not shown in the figure all three curves match the Theis type curve very well. The resulting aquifer parameters are listed in Table 7-2, Q is 50 L/min and r is 152m (between bottom of sections).

Table 7-2 Aquifer parameters in section 187.0-196m of KA2563A calculated for different response times.

Response time (min)	$T \cdot 10^{-5}$ (m/s^2)	$S \cdot 10^{-6}$ (-)
0	6.26	5.20
30	6.38	5.08
60	6.44	5.13

From the table it is seen that the response of up to one hour makes a little difference on the calculated aquifer parameters T and S. Hence a response time of zero minutes is hereby adopted.

The shut-in flow rate is controlled by the following circumstances.

- the maximum flow rate is approximately 72L/min, based on flow logging
- the hole had been flowing for 5 hours, where the rate is is assumed to decrease exponentially
- a lower flow rate when extracting the packers during the studied flow phase (demobilisation) relative open hole

In Table 7-3 a sensitivity analysis for different flow rates and zero response time is presented.

Table 7-3 Sensitivity in transmissivity and storage coefficient calculated for section 187-196 m of KA2563A to different shut-in flowrates in KI0025F.

Flow (L/min)	T ($\cdot 10^{-5}$ m/s^2)	S ($\cdot 10^{-6}$)
14	1.73	1.12
26	3.18	2.12
50	5.95	4.24
65	7.74	5.51

1. Since the storage coefficient is controlled by the bulk elastic properties of a rock volume it is also interesting to compare the above storage coefficients with those calculated as part of other projects on Äspö. Table 7-4 below shows results from interference tests in the TRUE-1 block (Winberg et al, 1996) and the LPT-2 experiment (Rhén et al 1992). The Tables 7-2 and 7-3 show storage coefficients of the same magnitude as those from the TRUE-1 experiment but up to a magnitude lower than those from the LPT-2 experiment. In both these experiments adopting theories of transient radial flow in a homogeneous porous medium arrived at the calculated parameters. It should however be emphasised that the block investigated in the LPT-2 experiment is 10 to 50 times larger than the TRUE-1 block.

Table 7-4 Storage coefficients from TRUE-1 and LPT-2 experiments on Äspö.

Project	n(*)	Median	Geometric Mean	Arithmetic Mean
TRUE-1	20	$1.95 \cdot 10^{-6}$	$1.62 \cdot 10^{-6}$	$4.49 \cdot 10^{-6}$
LPT-2	22	$7.60 \cdot 10^{-5}$	$2.94 \cdot 10^{-5}$	$4.35 \cdot 10^{-5}$

(*) n= number of evaluated tests

With the above in mind this exercise is concluded by adopting a storage coefficient of $5.5 \cdot 10^{-6}$ for the subsequent analysis of the hydraulic tests in KI0025F.

7.4 Skinfactor

A surprising result of the analysis is the generally high positive skin factors. The pressure recovery due to skin, being the difference in pressure at shut-in and one second later, is in all cases very high. It accounts for between 76% and 93% of the total recovery.

Due to the fact that the storage coefficient has not been calculated from these tests it is possible that the adopted S is incorrect, which would impact on the calculation of the skin. The implication is therefore that it would be better to also conduct interference testing in order to calculate the storage coefficient. Then it would not be necessary to make any *a priori* assumption on either S or assuming a skin of zero.

This can be readily shown by reverting to the dimensional relation shown in Appendix 4 for a constant rate test expressing the drawdown during IARF

$$\Delta p_{Dd}(\Delta t) = \frac{1}{2} \cdot \frac{Q}{2\pi T}\left[\ln\left(\frac{T}{Sr_w^2}\Delta t\right) + 0.80909 + \xi\right]$$

When reshaping the equation with the purpose to obtain the easily recognisable form for the straight line with respect to the pressure and time variables, the following expression is obtained

$$\Delta p_{Dd}(\Delta t) = \frac{Q}{4\pi T} \cdot \ln(\Delta t) + \frac{Q}{4\pi T}\left[\ln\left(\frac{T}{Sr\ w}\right) + 0.80909 + \xi\right]$$

From this we can see that the slope of the straight line during IARF on a semilog plot gives T since Q is known. However, the intercept ($\ln(\Delta t)=0$) is a function of both S and ξ and there is no way to calculate the skin without prior knowledge of the storage coefficient and vice versa.

Or simply put, the equation contains two variables, Δp and Δt, and three unknown parameters, T, S and skin. It can thus not be solved without decreasing one unknown. This may be achieved through a properly designed interference test. Since, the skin is then zero and the drawdown equation may be solved for T and S.

As an example, the test in section 165.3-166.3 m was analysed by assuming a zero skin and solving for the storage coefficient. This resulted in an equally good match and similar K and C values as with for the previous simulation when S is known, but the S is 10^{-27}, far from the values calculated from actual interference tests. This indicates that the zero skin assumption is unrealistic in this case.

A further potential problem in calculating the skin factor is the definition of the IARF period. This is taken from the horizontal derivative on the log-log plot that is badly defined in four out of the six tests. The result is a deficiency in the data where it is unclear whether IARF is truly established. However, the two tests that do exhibit a complete derivative curve actually indicate a clear horizontal plateau in the derivative.

An alternative explanation to the high skin factors obtained from the evaluation could possibly be that they are overestimated due to the assumption of radial flow, i.e. that flow of higher dimension occurred during the tests. A transient (pseudo)spherical flow model evaluation would possibly result in lower skin factors (and transmissivity values)

8 Conclusions

All of the tests that were analysed with Saphir were interpreted to display an infinite acting radial flow regime without encountering outer boundaries. However, the dp'=0.5 dimensionless pressure derivative, which is the basis for establishing whether IARF has developed or not, is in all tests except for section 165.3-166.3 m and 186.0-193.8 m uncertain.

The reason for such discontinuous derivative plot is attributed to the small amount of pressure build-up that generates many non-variable pressures, which produces a zero derivative and can not be plotted. The IARF model is verified by the matching of the complete test sequence (i e drawdown and build-up). This history match shows rather good agreement between data and model. In order to avoid such a situation in tests it is necessary to have longer period of flow and/or use a pressure measuring system which have higher resolution than the present one. This also impacts on the size of the volume, which is investigated. A larger perturbation might reach outer boundaries. The implication of a badly defined derivative plot is the embedded uncertainty on which flow regime is to be modelled.

It should also be reiterated that Saphir uses unit slope WBS line in the log-log plot in order to generate a first estimate of aquifer parameters. For constant pressure tests this line might be non-existent as the tests were designed to minimise the WBS period. Nevertheless, confidence in the generated model is enhanced considerably by modelling the complete pressure history.

Utilisation of steady-state hydraulic test evaluation methods, such as Moye's method, which do not require the use of the storage coefficient does not seem viable since this Saphir evaluation has shown that there often are quite high skin at the wellbore and the skin can only be calculated with transient evaluation methods.

Generally, high skin values were obtained which is indicative for damaged wells. One uncertainty in the skin estimates is the lack of measured storage coefficients since the skin factor can not be calculated without prior knowledge of the storage coefficient. For this reason it is necessary to conduct interference tests in order to obtain a value of the storage coefficient in order to calculate the skin factor.

REFERENCES

Agarwal, R.G., 1980: A New Method to Account for Producing Time Effects When Drawdown Type Curves Are Used to Analyze Pressure Buildup and Other Test Data. - Soc. of Petroleum Engineers, SPE Paper 9289, presented at SPE-AIME Meeting, Dallas, Texas, September 21-24, 1980.

Almén, K-E and Hansson, K., 1996: Hydrotestutrustning för underjordsmätningar i Äspölaboratoriet – Konstruktion och tillverkning, SKB Äspölaboratoriet, Stockholm. Internal Report (In Swedish)

Bourdet,D., Ayoub, J.A., and Pirard,Y.,M,1989: Use of Pressure Derivative in Well-Test Interpretation. Soc. Pet. Eng. Formation Evaluation, June 1989, pp 293-302.

Cooper, H.H. Jr. & Jacob, C.E., 1946: A Generalized Graphical Method for Evaluating Formation Constants and Summarizing Well-Field History. - Am. Geophys. Union Trans., Vol. 27, No. 4, pp. 526-534.

Carlsten, S. 1997: True Block Scale Experiment. Results from borehole radar measurements in KI0025F. SKB Internal Report.

De Marsily : Quantitative Hydrogeology. Academic press 1986.

Earlougher R. C., 1977: Advances in well test Analysis. SPE monograph Volume 5, Henry L, Doherty Series.

Gentzschein, B., 1994: ÄSPÖLABORATORIET. Manual för tryckuppbyggnadstester. SKB Internal Report (in Swedish).

Gentzschein, B. 1997: True Block Scale Experiment. Detailed flow logging of coreboreholes KA2511A, KI0025F and KA3510A using double packer system. SKB Internal Report.

Gustafsson, G. 1997: True Block Scale Experiment. Loggning med UCM flödessond i KI0025F. SKB Internal Report.

Hansson, K. 1997: Manual för Underground Hydraulic Testsystem UHT 1. Del 1, Handhavande. SKB Internal Report (in Swedish).

Hermanson, J. and Follin, S. 1997: Update of the structural model using characterization data from KA2563A, KA3510A and KA2511A. SKB Internal Report.

Johansson, B., and Olsson, O., 1994: IPPLOT, Konverterings- och plottprogram för data från injektions- och pumptester. Användarhandledning. Ver. 1.3 .ERGODATA AB. (In Swedish)

Lindström, D. 1997: True Block Scale Prototype Packer and Prototype Dummy. SKB Internal Report.

Moye, D. G., 1967: Diamond Drilling for Foundation Exploration. Civil Eng. Trans.,Inst. Eng. Australia, Apr. 1967, pp 95-100.

Rhén, I. and Nilsson, L., 1991: Pressure build-up tests in sounding boreholes - performance and evaluation. SKB Internal Report.

Rhén, I.(ed.) and Svensson, U.(ed.), 1992: Äspö Hard Rock Laboratory: Evaluation of the combined long-term pumping and tracer test (LPT2) in borehole KAS06. SKB-TR 92-32

Nyberg, G. 1994: Manual för Hydro Monitoring System (HMS), Del 3:4; Mekaniska installationer. SKB Internal Report.

Stråhle, A. 1997: True Block Scale Experiment. Borehole images of boreholeKI0025F. SKB Internal Report.

Winberg, A. (editor) 1996: First TRUE Stage – Tracer Retention Understanding Experiment. Descriptive structural-hydraulic models on block and detailed scales of the TRUE-1 site. SKB ICR 96-04

APPENDICES

APPENDIX 1: Borehole logg of KI0025F

APPENDIX 2: Description of the UHT 1 diagrams

APPENDIX 3: Symbols and calculations of the UHT 1 diagrams and description of the MIO-file

APPENDIX 4: Parameter equations used for the Saphir evaluation.

APPENDIX 5: Diagrams of the pressure build-up test in section 43.0 - 44.0 m

APPENDIX 6: Diagrams of the pressure build-up test in section 86.0 - 87.0 m

APPENDIX 7: Diagrams of the pressure build-up test in section 165.3 - 166.3 m

APPENDIX 8: Diagrams of the pressure build-up test in section 166.3 - 167.3 m

APPENDIX 9: Diagrams of the pressure build-up test in section 167.3 - 168.3 m

APPENDIX 10: Diagrams of the pressure build-up test in section 186.0 - 193.8 m

Appendix 1: Borehole logg of KI0025F

Title	**Borehole logs for KI0025F**		
Site	Äspötunnel	**Coordinate System**	Äspö96
Borehole	KI0025F	**Northing**	7238.153m
Diameter	76mm	**Easting**	1954.69m
Length	193.8m	**Elevation**	-448.229m
Bearing	187.143 °	**Completion Date**	1997-04-25
Inclination	-20.73°		
Remark	An inflow of 40L/min at 6-8m was grouted. Referens: TN-97-22b, TN-97-09b and TN-97-07b.		

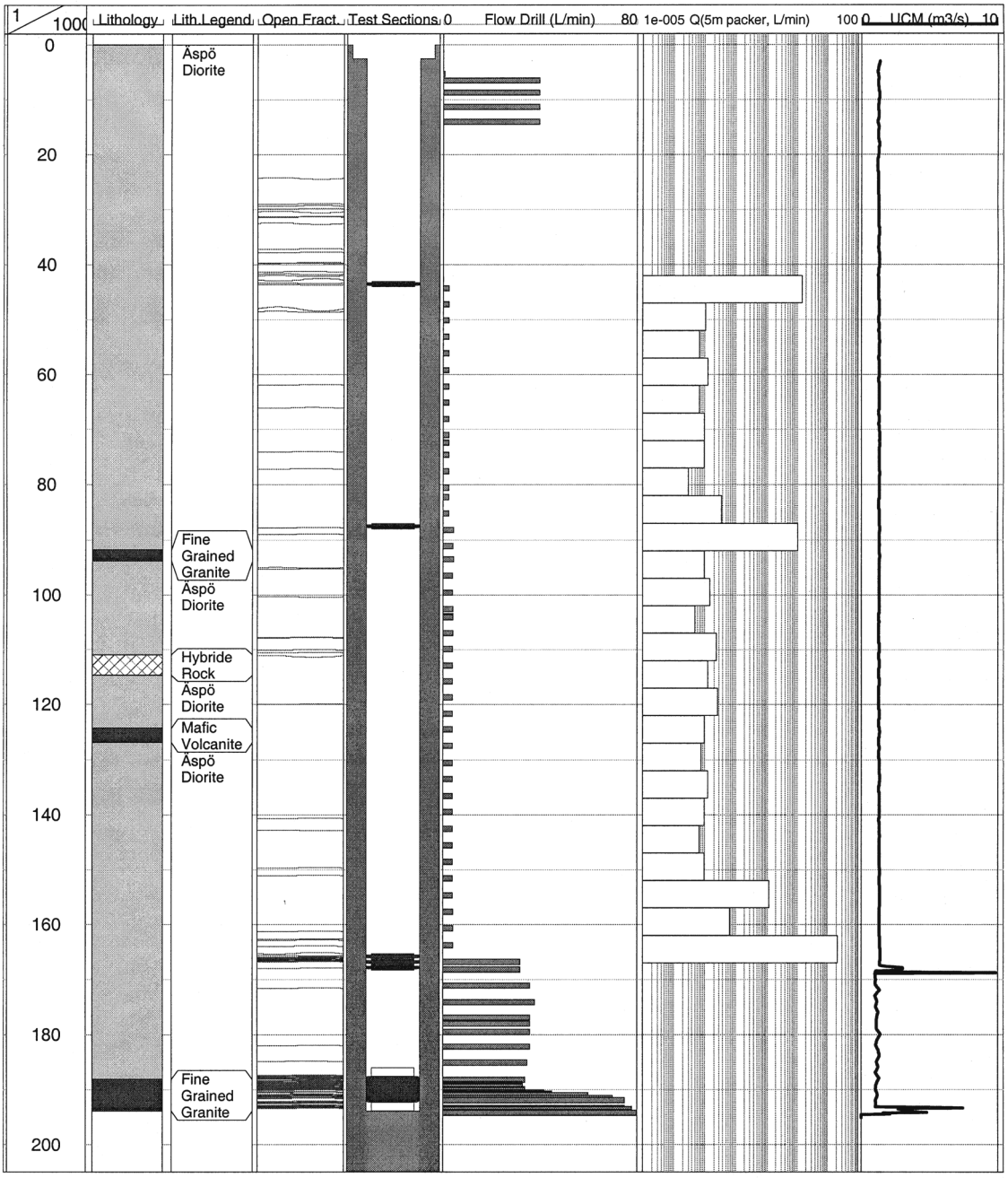

Appendix 1:

Selective description of open fractures in borehole KI0025F. Data is from Stråhle, A. 1998: True Block Scale Experiment. Borehole images of borehole KI0025F. SKB TN-97-09b

Depth(m)	Strike(°)	Dip(°)	Form	Aperture(mm)
Section 43.0 – 44.0m				
43.139	140	78	Open & planar	1.0
43.362	339	74	Open & stepped	3.0
43.396	134	87	Open & planar	2.0
Section 87.0 – 88.0m				
87.425	336	77	Cavities & undulating	2.0
87.546	015	86	Cavities & undulating	1.0
87.889	295	43	Cavities & planar	2.0
Section 165.3 – 166.3m				
165.049	147	90	Cavities & irregular	2.0
165.211	291	72	Cavities & undulating	1.0
165.400	248	63	Cavities & planar	2.0
165.498	338	74	Open & undulating	5.0
165.611	337	78	Cavities & planar	4.0
165.734	248	66	Cavities & network	7.0
165.751	289	56	Cavities & planar	3.0
165.829	270	08	Cavities & undulating	2.0
165.935	287	31	Cavities & planar	2.0
Section 166.3 – 167.3				
166.069	336	84	Open & planar	6.0
166.075	222	66	Cavities & planar	1.0
166.192	322	79	Cavities & planar	2.0
Section 167.3 – 168.3				
167.116	249	42	Cavities & undulating	2.0
167.243	253	60	Cavities & undulating	2.0
167.420	156	90	Open & undulating	1.0
167.750	211	78	Cavities & planar	1.0
Section 186.0 – 193.8m				
186.747	252	56	Cavities & planar	13.0
186.825	270	43	Cavities & planar	4.0
186.982	218	35	Cavities & planar	2.0
187.161	238	77	Cavities & network	4.0

Depth(m)	Strike(°)	Dip(°)	Form	Aperture(mm)
187.204	267	77	Cavities & network	7.0
187.349	256	82	Cavities & network	2.0
187.406	236	82	Cavities & network	2.0
187.471	246	87	Cavities & network	1.0
187.659	266	59	Cavities & network	3
187.807	276	16	Cavities & network	2
187.936	061	90	Cavities & network	4
187.947	326	78	Cavities & network	2
188.154	240	87	Cavities & network	3
188.197	310	85	Cavities & network	4
188.386	236	74	Cavities & network	2
188.464	239	73	Cavities & network	9
188.607	215	76	Cavities & network	12
188.835	343	85	Cavities & undulating	4
188.967	226	62	Cavities & planar	4
189.019	335	61	Cavities & planar	7
189.117	332	78	Cavities & planar	3
189.203	140	84	Cavities & planar	1
189.206	229	59	Cavities & planar	3
189.309	307	75	Cavities & planar	4
189.346	334	70	Cavities & planar	3
189.678	319	68	Cavities & planar	2
189.789	225	60	Cavities & planar	3
190.189	249	59	Open & planar	6
190.551	219	50	Cavities & crushed	55
190.730	296	87	Cavities & planar	3
190.849	292	74	Cavities & planar	1
191.448	237	87	Cavities & planar	4
191.507	236	79	Cavities & planar	2
191.546	241	78	Cavities & planar	4
191.627	243	77	Cavities & planar	6
191.673	249	74	Cavities & planar	3
191.727	254	69	Cavities & planar	3
192.625	107	75	Cavities & planar	3

APPENDIX 2

Description of flow and pressure build-up test diagrams produced by the UHT 1-system.

A flow and pressure build-up test with the UHT 1-equipment comprises 8 stages:

Stage 0: Start of registration
Stage 1: Storing of initial values
Stage 2: Start of packer inflation
Stage 3: Evacuation of air from the pipe string and the measurement hose.
Stage 4: The test valve is opened, the flowing phase is started
Stage 5: The test valve is closed, the flowing phase is stopped, and the pressure recovery phase is started
Stage 6: The recovery ends and the packers are deflated.
Stage 7: Stabilisation of the borehole pressure after the test.

A-diagrams show flow-, pressure-, electric conductivity- and temperature variations during the entire test cycle.

A0 A flyleaf showing background data as well as measured and calculated data from the test.

A1 X : Absolute time, stage 0 - 3
Y1: P

A2 X : Absolute time, stage 1 - 7
Y1: Q
Y2: Elcond

A3 X : Absolute time, stage 0 - 7
Y1: P
Y2: Pa
Y3: Pb

A4 X : Absolute time, stage 0 - 7

Y1: Tsec
Y2: Tsurf
Y3: Tair

A5 X : Absolute time, stage 0 - 7
Y1: Ppack
Y2: Pair
Y3: W

B-diagrams show test parameter variations during the flowing phase (stage 4).

B1 X : log (t)
Y1: P
Y2: Tsec
Y3: Elcond

B2 X : $t^{¼}$ and t
Y1: 1/Q

B3 X : $t^{1/2}$ and t
Y1: 1/Q

B4 X : log (t)
Y1: 1/Q
Y2: der(1/Q)

B5 X : log (t)
Y1: log (Q)
Y2: log(der(1/Q))

B6 X : $t^{1/2}$ and t
Y1: Q

C-diagrams show test parameter variations during the recovery phase (stage 5).

C1 X : $t^{¼}$ and dt
Y1: P

C2 X : $t^{1/2}$ and dt
Y1: P

C3 X : $(tpp + dt)^{1/2} - dt^{½}$ and dt
Y1: P

C4 X : log(dt) and dt
Y1: P
Y2: der(P)
Y3: Q

C5 X : log(dt/ (tp+dt)) and dt
Y1: P
Y2: Tsec

Appendix 2 (3)

C6 X : log(dte) and dt
Y1: log(P-Pp)
Y2: log(der(P-Pp))

C7 X : $(1/dt)^{1/2}$ - $(1/(tpp+dt))^{1/2}$ and dt
Y1: P

C8 X : log(dt)
Y1: P
Y2: der(P)
Y3: Q

C9 X : log(dt)
Y1: log(P-Pp)
Y2: log(der(P-Pp))

APPENDIX 3: Symbols and calculations of the UHT 1 diagrams and description of MIO-files

Symbols

(from Johansson and Olsson 1994)

TT	Test type
DW	Borehole diameter
X	x-coordinate, top of casing
Y	y-coordinate, top of casing
Z	altitude, top of casing
AW	Borehole azimut
IW	Borehole inclination
TC	Test crew
EC	Equipment code
TB	Time (YYMMDDhhmmss) when PB and BB are measured
PB	Barometric pressure at time TB(measured by P-the test section sensor)
BB	Barometric pressure at time TB(measured by Pair, not in use)

tabs	absolute time
t	elapsed time from pump start
dt	elapsed time from pump stop
tp	duration of flow phase
tpp	corrected tpp
dte	equivalent time
dtf	duration of the pressure recovery
Vtot	total flowing volume during the flowing phase

Measured variables

P	ground-water pressure of the test section
Pa	ground-water pressure of the borehole intervals around the test section
Pb	ground-water pressure of the test section
Ppack	Packer-pressure
Pw	Pressure of the ground-water level sensor (not in use)
Q1	flow rate of the small flow meter
Q2	flow rate of the big flow meter
Q	Flow rate from the test section, one of Q1 or Q2
Tsec	Temperature of the test section (not in use)
Tsurf	Temperature of the flow water at surface (not in use)
Tair	Air temperature in the measurement container (not in use)
Pair	Barometric pressure (not in use)

Calculations

W Ground-water level (not in use)

From the variables P, Pa, Pb, W and Q constants, with indices i, o, f, e and p, are determined according to:

i The first value of stage 1
o Average of the 4 last values of stage 3.
f The lasts value of stage 5
e The lasts value of stage 7
p Average of the 5 last values of stage 4, excluding the last value.

Vtot = the integral of the flow rate (Q) during the flowing phase (stage 4)
tpp = Vtot/Qp or = tp
dte = dt * tp/ (dt + tp)

dPim Average of Pi - P during the flow phase (stage 4)
dPom Average of Po - P during the flow phase (stage 4)

Kiss $(Qp * 9.81 * (1 + \ln(L/DW * 1000))) / dPim * L * 2\pi$
Koss $(Qp * 9.81 * (1 + \ln(L/DW * 1000))) / dPom * L * 2\pi$

Appendix 3 (3)

Description of the MIO - file

The MIO-file consists of two parts, one command part and one data part. The data part has a table structure with columns. The first column is as rule a time column followed by the parameters defined in the command part.

The commands are in the beginning of the file. Only one command on each line is allowed and the commands are first in the lines. Commands and parameters are separated by a space character.

The data types of the parameters are:

s - string of ASCII symbols
d - integer
f - decimal number
e - floating point
D - date (YYMMDD)
t - time (hhmmss) or [(YY)YYMMDDhhmmss]

The commands used are as follows:

Commands	**(data type)**	**Description**
l	d	number of command rows(including this row)
hs	[s . .]	general head line
t	s	name of table
f	s	file name of the data part (if data are in a separate files)
s	d	number of rows to skip before reading data
c	s c d d d	column description, the parameters are : name of the column, data type, offset (position on the row, first pos.= 0), width of column, number of decimals(-1 if no decimal number). This description is repeated for each column.
cm	s e e	name of column, min. value, max.value.
cu	s s	unit of column
;	s[ss. .]	comment row

Appendix 4: Theory for parameter evaluation employed in the Saphir modelling

In the following a condensed outline is given of the interpretation equations as they are implemented in the software utilised for the interpretation (Saphir) of the tests. This is done for the simplest boundary conditions and most idealised flow regime, ie two dimensional confined radial flow to a borehole producing at constant or multiple rate through a homogenous and isotropic porous medium of infinite lateral extent.

Log-Log Diagnostic

The starting point is the solution of the governing diffusivity equation for this problem, the Theis equation:

$$\Delta p_{Dd} = \frac{Q}{4\pi T} \int_{1/u}^{\infty} \frac{e^{-\tau}}{\tau} d\tau \quad where \quad u = \frac{Sr^2}{4T\Delta t}$$

where Q is the flow rate, Δp the pressure drawdown, T the transmissivity, S the storage coefficient, r the distance and Δt the time difference. The integral in this equation can be approximated by its limit form for small arguments, i e longer time, called Jacob's logarithmic approximation

$$\int_{1/u}^{\infty} \frac{e^{-\tau}}{\tau} d\tau \approx -\ln(u) - 0.5772 = \ln\left(1/u\right) - 0.5772$$

In practice Jacob's approximate equation valid is when u ≥ 100 which is always the case for the pumped section (active well) while it has to be checked for the observed section when conducting an interference test. The resulting Jacobs equation is :

$$\Delta p_{Dd} = \frac{Q}{4\pi T} \cdot \left[\ln\left(1/u\right) - 0.5772\right]$$

Jacob's approximate equation is fundamental to the interpretation with Saphir.
By introducing dimensionless parameters a functional relationship is established for p_D, t_D and C_D. The dimensionless parameters are defined as follows:

$$t_D = \frac{T}{Sr_w^2} \cdot \Delta t; \quad p_D = \frac{2\pi T}{Q} \cdot \Delta p; \quad C_D = \frac{\rho g}{2\pi S r_w^2} \cdot C$$

For a confined aquifer the wellbore storage, C, is defined as:

$$C = c_w + V_w = \frac{V}{\Delta p} \quad \text{where V is the volume produced by the wellbore}$$

With the above definitions of the dimensionless parameters a dimensionless form of Jacobs equation is obtained,

$$p_D \approx \frac{1}{2}\left[\ln(t_D) + 0.80907\right]$$

Taking the logarithm of the definitions of t_D and p_D above yields

$$\log(t_D) = \log(\Delta t) + \log\left(\frac{T}{Sr_w^2}\right)$$

$$\log(p_D) = \log(\Delta p) + \log\left(\frac{2\pi T}{Q}\right)$$

Hence there is a direct relationship between dimensional and dimensionless models where the two are shifted by an amount equal to the last term of each equation along the abscissa and the ordinata respectively.

When data and model match, the ratio between the dimensional and dimensionless parameter (t_r and p_r) is constant and equal to:

$$t_r = \frac{(t_D)_{match}}{(\Delta t)_{match}} = \frac{T}{Sr_w^2} \qquad \textit{and} \qquad p_r = \frac{(p_D)_{match}}{(\Delta p)_{match}} = \frac{2\pi T}{Q}$$

Including wellbore storage and skin

When introducing wellbore storage and skin the diffusivity equation is solved in Laplace space and obtained in real space through numerical inversion. The resulting solution (not shown here) shows that the pressure can be expressed as a function of time, wellbore storage and skin, $\Delta p = f(\Delta t, C, \xi)$. In dimensionless terms, functional relations are established between p_D, t_D, C_D and the correlation group $C_D e^{2\xi}$. Where C_D is defined as:

$$C_D = \frac{\rho g}{2\pi S r_w^2} \cdot C$$

For a dimensionless solution including wellbore storage and skin, the abscissa is not expressed as a function of t_D but of t_D/C_D instead. Where t_D/C_D is defined as

$$\frac{t_D}{C_D} = \frac{2\pi T}{\rho g C} \cdot \Delta t$$

For a chosen value of the correlation group $C_De^{2\xi}$ the resulting relationship between dimensional and dimensionless time is then

$$\log\left(\frac{t_D}{C_D}\right) = \log(\Delta t) + \log\left(\frac{2\pi T}{\rho g C}\right)$$

When the dimensionless model (type curve) is fitting the data one point is selected, anyone, and the values on the abscissa and ordinata are retrieved i e $(t_D/C_D)_{match}$, $(p_D)_{match}$, $(\Delta t)_{match}$ and $(\Delta p)_{match}$. Upon inserting these values in the relationships above and for practical reasons selecting the dimensionless values as 1, the following is obtained for the matchpoint

$$(\Delta t)_{match} = \frac{Sr_w^2}{T} \quad : \quad linesource$$

$$(\Delta t)_{match} = \frac{\rho g C}{2\pi T} \quad : \quad with\ WBS\ and\ skin$$

$$(\Delta p)_{match} = \frac{Q}{2\pi T}$$

The pressure match on the log-log plot will give the transmissivity and the time match gives the wellbore storage for the WBS/skin solution or the aquifer storage coefficient for the linesource solution, since Q and r_w are know entities. The skin is arrived through the value of the correlation parameter ($C_De^{2\xi}$) which is unique for the matched model.

Having chosen unit dimensionless parameters, the sequence of calculating the aquifer and wellbore parameters from a log-log plot, when the aquifer storage coefficient is known, is the following:

1. Pressure match $\Rightarrow$ transmissivity

$$T = \frac{Q}{2\pi(\Delta p)_{match}}$$

2. Time match $\Rightarrow$ WBS constant, C

$$C = \frac{2\pi T(\Delta t)_{match}}{\rho g} \quad \Rightarrow \quad C_D = \frac{T(\Delta t)_{match}}{Sr_w^2}$$

3. Correlation group value, $\beta=C_De2^{\xi}$ $\Rightarrow$ skin(ξ)

$$\xi = \frac{1}{2}\ln\left(\frac{\beta}{C_D}\right) = \frac{1}{2}\ln\left(\beta \cdot \frac{Sr_w^2}{T(\Delta t)_{match}}\right)$$

When model and data match and the IARF regime has been reached the relation between dimensional and dimensionless parameters is,

$$\Delta p_{Dd}(\Delta t) \approx \frac{(\Delta p)_{match}}{(p_D)_{match}} \cdot \frac{1}{2}\left[\ln\left(\frac{(t_D)_{match}}{(\Delta t)_{match}} \cdot \Delta t \right) + 0.80909 \right]$$

This equation may be used to model to model the pressure response due to constant rate punping.

Use of the pressure derivative

Since many different typecurves are similar in shape the above mentioned typecurve matching procedure is insensitive. This was resolved by introducing the pressure derivative. In this case the functional relationship is sought for the rate of change of the pressure with respect to the time function. It is obtained by simply differentiating the dimensionless form of the previously obtained approximate solution to the diffusivity equation (Jacob's equation).

The derivative is calculated from the Jacob's approximate solution, which is valid during infinite acting radial flow (IARF) phase.

$$\Delta p = \frac{Q}{4\pi T} \cdot \left(\ln(u) - 0.5772 \right) \quad ; \quad u = t_D = \frac{T}{Sr_w^2} \cdot \Delta t \text{ and } p_D = \frac{2\pi T}{Q} \cdot \Delta p$$

$$\Rightarrow \quad p_D = \frac{1}{2}\left(\ln(t_D) - 0.5772 \right) \quad \textit{for a linesource}$$

$$\Rightarrow \quad p_D = \frac{1}{2}\left(\ln\left(\frac{t_D}{C_D} \right) - 0.5772 + skin \right) \quad \textit{with WBS and skin}$$

The pressure derivative curve have two characteristic features:

- When flow is purely from WBS the slope of the pressure derivative in a log-log plot is equal to one and coincides with the slope of the pressure drawdown.
- When IARF is reached the derivative on a log-log plot is constant, i e a horizontal line on the plot. In dimensionless terms the derivative stabilizes at a value of 0.5:

$$p_D'(IARF) = \frac{dp_D}{d\ln(t_D)} = \frac{1}{2}$$

Hence, on a log-log plot with both pressure and pressure derivative the interpreter identifies the unit slope and the stabilisation level which indicates IARF. This gives the match between data and model, if the shapes of the two curves do match.

However, when no-flow boundaries are encountered the slope of the pressure vs time response will alter accordingly, e g

- single no flow boundary will double the slope $\Rightarrow P'_D = 1$
- two faults at 90^o angle will quadruple the slope $\Rightarrow P'_D = 2$

The relation between the dimensional and dimensionless pressure derivatives is obtained from the definition of the derivative of a variable including two functions. For the line source solution above the derivative is:

$$p'_D = \frac{dp_D}{d\ln(t_D)} \left[= \frac{dp_D}{\frac{1}{t_D} \cdot dt_D} = t_D \cdot \frac{dp_D}{dt_D} \right]$$

$$\Delta p' = \frac{d\Delta p}{d\ln(\Delta t)} \left[= \frac{d(\Delta p)}{\frac{1}{\Delta t} \cdot d(\Delta t)} = \Delta t \cdot \frac{d(\Delta p)}{d(\Delta t)} \right]$$

Then the ratio between the derivatives is:

$$\frac{p'_D}{\Delta p'} = \frac{\frac{dp_D}{d\ln(t_D)}}{\frac{d\Delta p}{d\ln(\Delta t)}}$$

But, since

$$d\ln(\Delta t) = \frac{d\Delta t}{\Delta t} \quad and \quad \Delta t = \frac{t_D}{t_r} \quad \Rightarrow \quad d\ln(\Delta t) = \frac{d\left(t_D / t_r \right)}{t_D / t_r} = \frac{dt_D}{t_D} = d\ln(t_D)$$

it follows that

$$\frac{p'_D}{\Delta p'} = \frac{d(p_D)}{d(\Delta p)} = \frac{p_D}{\Delta p} = p_r$$

From this relationship between the dimensional and dimensionless pressure derivative and since $p'_D = 0.5$ the transmissivity is obtained as

$$T = \frac{1}{4\pi} \cdot \frac{Q}{\Delta p'_{IARF}}$$

For the analysed flow phase (pressure build-up) the parameter estimation is performed on the pressure data (dP) and not on the derivative (dP'). For this purpose a non-linear reiterative regression is performed on a more widely spaced data set than the actual test data. This is specified by the user who is controlling the number of points as well as their position in time to be included in the non-linear regression. As a consequence the simulated derivative may not lie exactly on the original pressure derivative data. It has no effect on the regression, which work on the pressure only. The derivative of the pressure build-up is obtained through the preferred algorithm of Bourdet et al (1989). The differentiation is made with respect to a point to the left and a point to the right of the point of interest. This opens a time window [$t-dt_{left}$, $t+dt_{right}$] around the point of interest t. The derivative is calculated using the point just before and the point just after this window. The minimum distance on the time axis between the points to the left and right relative the point of interest is called the smoothing intervall, L. It is specified by the well test interpreter and the differentiation algorithm selects dt such that L< dt. The time function t can be log(time), Agarwal time or superposition time. Hence

$\ln(t_{right}) - \ln(t) > L$ and $\ln(t) - \ln(t_{left}) > L$.

Multiple rate analysis

In many instances the flow rate prior to the period of analysis have fluctuated. This rate variation may influence the analysis to a greater or lesser extent and should consequently be included in the analysis of a test. Normaly two kind of situations occur:

- Variable rates prior to a pressure drawdown phase
- Variable rates prior to a pressure build-up phase

The solution to these two situations is somewhat different since the build-up solution also considers the shut-in pressure, as will be shown later.

When considering the pressure response at a certain time, t, which is influenced by previous variable flow rates the principle of superposition may be applied, since the solution to the diffusivity equation is linear with respect to the variable p. This principle states that the drawdown Δp_t at a time t can be viewed as the linear addition of several different drawdowns each caused by a constant rate flow,

Hence, the variable flow rate history is discretized into N different flow periods, each with a constant flow rate Q_j as follows

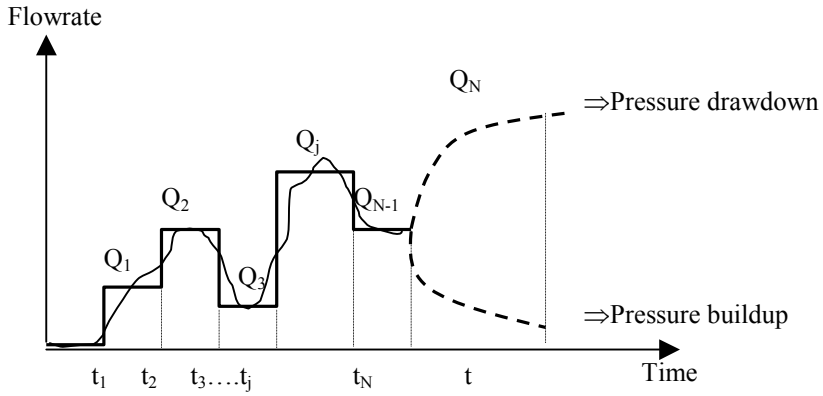

Multiple rate drawdown solution

The pressure drawdown, Δp_j, due to the flow rate Q_j is

$$\Delta p_j = \frac{\Delta Q_j}{4\pi T} \cdot W\left(1/u_j\right)$$

The total drawdown at time t, after a flow history with variable rates is the linear combination (additions) of drawdowns due to flows with constant rate. Since the skin is a wellbore effect it is only dependent on the last flow rate and not on the flow history, as such the pressure drop due to the skin may simply be added to the pressure drop induced by the formation,

$$\Delta p(t) = \sum_{j=1}^{N} \left\{ \left(Q_j - Q_{j-1}\right) \cdot \frac{W\left(1/u_j\right)}{4\pi T} \right\} + \Delta p_\xi$$

In order to relate this solution to the traditional constant rate solution for a reference constant flow Q, we divide the right hand side of the above equation with Q to obtain the multirate drawdown solution for a unit rate. Then the right hand side is multiplied with Q to obtain the multirate drawdown solution for the actual flow rate of the analysed flow phase(Δp_{MR}):

$$\Delta p_{MR}(\Delta t)=\sum_{j=1}^{N}\left\{\frac{(Q_j-Q_{j-1})}{Q}\cdot\frac{Q}{4\pi T}W\left(1/u_j\right)\right\}+\Delta p_\xi=\sum_{j=1}^{N}\left\{\frac{(Q_j-Q_{j-1})}{Q}\cdot\Delta p_{Dd}\left(t-t_j\right)\right\}+\Delta p_\xi$$

During IARF the Jacob approximation is applicable, hence

$$\Delta p_{Dd}(\Delta t)=\frac{1}{2}\cdot\frac{Q}{2\pi T}\left[\ln\left(\frac{T}{Sr_w^2}\Delta t\right)+0.80909+\xi\right]$$

and when the model and data match the multirate equation may be expressed in terms of the matching parameters, as follows,

$$\Delta p_{MR}(\Delta t)\approx\frac{1}{2}\cdot\frac{Q}{2\pi T}\sum_{j=1}^{N}\left\{\frac{(Q_j-Q_{j-1})}{Q}\left[\ln\left(t-t_j\right)+\ln\left(\frac{T}{Sr_w^2}\right)+0.80909+\xi\right]\right\}=$$

$$=\frac{1}{2}\frac{(\Delta p)_{match}}{(p_D)_{match}}\sum_{j=1}^{N}\left\{\frac{(Q_j-Q_{j-1})}{Q}\left[\ln\left(t-t_j\right)+\ln\left(\frac{(t_D)_{match}}{(\Delta t)_{match}}\right)+0.80909+\xi\right]\right\}$$

Any value of Q will work. In dimensionless terms Q could be the stabilized flow rate and in real terms Q could be the last acquired rate. From the above multirate equation the constant terms may be extracted to yield the form of equation for the straight line according to

$$\Delta p_{MR}(\Delta t)\approx\frac{1}{2}\frac{(\Delta p)_{match}}{(p_D)_{match}}\sum_{j=1}^{N}\left\{\frac{(Q_j-Q_{j-1})}{Q}\left[\ln\left(t-t_j\right)\right]\right\}+\frac{1}{2}\frac{(\Delta p)_{match}}{(p_D)_{match}}\cdot\left\{\ln\left(\frac{(t_D)_{match}}{(\Delta t)_{match}}\right)+0.80909+\xi\right\}$$

the summation defines the superposition time $\mathrm{Sup}(t)=\sum_{j=1}^{N}\left\{\frac{(Q_j-Q_{j-1})}{Q}\left[\ln\left(t-t_j\right)\right]\right\}$

The above equation may be used to model the pressure response due to multirate flows preceding the pressure drawdown phase. On the right hand side of this equation the second term is a constant, hence the derivative of the multirate pressure with respect to superposition time is

$$\Delta p'_{MR}(\Delta t)=\frac{1}{2}\frac{(\Delta p)_{match}}{(p_D)_{match}}$$

Multirate buildup solution

From shut-in time onward transients from the WBS in the hole might influence the pressure build-up. As before, by discretizing the flow rates during the build-up phase into k different periods of constant rates we obtain (N+k-1) number of rates. These will tend the flow toward zero during the build-up instead of being equal to zero, i e $Q_N \rightarrow 0$ instead on $Q_N=0$. This means that due consideration has to be taken to variable flow rate into the wellbore after shut-in. The simplest case is when the flow after shut-in time goes instantly to zero, then k=1 and the number of rates is N, as for the multirate drawdown solution

The duration of the active rate (i e the actual flow rate during which the pressure is calculated) is $t_N+\Delta t$ where Δt is the duration of the pressure build-up. The pressure build-up for the build-up phase ($\Delta p_{MRBu}(\Delta t)$) is done relative the last flowing pressure, $p_{shut\text{-}in}$ (shut-in pressure) at shut-in time t_N,

$\Delta p_{MRBu}(\Delta t) = p(t_N+\Delta t) - p_{shutin}$

The pressure at the time $t_N+\Delta t$ may be expressed in terms of multirate pressure as previously shown for the drawdown case,

$$p(t_N + \Delta t) = p_i - p_{MR}(\Delta t)$$

By inserting the latter equation into the former we obtain the relation for the multirate build-up pressure,

$$\Delta p_{MRBu}(\Delta t) = p(t_N + \Delta t) - p_{shut-in} = (p_i - \Delta p_{MR}(\Delta t)) - p_{shut-in} =$$
$$= p_i - p_{shut-in} - \left[\sum_{j=1}^{N-1} \left\{ \frac{(Q_j - Q_{j-1})}{Q} \cdot \Delta p_{Dd}\left((t_N + \Delta t) - t_j\right) \right\} + \Delta p_\xi \right]$$

Here, Q is the last acquired flow rate prior to åressure build-up. If the IARF regime has developed during the last flow period prior to shut-in the Jacob approximation is applicable and the pressure response is given by,

$$\Delta p_{MRBu}(\Delta t) \approx p_i - p_{shut-in} - \frac{1}{2} \cdot \frac{Q}{2\pi T} \sum_{j=1}^{N-1} \left\{ \frac{(Q_j - Q_{j-1})}{Q} \left[\ln\left((t_N + \Delta t) - t_j\right) + \ln\left(\frac{T}{Sr_w^2}\right) + 0.80909 + \xi \right] \right\} =$$
$$= p_i - p_{shut-in} - \frac{1}{2} \frac{(\Delta p)_{match}}{(p_D)_{match}} \sum_{j=1}^{N-1} \left\{ \frac{(Q_j - Q_{j-1})}{Q} \left[\ln\left((t_N + \Delta t) - t_j\right) + \ln\left(\frac{(t_D)_{match}}{(\Delta t)_{match}}\right) + 0.80909 + \xi \right] \right\}$$

As previously, extracting the constant terms from the above equation we obtain an expression for the intercept from which the skin may be calculated

$$\Delta p_{MR}(\Delta t) \approx p_i - p_{shut-in} - \left[\frac{1}{2}\frac{(\Delta p)_{match}}{(p_D)_{match}}\sum_{j=1}^{N-1}\left\{\frac{(Q_j - Q_{j-1})}{Q}\left[\ln\left((t_N + \Delta t) - t_j\right)\right]\right\} + \left[\frac{1}{2}\frac{(\Delta p)_{match}}{(p_D)_{match}} \cdot \left\{\ln\left(\frac{(t_D)_{match}}{(\Delta t)_{match}}\right) + 0.80909 + \xi\right\}\right]\right]$$

$$\text{the summation defines the superposition time,} \quad Sup(t) = \sum_{j=1}^{N}\left\{\frac{(Q_j - Q_{j-1})}{Q}\left[\ln\left((t_N + \Delta t) - t_j\right)\right]\right\}$$

$$\text{the intercept is :} \quad p_i - p_{shut-in} - \left[\frac{1}{2}\frac{(\Delta p)_{match}}{(p_D)_{match}} \cdot \left\{\ln\left(\frac{(t_D)_{match}}{(\Delta t)_{match}}\right) + 0.80909 + \xi\right\}\right]$$

The above equation may be used to model the pressure response due to multirate flows preceding the pressure drawdown phase. Taking the derivative with respect to the superposition time function yields,

$$\Delta p'_{MRBu}(\Delta t) = \frac{Q}{4\pi T} = \frac{1}{2}\frac{(\Delta p)_{match}}{(p_D)_{match}}$$

It should be recognised that the pressure derivative discussed above is the same as taking the slope of the pressure function vs time function on a semi-log plot and displaying it on a log-log plot.

APPENDIX 5: Diagrams of the pressure build-up test in section 43.0 - 44.0 m

Borehole: KI0025F

Section : 43.0 - 44.0 m

A0 (Pump const P) Konst P

Start : 1997-06-18 14:54:11

Pi	4156.73 kPa	tp	3793 s
Po	4161.58 kPa	tpp	3840 s
Po-Pi	4.85 kPa	dtf	1941 s
Pp	2150.26 kPa	Qp	1.472e-005 m3/s
Pp-Pi	-2006.47 kPa	Vtot	5.654e-002 m3
Pf	4157.47 kPa	dPim	2020.34 kPa
Pf-Pi	0.74 kPa	dPom	2025.19 kPa
Pe	4171.71 kPa	Kiss	4.06e-008 m/s
Pe-Pi	14.98 kPa	Koss	4.05e-008 m/s
Wi		tdiffstart:	9 s
Wo-Wi		tdiffstop	8 s
Wp-Wi		PB	110 kPa
Wf-Wi	0.000 m	BB	999 kPa
We-Wi		TB	:970617095500
Pai	4121.85 kPa	X	999 m
Pao-Pai:	3.25 kPa	Y	999 m
Pap-Pai:	50.05 kPa	Z	-449 m.a.s.l.
Paf-Pai:	64.03 kPa	AW	999 Degrees
Pae-Pai:	60.10 kPa	IW	20 Degrees
Pbi	4157.18 kPa	DW	76.5 mm
Pbo-Pbi:	1.16 kPa	EC	:UHT1
Pbp-Pbi:	-2007.62 kPa	TC	:MM,KR,JO
Pbf-Pbi:	0.24 kPa	COMMENT	:Succesful test 43-44m! File:KI0025F4.HT2
Pbe-Pbi:	14.23 kPa	Crit 4	:Q > 1E-5 or Po - P > 10
dL4	0.5	Difft 4	-1 s
dL5	0.5	Crit 5	:Q < 1E-6 or P - Pp > 10
infile	:Ki0025f4.ht2'	Difft 5	-1 s

Thu Aug 13 13:56:58 1998

Borehole: KI0025F

Section : 43.0 - 44.0 m

A2 (Pump const P) Konst P

Start : 1997-06-18 14:54:11

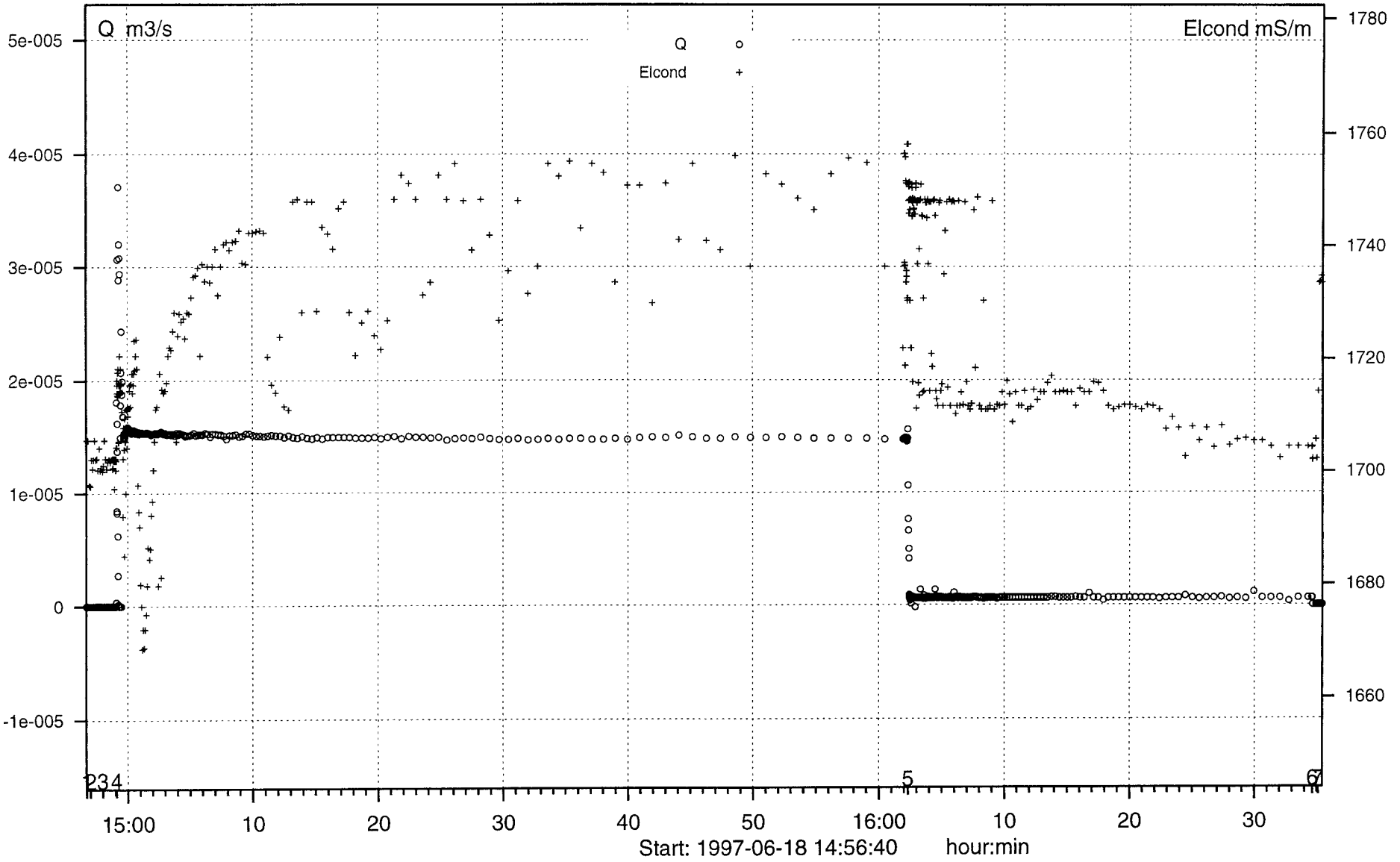

Thu Aug 13 13:56:40 1998

Borehole: KI0025F

Section : 43.0 - 44.0 m

C4 (Pump const P) Konst P

Start : 1997-06-18 14:54:11

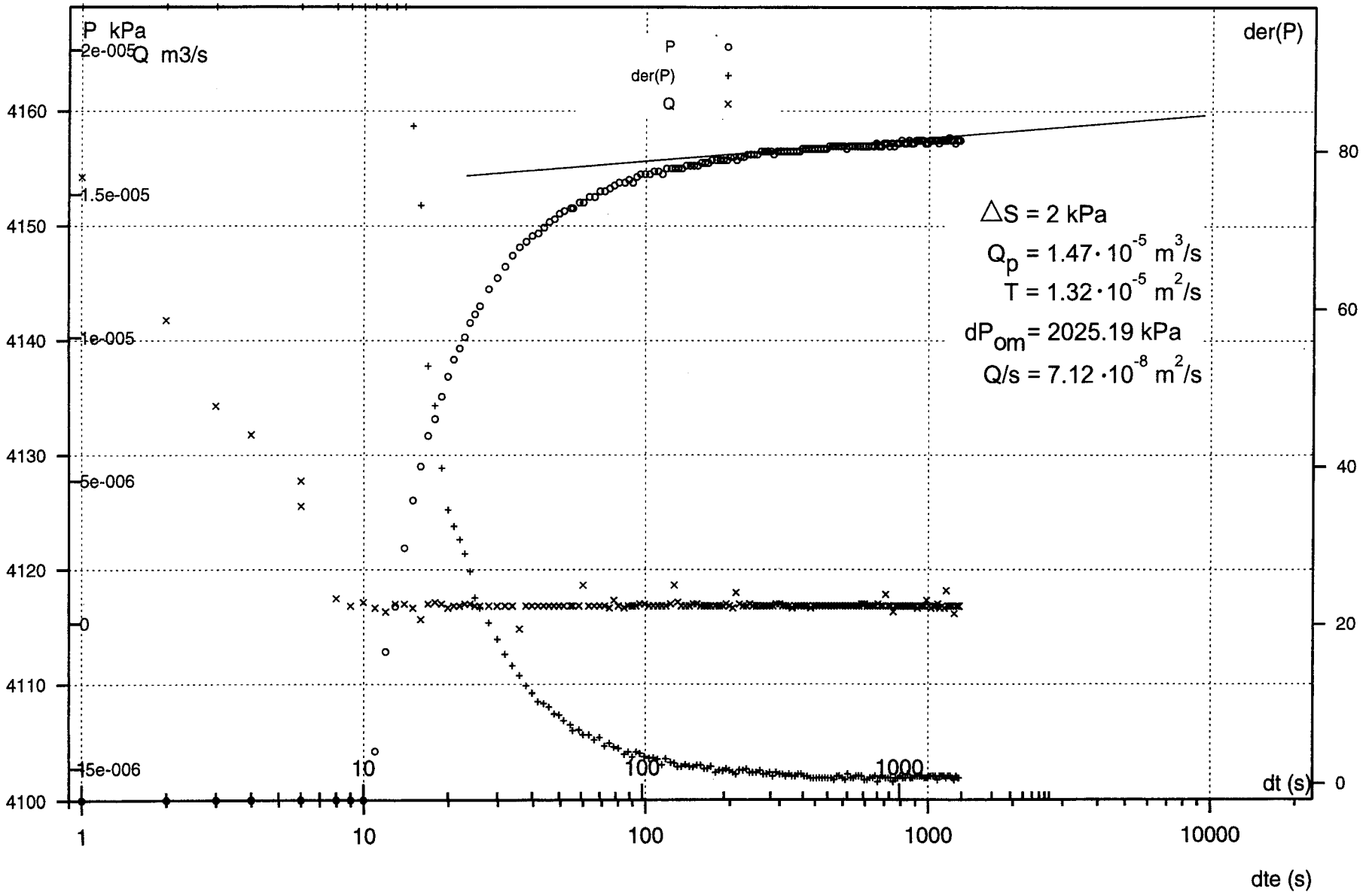

Borehole: KI0025F

Section : 43.0 - 44.0 m

C6 (Pump const P) Konst P

Start : 1997-06-18 14:54:11

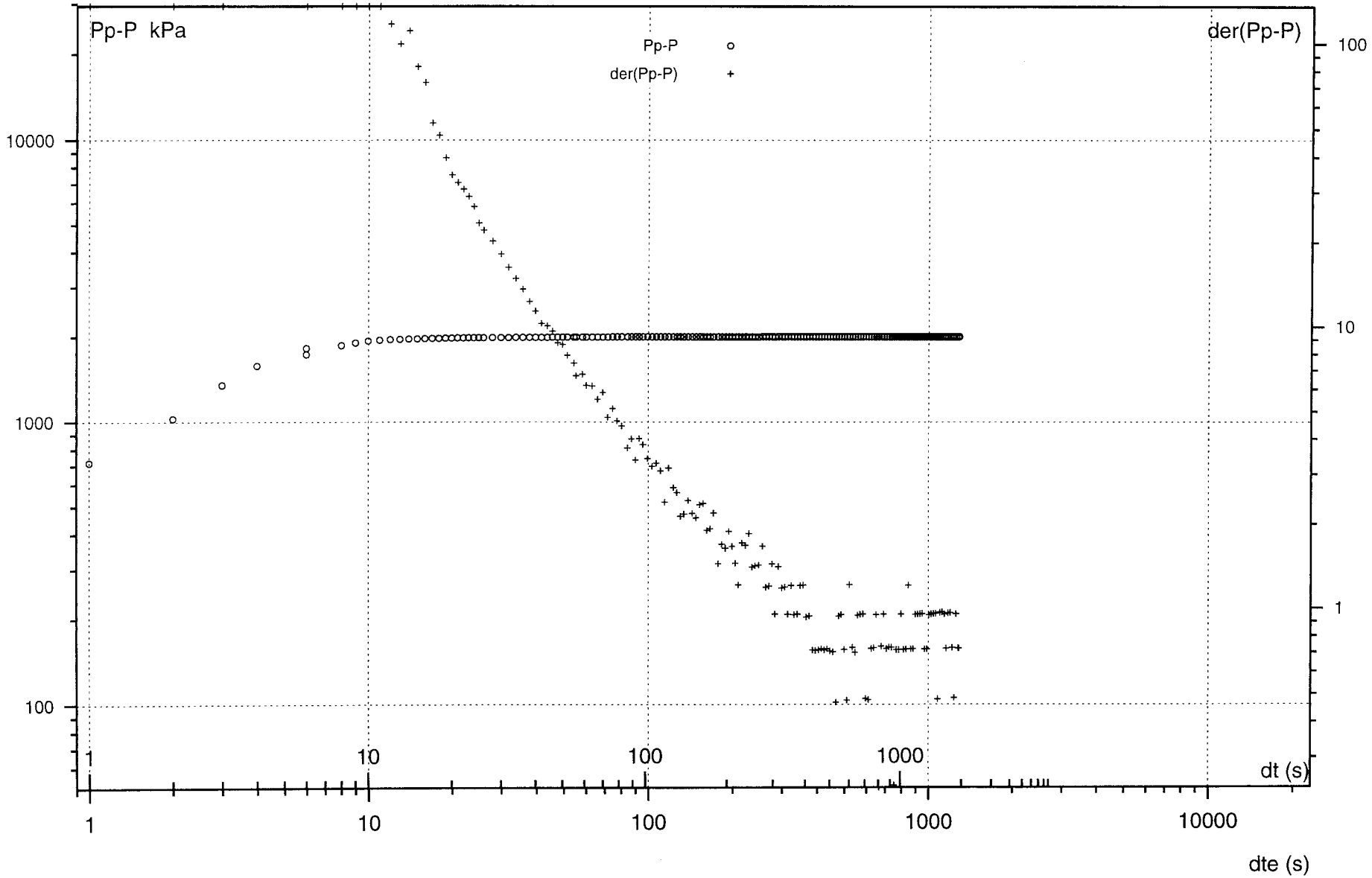

Thu Aug 13 13:56:40 1998

APPENDIX 6: Diagrams of the pressure build-up test in section 86.0 - 87.0 m

Borehole: KI0025F

Section : 87.0 - 88.0 m

A0 (Pump const P) Konst P

Start : 1997-06-18 18:06:16

Pi	4193.79 kPa	tp	3342 s
Po	4224.59 kPa	tpp	3483 s
Po-Pi	30.80 kPa	dtf	1795 s
Pp	2216.82 kPa	Qp	5.710e-006 m3/s
Pp-Pi	-1976.97 kPa	Vtot	1.989e-002 m3
Pf	4223.24 kPa	dPim	1982.51 kPa
Pf-Pi	29.45 kPa	dPom	2013.31 kPa
Pe	4217.84 kPa	Kiss	1.61e-008 m/s
Pe-Pi	24.05 kPa	Koss	1.59e-008 m/s
Wi		tdiffstart:	5 s
Wo-Wi		tdiffstop	3 s
Wp-Wi		PB	110 kPa
Wf-Wi	0.000 m	BB	999 kPa
We-Wi		TB	:970617095500
Pai	4190.30 kPa	X	999 m
Pao-Pai:	10.55 kPa	Y	999 m
Pap-Pai:	20.91 kPa	Z	-449 m.a.s.l.
Paf-Pai:	24.52 kPa	AW	999 Degrees
Pae-Pai:	24.03 kPa	IW	20 Degrees
Pbi	4193.73 kPa	DW	75.8 mm
Pbo-Pbi:	30.91 kPa	EC	:UHT1
Pbp-Pbi:	-1977.87 kPa	TC	:MM,KR,JO
Pbf-Pbi:	29.69 kPa	COMMENT	:Test 5 87-88m using valve on pipe string
Pbe-Pbi:	24.29 kPa	Crit 4	:Q > 1E-5 or Po - P > 10
dL4	0.5	Difft 4	-1 s
dL5	0.5	Crit 5	:Q < 1E-6 or P - Pp > 10
infile	:Ki0025f6.ht2'	Difft 5	-1 s

Thu Aug 13 15:33:33 1998

Borehole: KI0025F

Section : 87.0 - 88.0 m

A2 (Pump const P) Konst P

Start : 1997-06-18 18:06:16

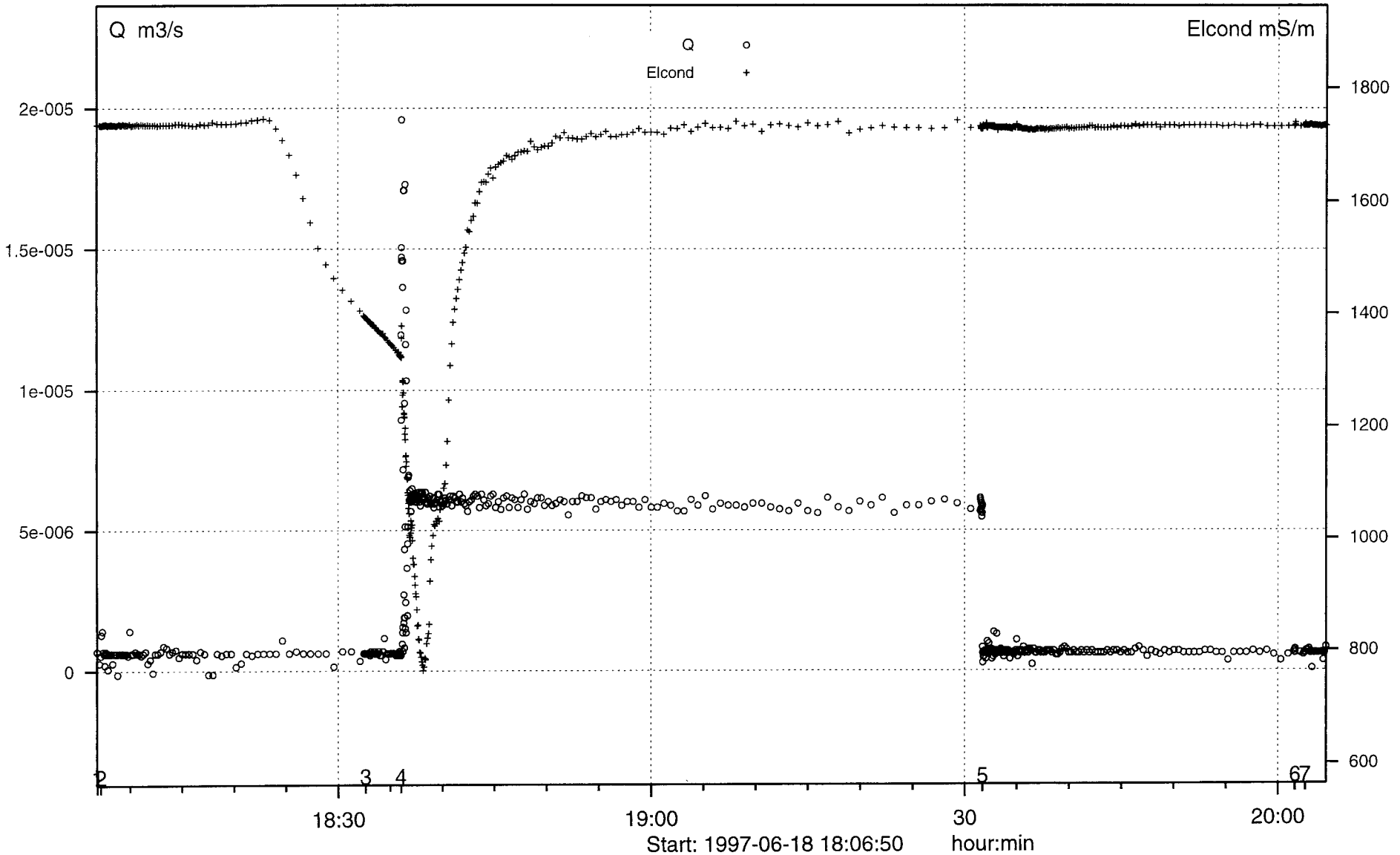

Thu Aug 13 15:33:33 1998

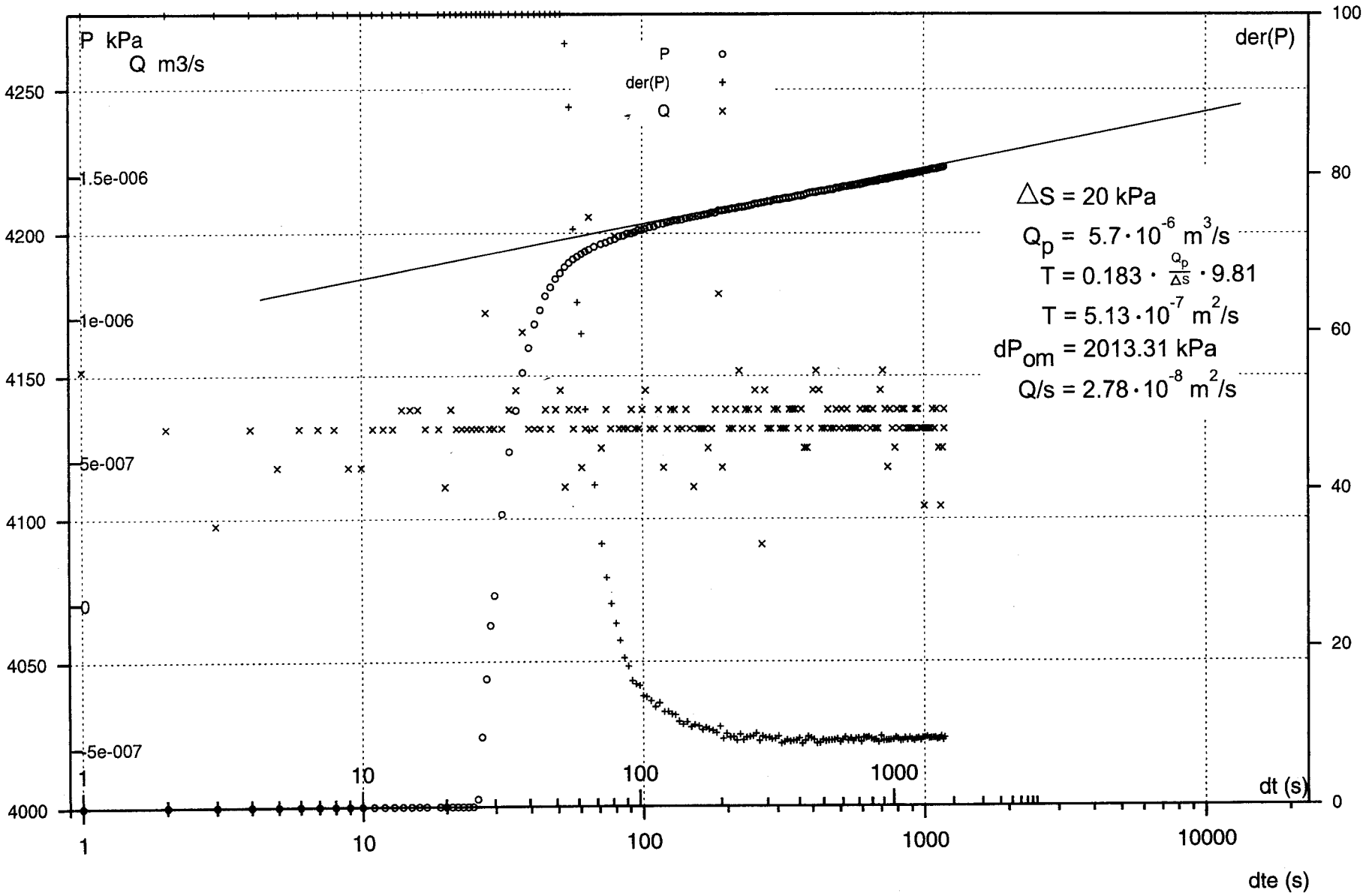
Borehole: KI0025F
Section : 87.0 - 88.0 m
C4 (Pump const P) Konst P
Start : 1997-06-18 18:06:16
P kPa
Q m3/s
der(P)
P
der(P)
Q
ΔS = 20 kPa
Qp = 5.7·10-6 m3/s
T = 0.183 · Qp/Δs · 9.81
T = 5.13·10-7 m2/s
dPom = 2013.31 kPa
Q/s = 2.78·10-8 m2/s
4250
4200
4150
4100
4050
4000
1.5e-006
1e-006
5e-007
0
5e-007
100
80
60
40
20
0
1
10
100
1000
10000
dt (s)
dte (s)

Borehole: KI0025F

Section : 87.0 - 88.0 m

C6 (Pump const P) Konst P

Start : 1997-06-18 18:06:16

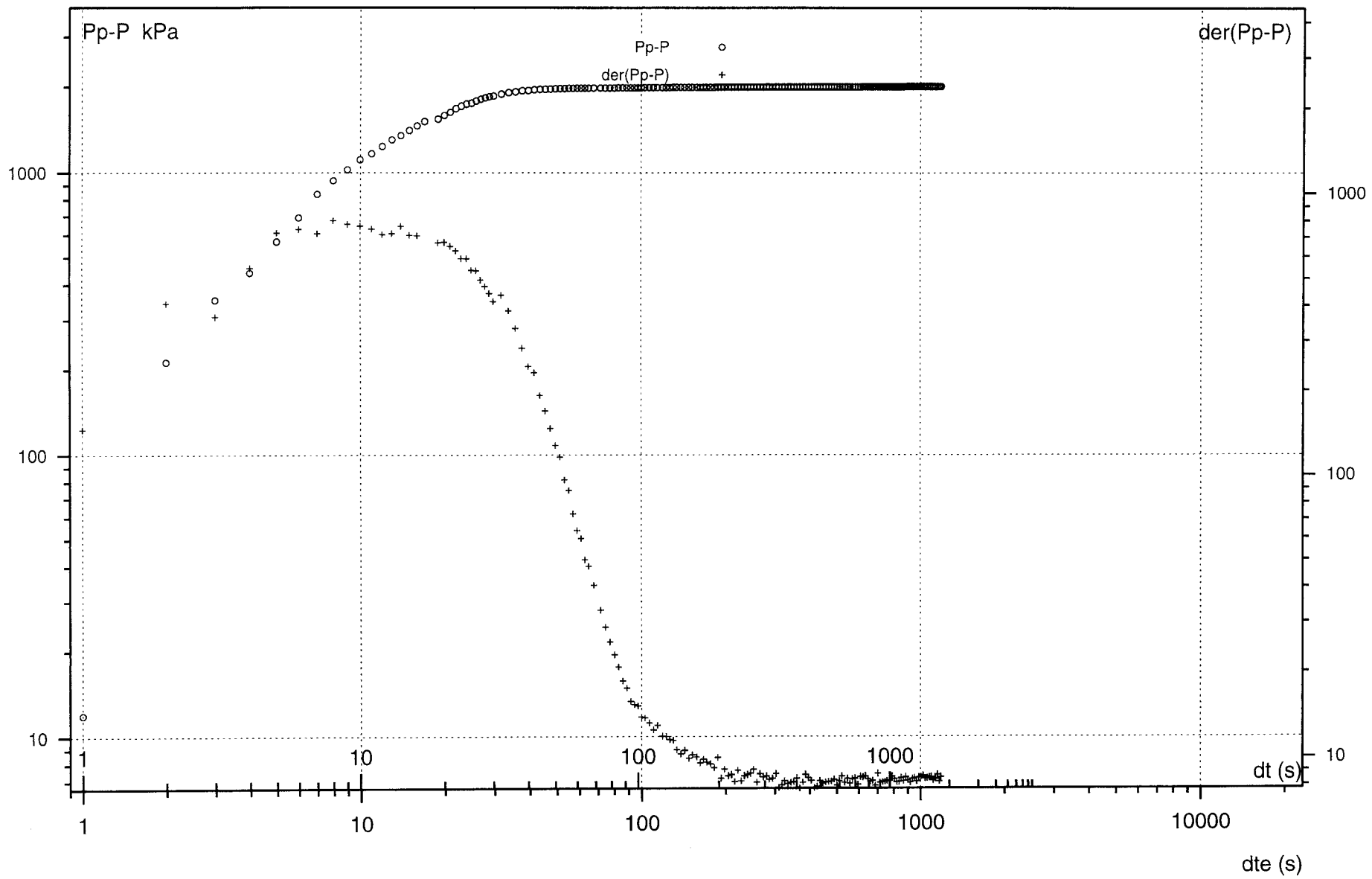

Thu Aug 13 15:33:34 1998

APPENDIX 7: Diagrams of the pressure build-up test in section 165.3 - 166.3 m

Borehole: KI0025F

Section : 165.3 - 166.3 m

A0 (Pump const P) Konst P

Start : 1997-06-19 09:50:09

Pi	4238.45 kPa	tp	2684 s
Po	4239.00 kPa	tpp	2710 s
Po-Pi	0.55 kPa	dtf	1338 s
Pp	2231.17 kPa	Qp	2.270e-004 m3/s
Pp-Pi	-2007.28 kPa	Vtot	6.154e-001 m3
Pf	4219.31 kPa	dPim	1996.85 kPa
Pf-Pi	-19.14 kPa	dPom	1997.40 kPa
Pe	4219.55 kPa	Kiss	6.35e-007 m/s
Pe-Pi	-18.90 kPa	Koss	6.35e-007 m/s
Wi		tdiffstart:	4 s
Wo-Wi		tdiffstop	5 s
Wp-Wi		PB	110 kPa
Wf-Wi	0.000 m	BB	999 kPa
We-Wi		TB	:970617095500
Pai	4227.83 kPa	X	999 m
Pao-Pai:	0.43 kPa	Y	999 m
Pap-Pai:	-44.83 kPa	Z	-449 m.a.s.l.
Paf-Pai:	-17.17 kPa	AW	999 Degrees
Pae-Pai:	-13.25 kPa	IW	20 Degrees
Pbi	4239.12 kPa	DW	75.8 mm
Pbo-Pbi:	-0.68 kPa	EC	:UHT1
Pbp-Pbi:	-2008.29 kPa	TC	:MM,KR,JO
Pbf-Pbi:	-19.63 kPa	COMMENT	:165.3-166.3m succesful
Pbe-Pbi:	-19.63 kPa	Crit 4	:Q > 1E-5 or Po - P > 10
dL4	0.5	Difft 4	-1 s
dL5	0.5	Crit 5	:Q < 1E-6 or P - Pp > 10
infile	:Ki0025f9.ht2'	Difft 5	-1 s

Thu Aug 13 16:02:59 1998

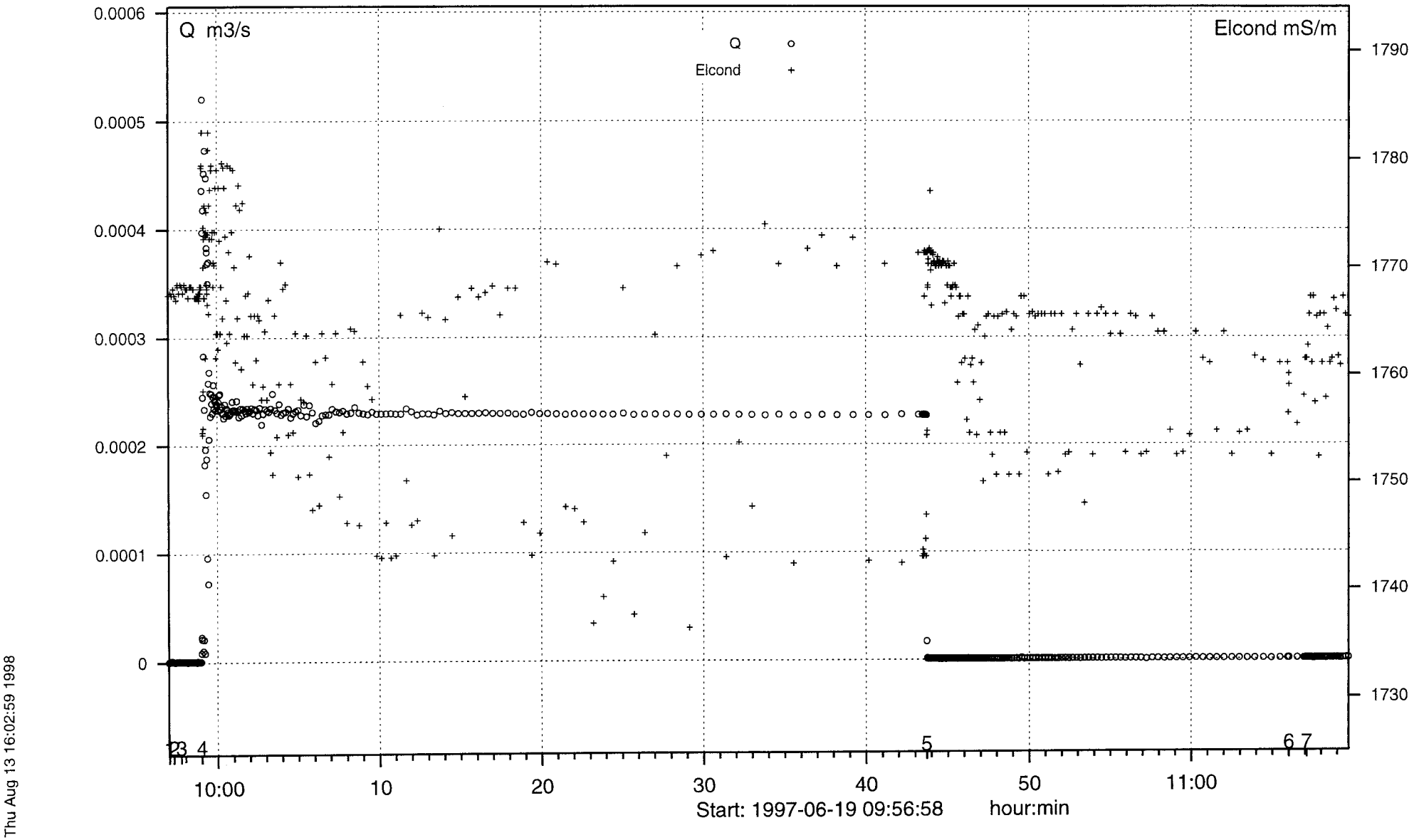
Borehole: KI0025F
Section : 165.3 - 166.3 m
A2 (Pump const P) Konst P
Start : 1997-06-19 09:50:09
Q m3/s
Elcond mS/m
Q
Elcond
0.0006
0.0005
0.0004
0.0003
0.0002
0.0001
0
1790
1780
1770
1760
1750
1740
1730
10:00
10
20
30
40
50
11:00
Start: 1997-06-19 09:56:58
hour:min
Thu Aug 13 16:02:59 1998

Borehole: KI0025F

Section : 165.3 - 166.3 m

C4 (Pump const P) Konst P

Start : 1997-06-19 09:50:09

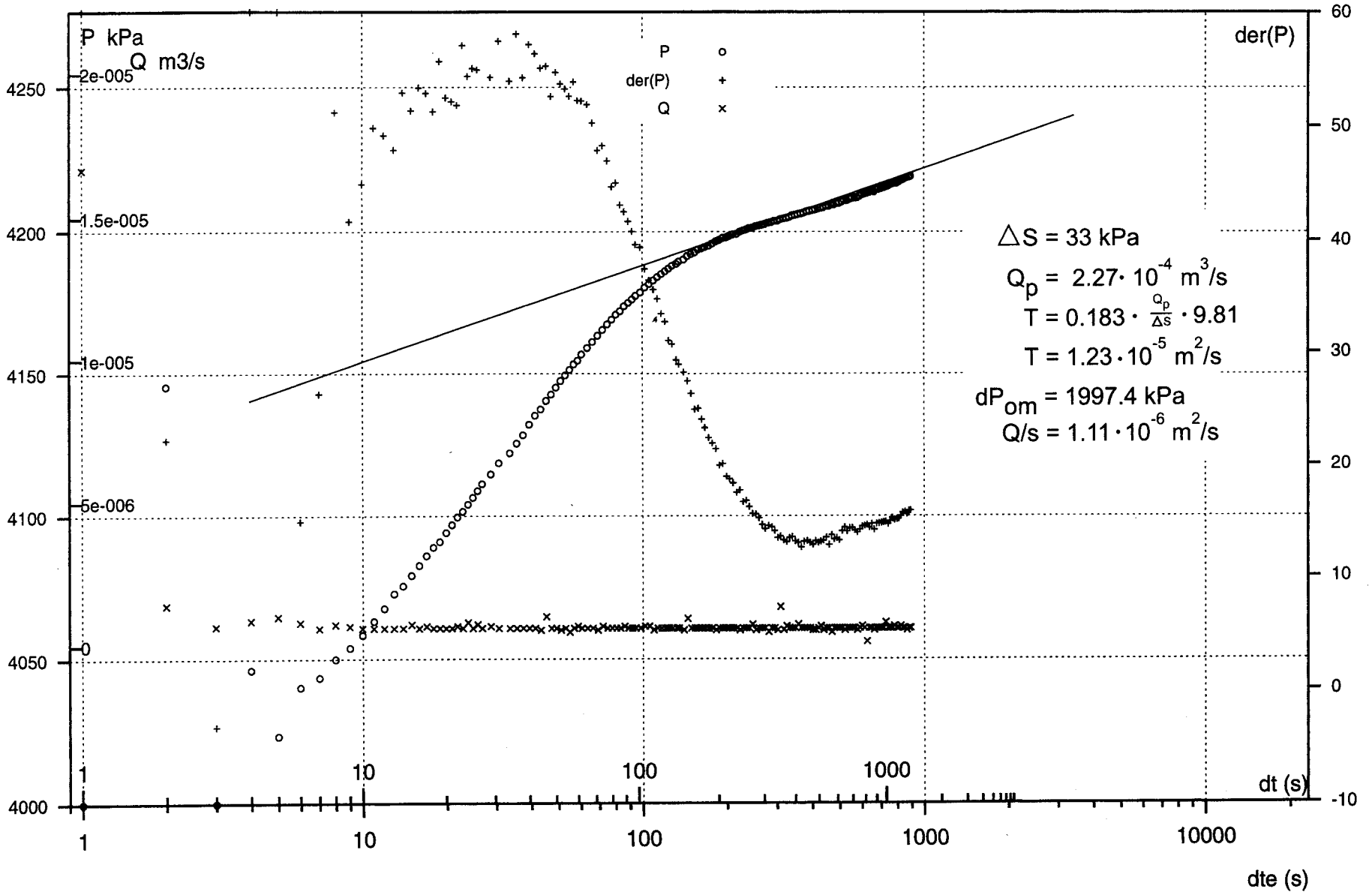

Borehole: KI0025F

Section : 165.3 - 166.3 m

C6 (Pump const P) Konst P

Start : 1997-06-19 09:50:09

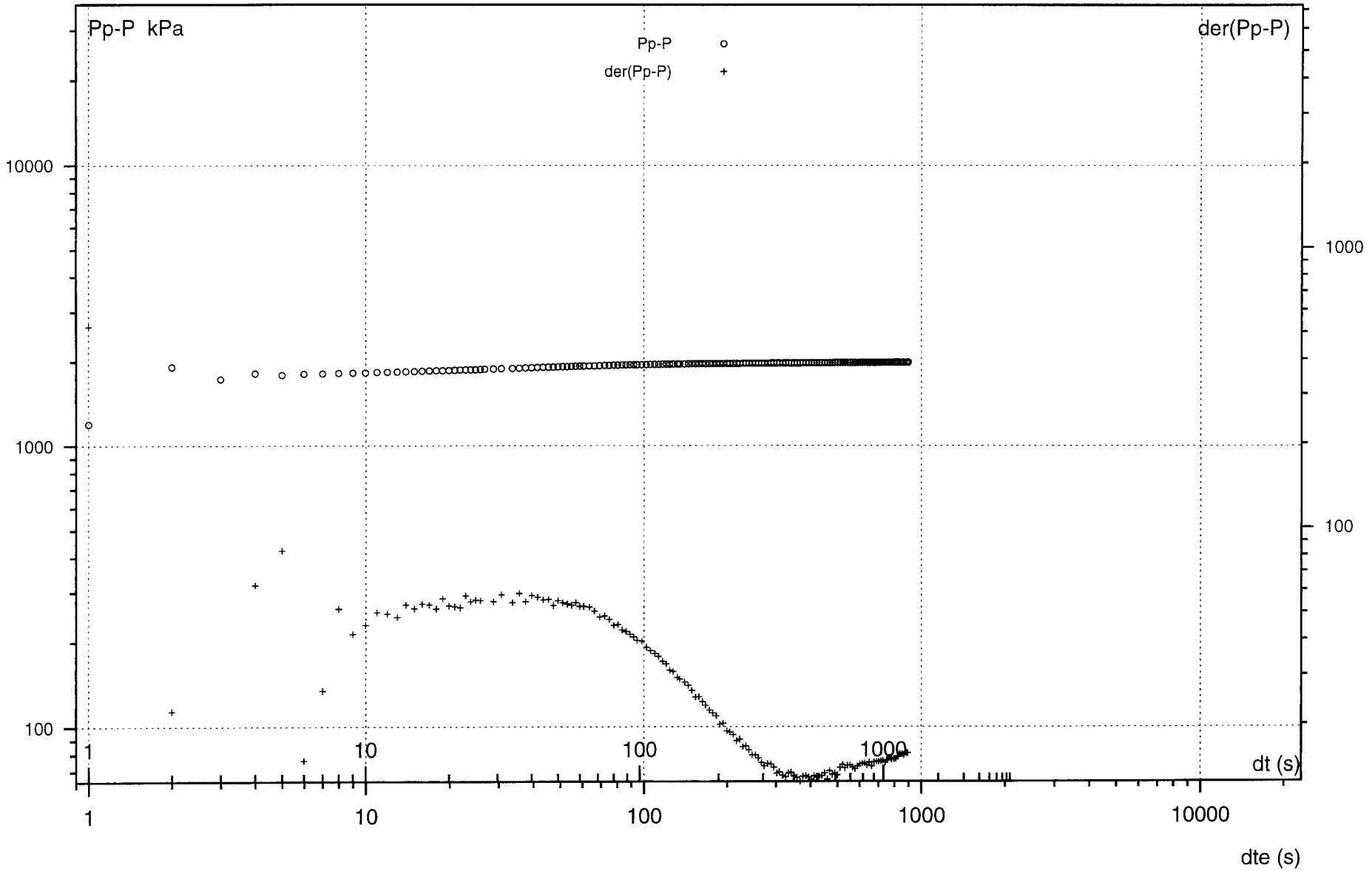

Thu Aug 13 16:03:00 1998

APPENDIX 8: Diagrams of the pressure build-up test in section 166.3 - 167.3 m

Borehole: KI0025F

Section : 166.3 - 167.3 m

A0 (Pump const P) Konst P

Start : 1997-06-19 14:27:41

Pi	4232.07 kPa	tp	1823 s
Po	4232.99 kPa	tpp	1848 s
Po-Pi	0.92 kPa	dtf	1354 s
Pp	3521.67 kPa	Qp	8.614e-005 m3/s
Pp-Pi	-710.40 kPa	Vtot	1.592e-001 m3
Pf	4232.31 kPa	dPim	708.54 kPa
Pf-Pi	0.24 kPa	dPom	709.46 kPa
Pe	4231.33 kPa	Kiss	6.79e-007 m/s
Pe-Pi	-0.74 kPa	Koss	6.79e-007 m/s
Wi		tdiffstart:	7 s
Wo-Wi		tdiffstop	4 s
Wp-Wi		PB	110 kPa
Wf-Wi	0.000 m	BB	999 kPa
We-Wi		TB	:970617095500
Pai	4222.18 kPa	X	999 m
Pao-Pai:	0.81 kPa	Y	999 m
Pap-Pai:	-10.24 kPa	Z	-449 m.a.s.l.
Paf-Pai:	0.25 kPa	AW	999 Degrees
Pae-Pai:	5.16 kPa	IW	20 Degrees
Pbi	4232.24 kPa	DW	75.8 mm
Pbo-Pbi:	1.23 kPa	EC	:UHT1
Pbp-Pbi:	-710.76 kPa	TC	:MM,KR,JO
Pbf-Pbi:	0.00 kPa	COMMENT	:Const p-700kpa 166.3-167.3
Pbe-Pbi:	-0.49 kPa	Crit 4	:Q > 1E-5 or Po - P > 10
dL4	0.5	Difft 4	-1 s
dL5	0.5	Crit 5	:Q < 1E-6 or P - Pp > 10
infile	:Ki025f12.ht2'	Difft 5	-1 s

Thu Aug 13 16:10:56 1998

Borehole: KI0025F

Section : 166.3 - 167.3 m

A2 (Pump const P) Konst P

Start : 1997-06-19 14:27:41

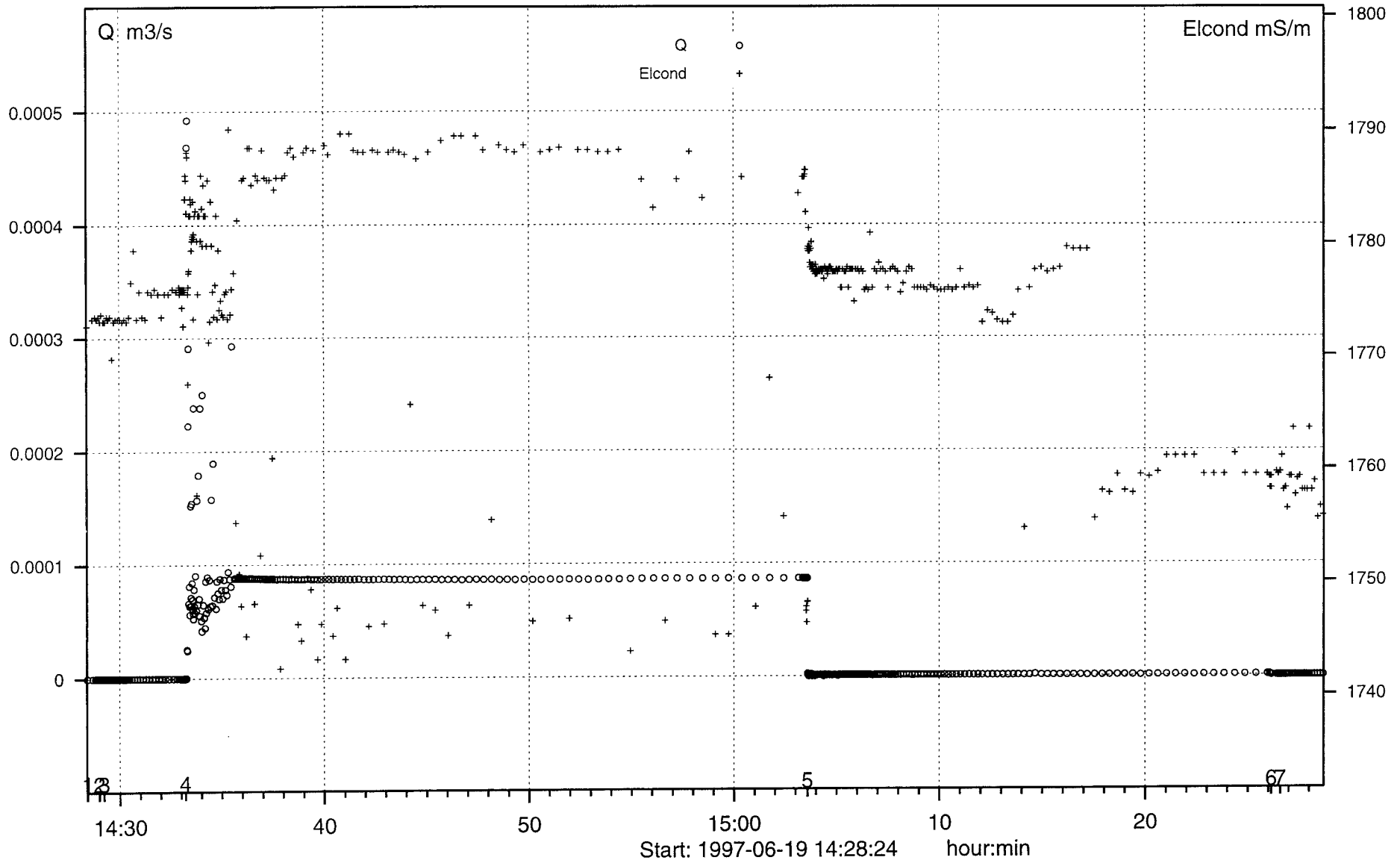

Thu Aug 13 16:10:56 1998

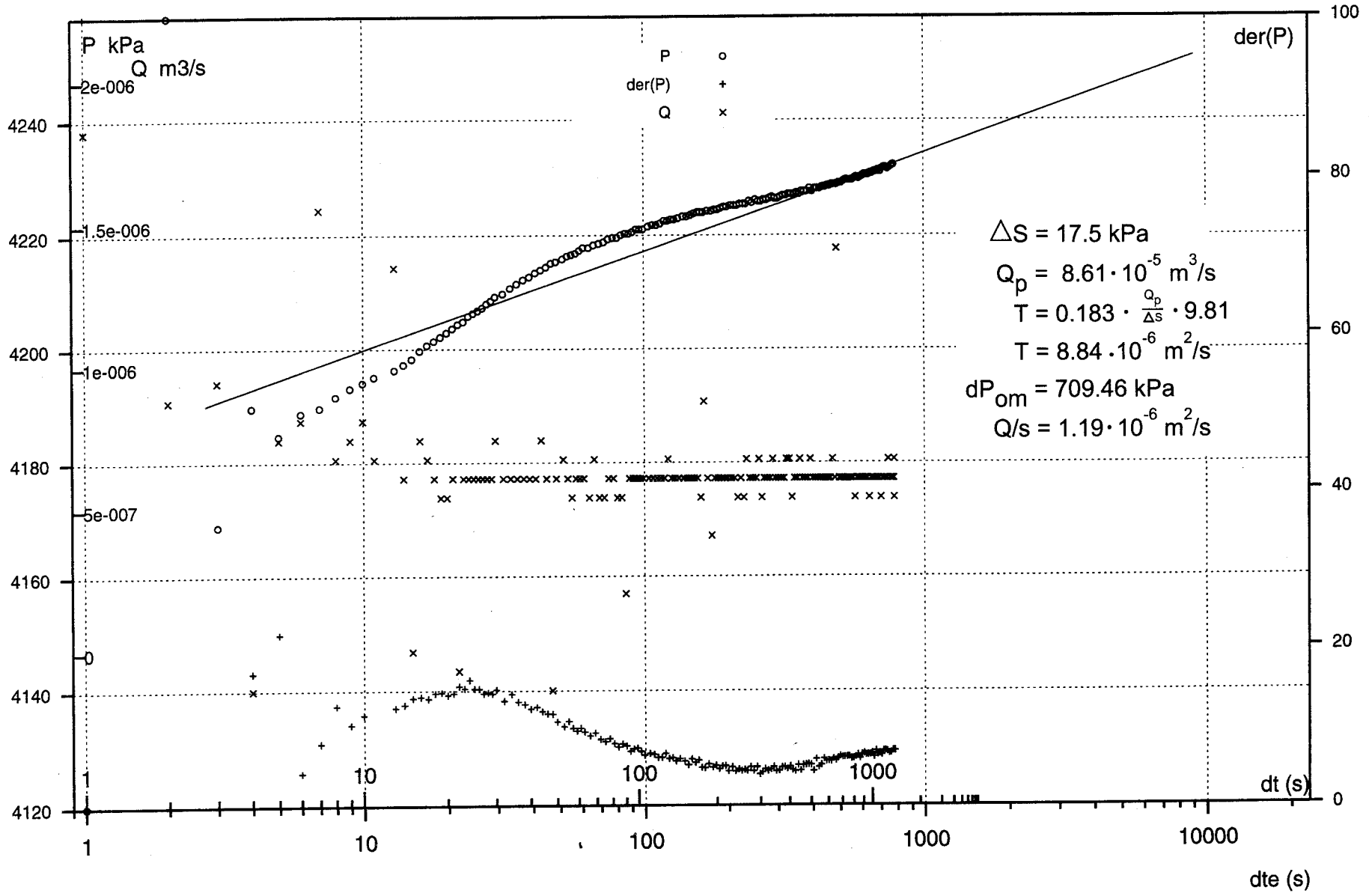
Borehole: KI0025F
Section : 166.3 - 167.3 m
C4 (Pump const P) Konst P
Start : 1997-06-19 14:27:41
P kPa
Q m3/s
der(P)
P
der(P)
Q
2e-006
1.5e-006
1e-006
5e-007
0
4240
4220
4200
4180
4160
4140
4120
100
80
60
40
20
0
1
10
100
1000
10000
dt (s)
dte (s)
ΔS = 17.5 kPa
$Q_p = 8.61 \cdot 10^{-5}$ m³/s
$T = 0.183 \cdot \frac{Q_p}{\Delta s} \cdot 9.81$
$T = 8.84 \cdot 10^{-6}$ m²/s
dP_{om} = 709.46 kPa
$Q/s = 1.19 \cdot 10^{-6}$ m²/s

Borehole: KI0025F

Section : 166.3 - 167.3 m

C6 (Pump const P) Konst P

Start : 1997-06-19 14:27:41

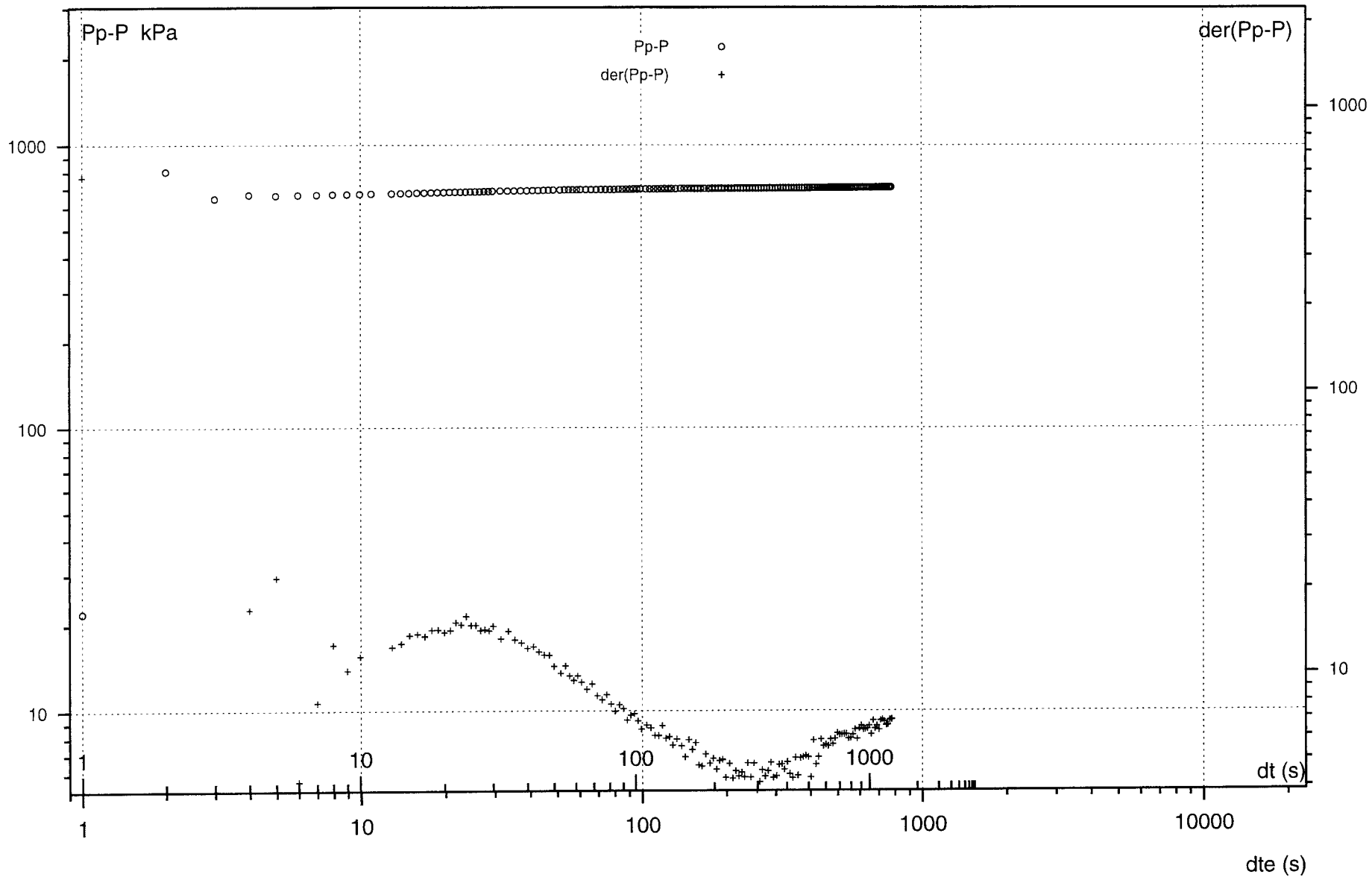

Thu Aug 13 16:10:56 1998

APPENDIX 9: Diagrams of the pressure build-up test in section 167.3 - 168.3 m

Borehole: KI0025F

Section : 167.3 - 168.3 m

A0 (Pump const P) Konst P

Start : 1997-06-23 11:18:05

Pi :	4249.25 kPa
Po :	4250.35 kPa
Po-Pi :	1.10 kPa
Pp :	2241.73 kPa
Pp-Pi :	-2007.52 kPa
Pf :	4247.78 kPa
Pf-Pi :	-1.47 kPa
Pe :	4240.41 kPa
Pe-Pi :	-8.84 kPa
Wi :	
Wo-Wi :	
Wp-Wi :	
Wf-Wi :	0.000 m
We-Wi :	
Pai :	4245.49 kPa
Pao-Pai:	1.17 kPa
Pap-Pai:	-13.18 kPa
Paf-Pai:	-1.47 kPa
Pae-Pai:	-8.83 kPa
Pbi :	4250.15 kPa
Pbo-Pbi:	0.74 kPa
Pbp-Pbi:	-2008.96 kPa
Pbf-Pbi:	-1.96 kPa
Pbe-Pbi:	-9.32 kPa
dL4 :	0.5
dL5 :	0.5
infile :Ki025f13.ht2'	

tp :	1945 s
tpp :	1987 s
dtf :	2522 s
Qp :	2.300e-005 m3/s
Vtot :	4.568e-002 m3
dPim :	1790.79 kPa
dPom :	1791.89 kPa
Kiss :	7.18e-008 m/s
Koss :	7.17e-008 m/s
tdiffstart:	3 s
tdiffstop :	5 s
PB :	110 kPa
BB :	999 kPa
TB :970617095500	
X :	999 m
Y :	999 m
Z :	-449 m.a.s.l.
AW :	999 Degrees
IW :	20 Degrees
DW :	75.8 mm
EC :UHT1	
TC :MM,KR	
COMMENT :167.3-168.3m.	
Crit 4 :Q > 1E-5 or Po - P > 10	
Difft 4 :	-1 s
Crit 5 :Q < 1E-6 or P - Pp > 10	
Difft 5 :	-1 s

Thu Aug 13 16:21:41 1998

Borehole: KI0025F

Section : 167.3 - 168.3 m

A2 (Pump const P) Konst P

Start : 1997-06-23 11:18:05

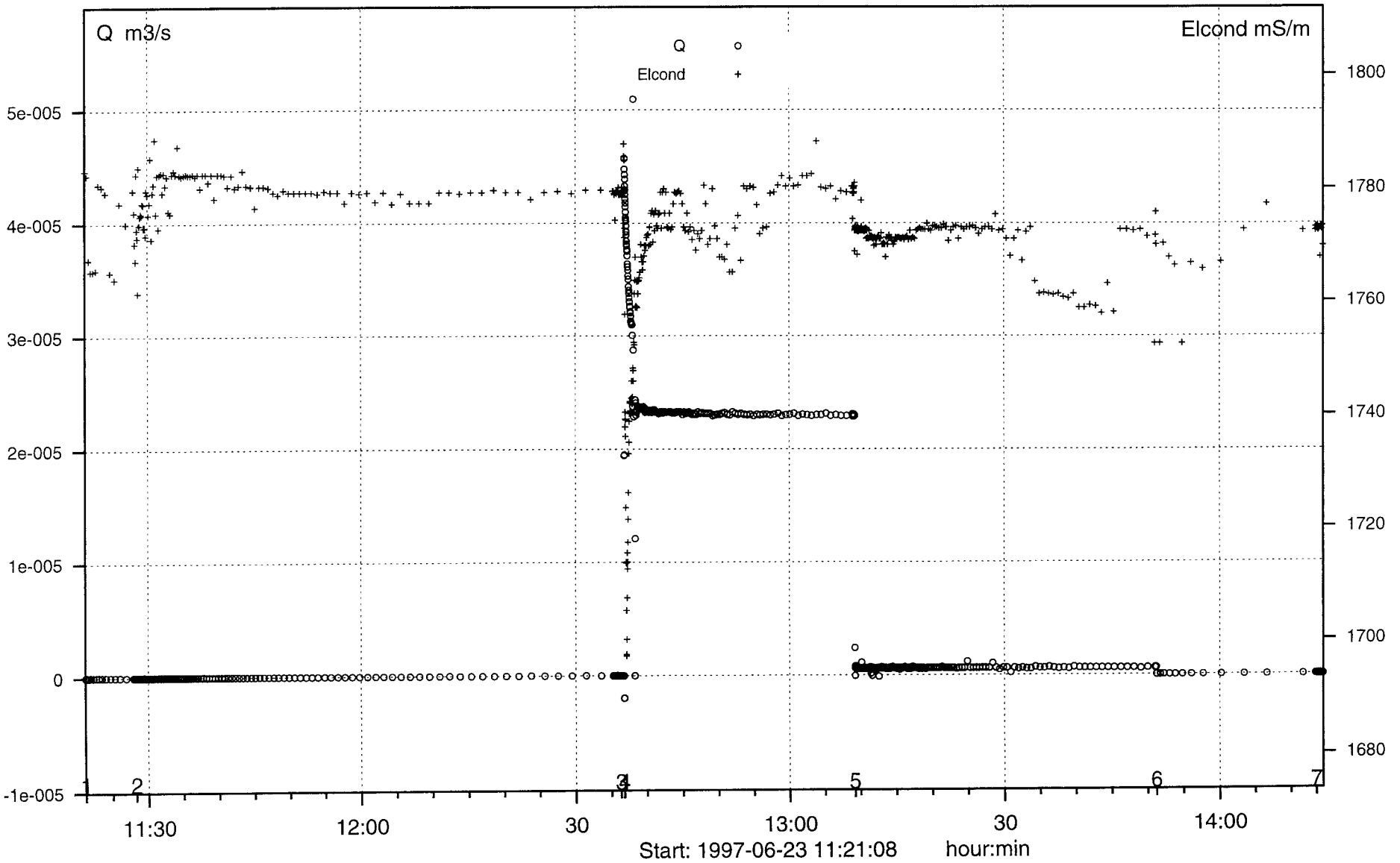

Thu Aug 13 16:21:41 1998

Borehole: KI0025F

Section : 167.3 - 168.3 m

C4 (Pump const P) Konst P

Start : 1997-06-23 11:18:05

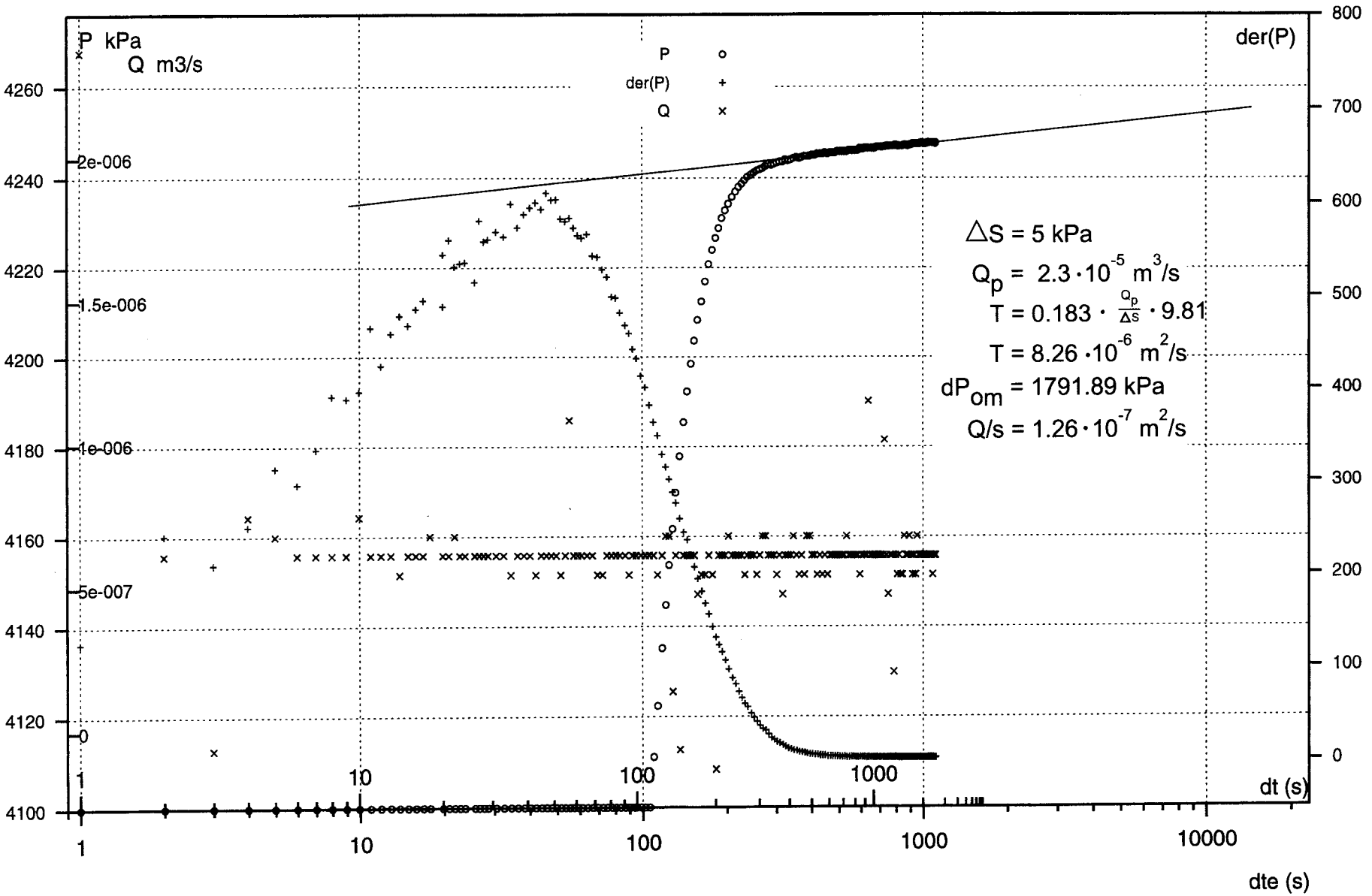

Borehole: KI0025F

Section : 167.3 - 168.3 m

C6 (Pump const P) Konst P

Start : 1997-06-23 11:18:05

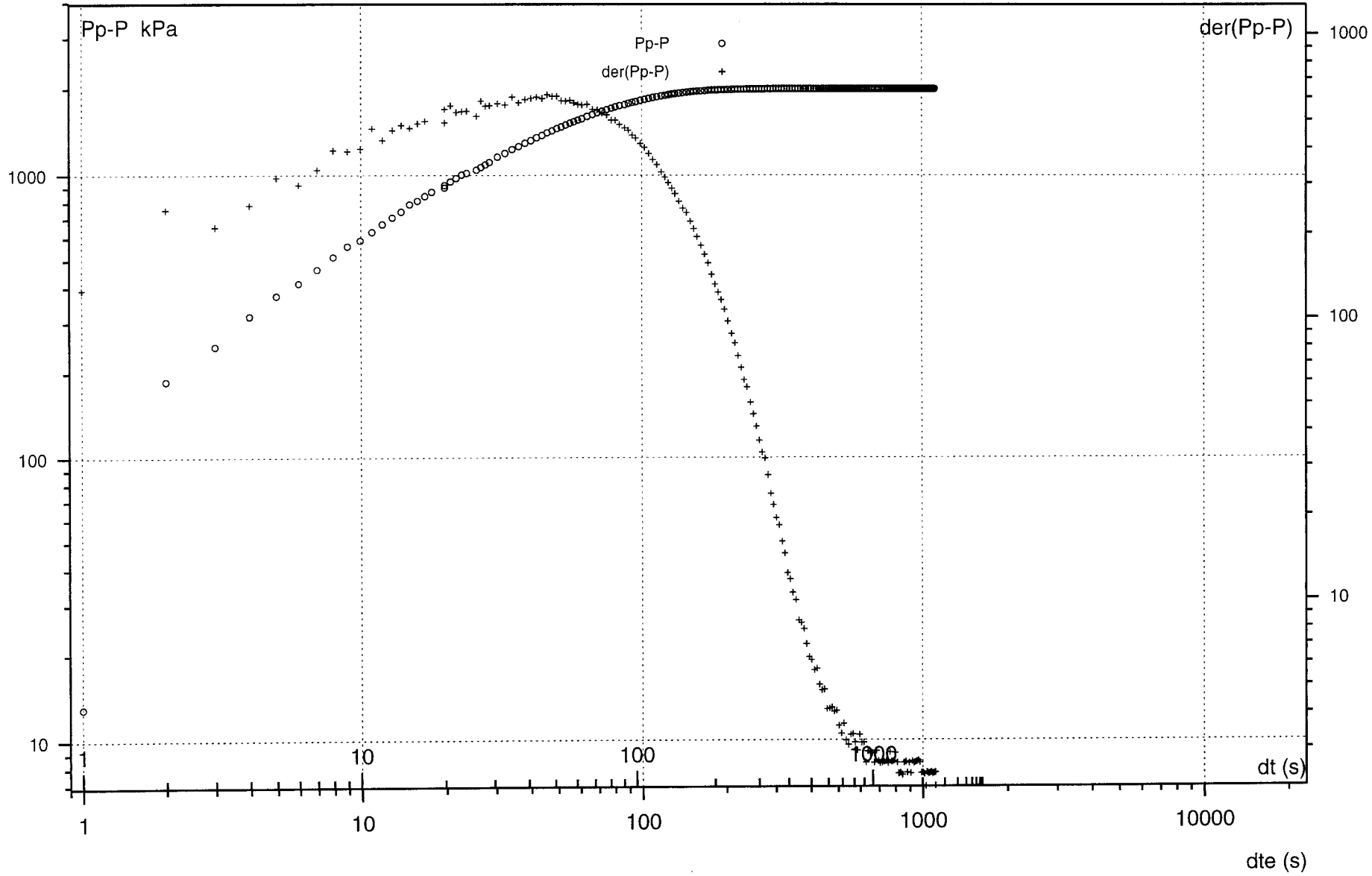

Thu Aug 13 16:21:41 1998

APPENDIX 10: Diagrams of the pressure build-up test in section 186.0 - 193.8 m

Borehole: KI0025F

Section : 186.0 - 193.8 m

A0 (Pump const P) Konst P

Start : 1997-06-24 12:54:45

Pi :	4181.52 kPa
Po :	4183.49 kPa
Po-Pi :	1.97 kPa
Pp :	2175.72 kPa
Pp-Pi :	-2005.80 kPa
Pf :	4215.38 kPa
Pf-Pi :	33.86 kPa
Pe :	4207.29 kPa
Pe-Pi :	25.77 kPa
Wi :	
Wo-Wi :	
Wp-Wi :	
Wf-Wi :	0.000 m
We-Wi :	
Pai :	4178.28 kPa
Pao-Pai:	1.53 kPa
Pap-Pai:	-57.23 kPa
Paf-Pai:	29.68 kPa
Pae-Pai:	24.53 kPa
Pbi :	4182.69 kPa
Pbo-Pbi:	1.84 kPa
Pbp-Pbi:	-2007.43 kPa
Pbf-Pbi:	33.36 kPa
Pbe-Pbi:	25.02 kPa
dL4 :	0.5
dL5 :	0.5

infile :Ki025f17.ht2'

tp :	2000 s
tpp :	2091 s
dtf :	7505 s
Qp :	4.540e-004 m3/s
Vtot :	9.491e-001 m3
dPim :	1970.12 kPa
dPom :	1972.08 kPa
Kiss :	2.60e-007 m/s
Koss :	2.60e-007 m/s
tdiffstart:	5 s
tdiffstop :	7 s
PB :	110 kPa
BB :	999 kPa
TB	:970617095500
X :	999 m
Y :	999 m
Z :	-449 m.a.s.l.
AW :	999 Degrees
IW :	20 Degrees
DW :	75.8 mm
EC	:UHT1
TC	:JO,KR
COMMENT	:OK
Crit 4	:Q > 1E-5 or Po - P > 10
Difft 4 :	-1 s
Crit 5	:Q < 1E-6 or P - Pp > 10
Difft 5 :	-1 s

Thu Aug 13 16:55:30 1998

Borehole: KI0025F

Section : 186.0 - 193.8 m

A2 (Pump const P) Konst P

Start : 1997-06-24 12:54:45

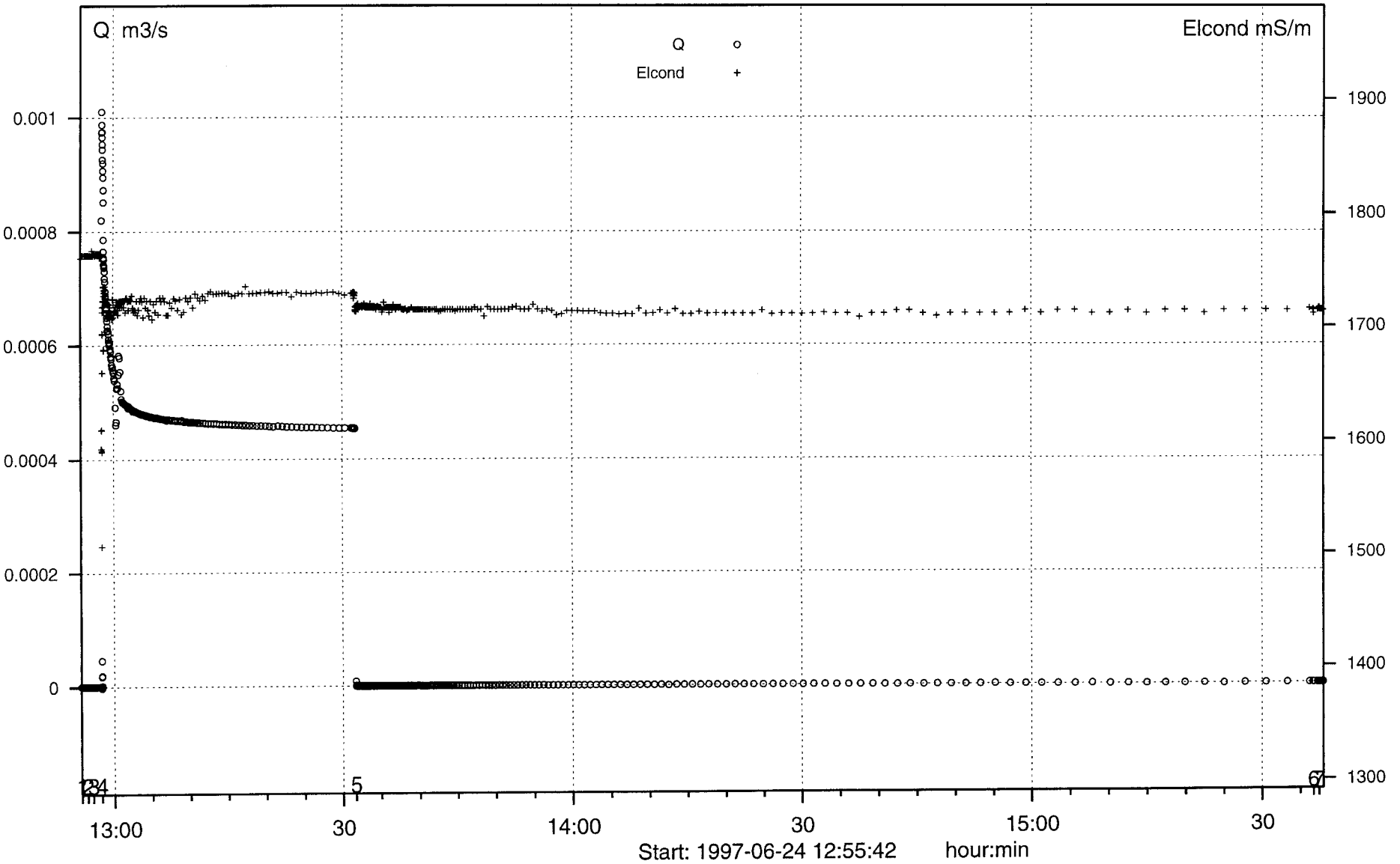

Thu Aug 13 16:55:31 1998

Borehole: KI0025F

Section : 186.0 - 193.8 m

C4 (Pump const P) Konst P

Start : 1997-06-24 12:54:45

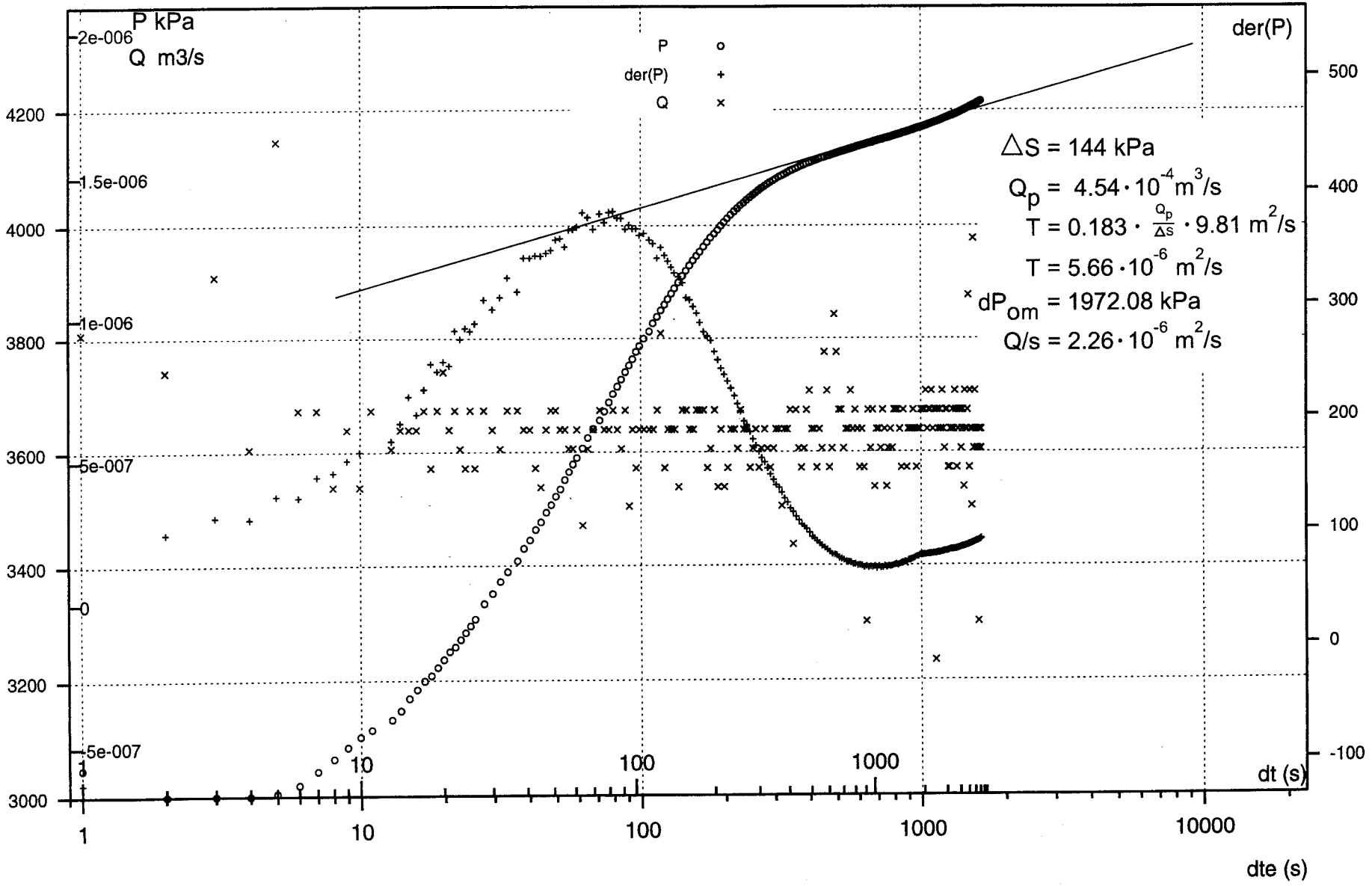

Borehole: KI0025F

Section : 186.0 - 193.8 m

C6 (Pump const P) Konst P

Start : 1997-06-24 12:54:45

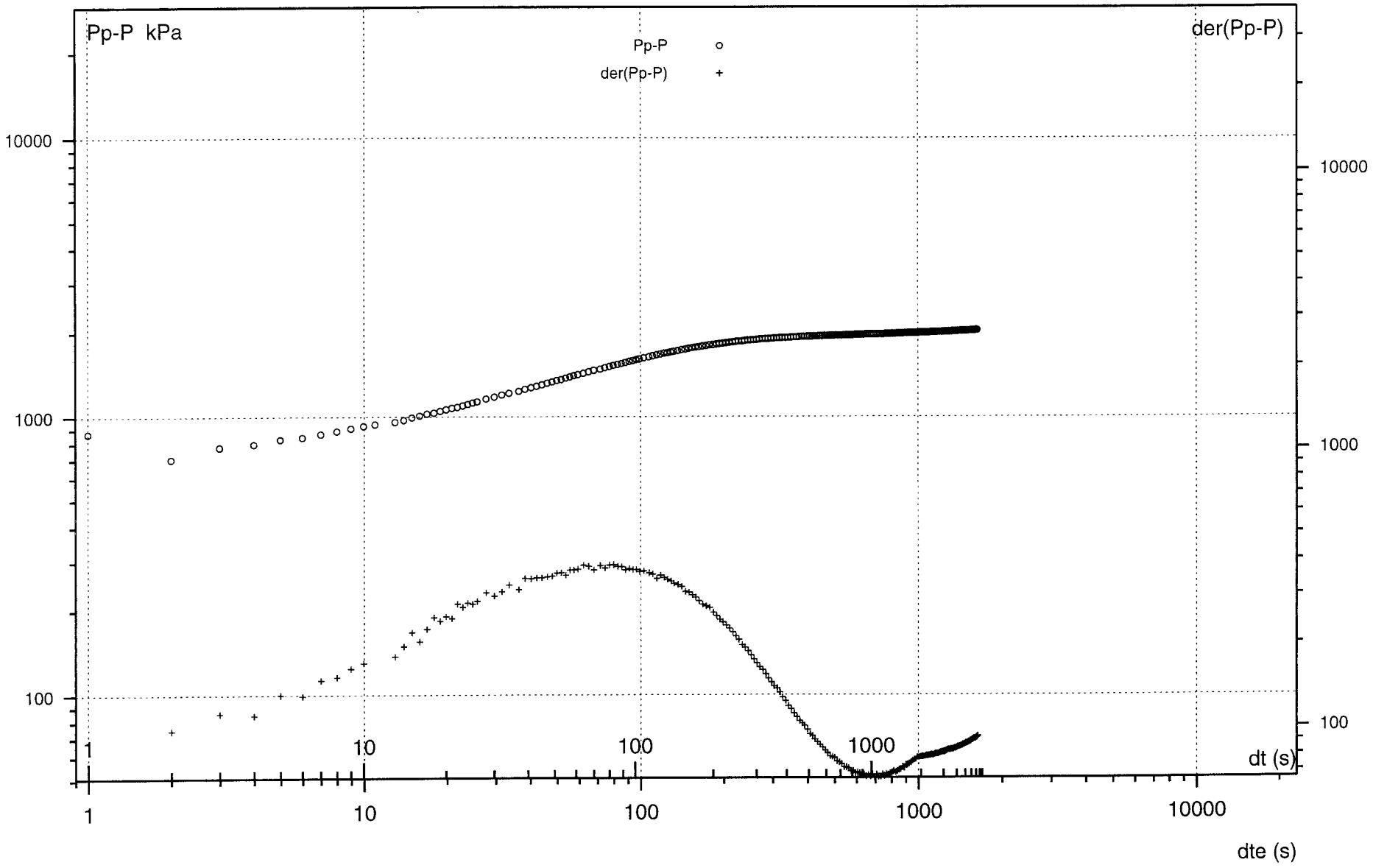

Thu Aug 13 16:55:31 1998